

AN ARCHAEOLOGICAL ANALYSIS OF LAYER V FAUNAL REMAINS FROM ABRIC  
DEL PASTOR, ALCOY ALICANTE SPAIN

A Thesis Submitted to the Committee on Graduate Studies in Partial Fulfillment of the  
Requirements for the Degree of Master of Arts in the Faculty of Arts and Sciences

TRENT UNIVERSITY

Peterborough, Ontario, Canada

© Copyright by Marissa Scott 2023

Anthropology M.A. Graduate Program

September 2023

## ABSTRACT

An Archaeozoological Analysis of Faunal Remains from Layer V of Abric Del Pastor, Alcoy, Alicante, Spain.

Marissa Scott

This thesis employs zooarchaeological, taphonomic, and spatial analysis to reconstruct subsistence behaviors of Middle Paleolithic Neanderthals using layer V of Abric del Pastor as a case study. Located in Alcoy, Alicante, Spain, Abric del Pastor is a cave shelter with occupation layers dated from MIS 5 through 3. The faunal assemblage is examined on two time scales: i) a longer time frame focused on large scale human occupation and use and ii) another, shorter time frame in an attempt to distinguish possible shorter anthropogenic events. The layer V assemblage is comprised of at least two occupation events, Occupation A and Occupation B. These are two relatively well-preserved anthropogenic accumulations dominated by medium sized taxa. In these occupations, the carcasses were likely transported from a separate kill site to the cave shelter to be processed and consumed. The taxonomic and taphonomic patterns uncovered in these occupation events are similar suggesting consistent behavioral patterns throughout Layer V. Ultimately, the faunal assemblage is typical of other MIS 5-3 rock shelters in the Iberian Peninsula. By examining the subsistence practices of layer V, dated to MIS 4, this work aims to fill a gap in the MIS 4 Iberian Peninsula literature and add to the conversation on how early hominins adapted to the changing climate.

**Keywords:** Archaeozoology, Middle Paleolithic, Abric del Pastor, Iberian Peninsula, Palimpsest, Time Perspectivism.

## DEDICATION

This thesis is dedicated to my past self. Thank you for putting in the work that allowed me to embark on the adventure that resulted in a body of work I can be proud of.

*“A work in progress. And the possibilities are endless.”*  
Elizabeth Eulberg

## ACKNOWLEDGMENTS

I would like to take this opportunity to thank quite a few people and organizations who without their support this thesis would not have been completed. Firstly, I would like to thank Dr. Jose Capriles for recommending Trent University's Anthropology Master's program and Dr. Eugène Morin to me. This was a necessary and life changing experience that has made me a better student, archaeologist, and person. I would like to extend my deepest gratitude to my supervisor Dr. Eugène Morin. I appreciate all of your patience, guidance, feedback, and faith that you have had in me over these past two years. Thank you for taking a chance on me and introducing me to Dr. Carolina Mallol without whom, this project would not have been possible. Thank you to Dr. Mallol and Dr. Cristo Hernández for allowing me to work with you and spearhead a zooarchaeological analysis on your material from Abric del Pastor. You both gave me the opportunity to do what I have always wanted to do as well as to experience a new country and culture. Dr. Leopold Pérez, I appreciate all of your guidance and assistance in the initial examination of this collection. You really helped me get on my feet and provided me with a significant number of resources. Thank you as well to all of the graduate students I encountered at Trent and while working in Spain. The knowledge that I gained from you and the feedback you provided me was incredibly helpful throughout this process.

A great deal of my appreciation is owed to the Trent Archaeology program, TUARC, and Trent University as a whole, for providing me with the opportunity and funding to create this body of work. Additionally, a thank you to my thesis committee (Dr. James Connolly and Dr. Paul Spzak) for all of the time and energy you dedicated to assisting me in this process. Lastly, to Yumi Pedoe for all of your administrative and emotional support over the past two years. I

appreciated every email, event, and meal that would not have been possible without your dedication to the archaeology program.

Personally, I would also like to express gratitude to my family and friends. Without your endless love and support I would not have been able to move to a new country on my own. Thank you specifically to my parents for supporting and encouraging my passions and to my partner, Brianna. Your constant support kept me going.

## TABLE OF CONTENTS

ABSTRACT.....	ii
DEDICATION.....	iii
ACKNOWLEDGMENTS.....	iv
TABLE OF CONTENTS.....	vi
LIST OF FIGURES.....	ix
LIST OF TABLES.....	xii
CHAPTER 1 INTRODUCTION.....	1
1.1 Research Objectives and Significance.....	1
1.2 Structure of Thesis.....	2
CHAPTER 2 BACKGROUND.....	4
2.1 Overview of MIS 5-MIS 3 in the Iberian Peninsula.....	6
2.1.1. MIS 5.....	7
2.1.2. MIS 4.....	9
2.1.3. MIS 3.....	10
2.2 Abric del Pastor.....	13
2.3 Time Perspectivism.....	18
CHAPTER 3 METHODS.....	21
3.1 Faunal Sample.....	22
3.1.1 Obtaining the Samples.....	22
3.1.2 Division of Time Scales.....	23
3.2 Database.....	23
3.3 Taxonomic Classification.....	25
3.4 Anatomic Group Classification.....	27
3.4.1 Anatomic Group.....	28
3.4.2 Tooth Database.....	29
3.4.3 Portion.....	30
3.4.4 Length and Circumference.....	31
3.4.5 Zone and Bone Region.....	33

3.4.6 Side.....	33
3.4.7 Age and Sex.....	33
3.4.8 Osteometry and the Osteo-metric Database.....	34
3.5 Taphonomy.....	35
3.5.1 Fractures.....	36
3.5.2 Refits.....	37
3.5.3 Post-depositional Damage.....	38
3.5.4 Marks.....	39
3.5.5 Thermo-alteration.....	40
3.5.6 Marks Database.....	41
3.6 Quantification.....	44
3.6.1 Counts.....	45
3.6.2 Statistical Analysis.....	47
3.6.3 Spatial Analysis.....	47
3.7 Summary.....	49
CHAPTER 4 RESULTS.....	50
4.1 Occupation A.....	51
4.2 Occupation B.....	57
4.3 Finer Time Scale: Patterns Between Sublayers in Occupation B.....	65
4.4 Comparison of the Two Occupation Events.....	74
4.5 Summary.....	77
CHAPTER 5 DISCUSSION AND CONCLUDING REMARKS.....	78
5.1. What species were exploited?.....	78
5.2 What agents and activities were involved in the deposition of fauna remains?.....	79
5.3 Can we identify finer periods of accumulation?.....	81
5.4 Limitations and Future Research Directions.....	81
5.5 Concluding Remarks.....	83
REFERENCES CITED.....	84

APPENDICES.....96



## LIST OF FIGURES

<b>2.1</b>	Map of MIS 5-3 sites in Spain.	<b>6</b>
<b>2.2</b>	Map of Spain showing Abric del Pastor with photos of the site. The top right photo is an aerial view of the cave shelter. The bottom right photo shows the opening of the rock shelter and the excavation area.	<b>13</b>
<b>2.3</b>	Stratigraphic diagram noting the type of sediment, the sublayers, as well as the presence of hearths.	<b>15</b>
<b>3.1</b>	Excavation map of Abric del Pastor. Along the X axis the squares occur in alphabetical order from D-V while the Y axis follows a numerical order from 1-6. The dotted line represents the drip line.	<b>21</b>
<b>3.2</b>	The principal layout for the Abric del Pastor database.	<b>24</b>
<b>3.3</b>	Example of how the information about provenience is recorded in the database.	<b>25</b>
<b>3.4</b>	The section of the database where taxonomic information is recorded.	<b>26</b>
<b>3.5</b>	The section in which the anatomical data for each specimen is recorded.	<b>28</b>
<b>3.6</b>	Tooth database layout.	<b>29</b>
<b>3.7</b>	The diagrams showing how the portion of the fragment is identified and recorded.	<b>31</b>
<b>3.8</b>	Diagrams describing how circumference and bone region are recorded.	<b>32</b>
<b>3.9</b>	The section where sex and age data are recorded.	<b>34</b>
<b>3.10</b>	The section where osteo-metric data are recorded. The link to the osteo-metric database is provided by the gray button in the lower right-hand corner.	<b>35</b>
<b>3.11</b>	The osteo-metric database layout.	<b>35</b>
<b>3.12</b>	Where the fracture data is recorded including the origin (i.e., fresh, ancient, or mixed) and the morphology.	<b>36</b>
<b>3.13</b>	The section where refits, photographs, and possible future revisions are noted.	<b>37</b>
<b>3.14</b>	The database layout where post-depositional damage is recorded.	<b>39</b>
<b>3.15</b>	The section of the database where anthropic marks are recorded.	<b>40</b>
<b>3.16</b>	The section where evidence of burning on fragments is noted.	<b>40</b>

<b>3.17</b>	Example of a burnt remain where only a “point” on the surface area was affected by thermo-alteration. The arrow indicates the burnt point.	<b>41</b>
<b>3.18</b>	Example of a burnt remain where “part” of the surface area was affected by thermo-alteration. The arrow indicates the part of the specimen where the surface area has been burnt.	<b>42</b>
<b>3.19</b>	Example of a burnt remain where the “total” amount of surface area was affected by thermo-alteration.	<b>42</b>
<b>3.20</b>	Marks database layout.	<b>43</b>
<b>3.21</b>	Diagrams explaining how the location of marks on a specimen are recorded.	<b>44</b>
<b>4.1</b>	Cross-section of the y axis showing the vertical distribution of all the faunal remains in Occupations A and B. The y-axis (in meters) correlates to rows 1-6 of the excavation surface	<b>50</b>
<b>4.2</b>	Cross-section of the x-axis showing the vertical distribution of all the faunal remains in Occupations A and B. The x-axis (in meters) correlates to columns D through W of the excavation surface.	<b>51</b>
<b>4.3</b>	Kernel density model of Occupation A. The darker the color the denser the accumulation of faunal material.	<b>56</b>
<b>4.4</b>	XZ plot of Occupation B with the sublayers color-coded as follows: Va is red, Vb is purple, Vc is green, Vd is pink, Ve is black, and Vf is blue. The x-axis (in meters) correlates to columns D through W of the excavation surface.	<b>57</b>
<b>4.5</b>	Kernel density model of Occupation B. The darker the color the denser the accumulation of faunal material.	<b>65</b>
<b>4.6</b>	The average level of erosion, weathering, and root mark damage in the sublayers of Occupation B.	<b>66</b>
<b>4.7</b>	The average level of manganese and concretion damage in the sublayers of Occupation B. Va is the topmost sublayer and Vf is the bottommost sublayer.	<b>66</b>
<b>4.8</b>	The percentages of determinate and indeterminate specimens through the sublayers of Occupation B. Va is the most recent sublayer and Vf is the oldest sublayer.	<b>67</b>
<b>4.9</b>	Percent of small-sized species through the sublayers of Occupation B.	<b>69</b>
<b>4.10</b>	Percent of variation in body size classes (small, medium, and large) through the sublayers of Occupation B. Va is the most recent sublayer and Vf is the oldest sublayer.	<b>70</b>
<b>4.11</b>	Comparing the percentage of caprines versus medium-sized mammals through the sublayers of Occupation B	<b>71</b>
<b>4.12</b>	Variation in the percentage of the anatomic groups (cranial, axial, forelimb, and	<b>72</b>

	hindlimb) through the sublayers of Occupation B. Va is the most recent sublayer and Vf is the oldest sublayer.	
<b>4.13</b>	The number of burnt specimens per sublayer of Occupation B. Vb is the topmost sublayer with burnt remains and Vf is the bottommost sublayer.	<b>73</b>
<b>4.14</b>	Anthropic marks through the sublayers of Occupation B.	<b>74</b>
<b>4.15</b>	Vertical distribution of anthropic marks. A) cut marks B) percussion notches C) scrape marks.	<b>77</b>
<b>A 2.1</b>	Figure that depicts the various morphotypes of long bone fractures and their corresponding database code.	<b>87</b>
<b>A 2.2</b>	Figure that depicts the various morphotypes of epiphyses fractures and their corresponding database codes.	<b>88</b>
<b>A 2.3</b>	Figure depicting the various morphotypes of mandible fractures and their corresponding database codes.	<b>89</b>
<b>A 2.4</b>	Figure depicting the various morphotypes of vertebra fractures and their corresponding database codes.	<b>90</b>
<b>A 2.5</b>	Figure depicting the various morphotypes of scapula fractures and their corresponding database codes.	<b>91</b>
<b>A 2.6</b>	Figure depicting the various morphotypes of pelvis fractures and their corresponding database codes.	<b>92</b>
<b>A 3.3</b>	Vertical distribution of specimens attributed to A) small-sized taxa, B) large-sized taxa, and C) medium-sized taxa.	<b>94</b>

LIST OF TABLES

<b>3.1</b>	Body size class classification.	<b>27</b>
<b>3.2</b>	Indeterminate anatomic group bones and the abbreviations that are used in the database.	<b>28</b>
<b>3.3</b>	Weathering stage criteria from Gifford-Gonzalez (2018).	<b>38</b>
<b>3.4</b>	Scale from 1-5 that corresponds to the percentage of surface area affected by post-depositional damage.	<b>39</b>
<b>4.1</b>	Number and percentage of the faunal remains from Occupation A exhibiting various types of post-depositional damage. Percentage is listed in parentheses.	<b>52</b>
<b>4.2</b>	Taxonomic breakdown of Occupation A.	<b>52</b>
<b>4.3</b>	Percentage of specimens identified to small- and medium-sized animals from Occupation A after merging the species with those identified to body size class.	<b>52</b>
<b>4.4</b>	Anatomic group for all species combined that are present in Occupation A.	<b>53</b>
<b>4.5</b>	MNE counts for Occupation A.	<b>53</b>
<b>4.6</b>	MNI counts for Occupation A.	<b>54</b>
<b>4.7</b>	The number and percentage of each type of anthropic mark identified in Occupation A. The percentage of anthropic marks in Occupation A, as a whole, is listed in the total row.	<b>54</b>
<b>4.8</b>	The number and percent of specimens for each type of mark separated by body size class in Occupation A.	<b>55</b>
<b>4.9</b>	The number and percent of specimens of each category of percent of circumference preserved for long bone fragments from Occupation A. The percentage of the assemblage is listed in the parentheses.	<b>55</b>
<b>4.10</b>	Number and percentage of long bone fragments with dry, fresh, and mixed fractures from Occupation A.	<b>55</b>
<b>4.11</b>	Average length of medium- and small-sized animal specimens from Occupation A.	<b>55</b>

<b>4.12</b>	Number and percent of the surface area of fragments affected by concretions and manganese for each sublayer of Occupation B. The percentage is listed in the parentheses. Va is the most recent sublayer and Vf is the oldest sublayer.	<b>58</b>
<b>4.13</b>	Percent of the surface area of the fragments affected by erosion and root mark damage for each sublayer in Occupation B. The percentage is listed in the parentheses.	<b>58</b>
<b>4.14</b>	Weathering stage for the fragments in each sublayer of Occupation B. Va is the topmost sublayer and Vf is the bottommost sublayer. The percentage is listed in the parentheses.	<b>59</b>
<b>4.15</b>	Taxa identified in each sublayer of Occupation B. Va is the most recent sublayer and Vf is the oldest sublayer.	<b>59</b>
<b>4.16</b>	Percent distribution by body size class in the sublayers of Occupation B after merging taxonomically identified specimens with those attributed to body size class.	<b>60</b>
<b>4.17</b>	Anatomic groups present in the sublayers of Occupation B. All species combined.	<b>60</b>
<b>4.18</b>	MNE counts for the sublayers of Occupation B.	<b>61</b>
<b>4.19</b>	MNI counts for the sublayers in Occupation B.	<b>61</b>
<b>4.20</b>	The number and percentage of specimens attributed to each category of the percentage of circumference preserved for long bone fragments in Occupation B. The percentage of specimens is listed in the parentheses.	<b>62</b>
<b>4.21</b>	The average length (in millimeters) of specimens per body size class in each sublayer of Occupation B. The number of specimens is in the parentheses.	<b>62</b>
<b>4.22</b>	The percentage of dry, fresh, and mixed fractures in each sublayer of Occupation B. Va is the most recent sublayer and Vf is the oldest sublayer. The percentage is listed in parentheses.	<b>63</b>
<b>4.23</b>	Number and percentage of anthropogenic marks identified in the sublayers of Occupation B.	<b>63</b>
<b>4.24</b>	Number and percentage of anthropogenic marks by species and type of mark in Occupation B.	<b>64</b>
<b>4.25</b>	Breakdown of burned specimens identified in the sublayers of Occupation B. Vb is the topmost sublayer with burnt remains and Vf is the bottommost sublayer.	<b>64</b>

<b>4.26</b>	Adjusted standardized residuals and <i>p</i> -values for the chi-square analysis of the distribution of identified and indeterminate specimens for the sublayers of Occupation B. Statistically significant outliers are in bold.	<b>68</b>
<b>4.27</b>	Adjusted standardized residuals and <i>p</i> -values for the chi-square analysis of the distribution of tortoises through the sublayers of Occupation B compared to other identified taxa. Statistically significant outliers are in bold.	<b>69</b>
<b>4.28</b>	Adjusted standardized residuals and <i>p</i> -values for chi-square analysis of the comparison of body size class distribution for each of the sublayers of Occupation B. Statistically significant outliers are in bold.	<b>71</b>
<b>4.29</b>	Residuals and <i>p</i> -values for comparison of the distribution of cranial versus axial remains in the sublayers of Occupation B. Statistically significant outliers are in bold.	<b>73</b>
<b>4.30</b>	Identified versus unidentified specimens per occupation and sublayer. Va is the most recent sublayer and Vf is the oldest sublayer.	<b>75</b>
<b>4.31</b>	Percentage of overall post-depositional damage including the effects of concretions, erosion, weathering, root marks, and manganese for Occupation A and Occupation B.	<b>75</b>
<b>A 3.1</b>	The number and percent of the determinate and indeterminate specimens through the sublayers of Occupation B.	<b>93</b>
<b>A 3.2</b>	Average Nearest Neighbor analysis output for both Occupation A and Occupation B.	<b>93</b>

## Chapter 1 Introduction

Spatial patterns are believed to be significant components for archaeologists to reconstruct past social and economic behaviors (Schiffer 1999). Traditionally, archaeologists have relied on stratigraphic units or layers in order to understand how sites were formed, if and how their use changed seasonality, as well as shifts in diet or subsistence practices. However, for many Middle Paleolithic sites (~300–40 ka), this is an imperfect strategy as most of these sites are palimpsests (superimposition of overlapping activities or occupations at a site) in nature. Therefore, more recent work has shifted to employing a spatiotemporal perspective to address the palimpsest problem and illuminate behavioral patterns like the subsistence behavior of Neandertals during the Middle Paleolithic. To accomplish this, researchers are relying on new methods (i.e., geoarchaeological and stratigraphic analyses) to examine excavation units at relatively high temporal resolutions (Bailey 2007; Machado et al. 2019; Pérez et al. 2020; Sossaríos et al. 2022). This thesis follows this approach as it explores the subsistence behavior of Middle Paleolithic Neanderthals in Eastern Iberia with an emphasis on the issue of temporal resolution using layer V of Abric del Pastor as a case study.

### 1.1 Research Objectives and Significance

This research combines zooarchaeological and taphonomic methods to analyze the faunal remains from layer V of Abric del Pastor in order to identify subsistence practices and periods of finer accumulation. Those results were then interpreted from a time perspectivist framework to better understand how Neandertals from MIS 4 in the Iberian Peninsula interacted with and adapted to their environment, a current gap in the literature. Specifically, the following research

questions will be addressed: What species were exploited by Neandertals at Abric del Pastor? What agents (i.e., hominins, carnivores, raptors, etc.) were involved in the deposition of the faunal remains? Which kinds of activities took place at the site, as indicated by the faunal remains? Ultimately, this thesis helps to fill the gap in the MIS 4 Iberian Peninsula literature as well as provide a source of evidence for later research to build upon.

## 1.2 Structure of Thesis

This thesis contains five chapters. In Chapter 2, I outline the necessary background information in order to provide the context of the faunal material. I begin by discussing the chronological period in which the site was inhabited (MIS 5 through MIS 3). This is followed by the history of Abric del Pastor including the environmental conditions, when it was excavated, how it was excavated, and the remains that have been identified so far. Lastly, a presentation on the theoretical framework—Time Perspectivism—through which I am approaching this research. Chapter 3 outlines the materials and methods that comprise this thesis. It details how the layer V material was obtained as well as at which time scales the material is divided upon. The taxonomic and taphonomic analyses that were performed and how they recorded are in the following sections. Lastly, there is a section on quantification, and statistical and spatial analyses.

In Chapter 4, the results of the analyses described in the previous chapter are presented. The results for Occupation A are presented first followed by Occupation B. Occupation B results are presented as the occupation as a whole and then on a finer time scale comparing the sublayers within Occupation B to each other. Lastly the results of Occupation A are compared to



Occupation B's results. In the last chapter, Chapter 5, the results of the analysis on the layer V faunal remains from Abric del Pastor are contextualized and interpreted in order to answer the research questions that were presented above.

## Chapter 2: Background

Abric del Pastor, the focus of this work, is a Middle Paleolithic rock shelter located in the southeastern portion of the Iberian Peninsula. The site has been dated to Marine Isotope Stages (MIS) 5-3. Globally, this period coincided with a shift from warmer climates in MIS 5 to cooler temperatures in MIS 4 and back to a warm period (MIS 3). During the MIS 5/4 transition, it is thought that the Iberian Peninsula was a place of refuge for Northern European Neanderthals (Carvalho and Bicho 2022; Finlayson et al. 2006; Finlayson and Carrión 2007; Galvan et al. 2014; Garralda et al. 2014; Mallol et al. 2019). However, there is a lack of sites that date securely to MIS 4 in the region (Daura et al. 2021; Mallol et al. 2019). Abric del Pastor thus provides a unique opportunity to provide insight into Neanderthal behavior during MIS 4.

In archaeology, spatial patterns are believed to be a key element in attempts to reconstruct past social and economic behavioral patterns (Schiffer 1999). To examine these patterns, archaeologists have traditionally used stratigraphic units or layers, as it can yield important information on site formation, seasonality, and changes in diet or subsistence practices. However, for many Middle Paleolithic sites (~300–40 ka), this has been an imperfect strategy for behavioral interpretation due to the palimpsest (superimposition of overlapping activities or occupations at a site) nature of most of these sites. Recently, a spatiotemporal perspective has been employed to address the palimpsest problem and illuminate the subsistence behavior of Neandertals during the Middle Paleolithic. Researchers have thus relied on new methods involving geoarchaeological and stratigraphic analyses to examine excavation units at relatively high temporal resolution (Bailey 2007, Pérez et al. 2020).

This thesis analyzes the faunal remains of Layer V from Abric del Pastor as a case study to explore the subsistence behavior of Middle Paleolithic Neanderthals in Eastern Iberia with an emphasis on the problem of temporal resolution. Specifically, I aim to answer the following questions using a time perspectivist framework: 1) what species were exploited at Abric del Pastor?; 2) what agents were involved in the deposition of the faunal remains?; 3) what activities (i.e., butchering, burning, etc.) took place at the cave shelter?; 4) Can we identify specific moments in which the cave was being utilized within layer V?

Below, I describe the climatic and environmental conditions of the Iberian Peninsula from MIS 5 through MIS 3. I then present overviews of the faunal assemblages from other MIS 5-3 rock shelter sequences throughout Spain. This is followed by a detailed discussion of the site history of Abric del Pastor. Finally, the time perspectivist framework is presented.



Figure 2.1: Map of MIS 5-3 sites in Spain.

## 2.1 Overview of MIS 5-MIS 3 in the Iberian Peninsula

Marine Isotope stages correspond to alternating periods of warming and cooling of the Earth's paleoclimate. Odd-numbered stages like MIS 5 and 3 correlate with periods of warming while even-numbered stages (i.e., MIS 4) correspond to periods of cooling. The oscillation between cold and warm is often referred to as stadial, meaning cooler, and interstadial, meaning warmer periods (Rabassa and Ponce 2013). However, MIS stages are not homogenous. The warmer periods tend to be shorter (i.e., 10-20ky) while the colder stages are longer (80-90ky). Each MIS stage has its own combination of oscillations between stadial and interstadial events

with each of these events being unique in length and average temperature (Rabassa and Ponce 2013). The more specific compositions of MIS 5-3 are detailed below.

The Iberian Peninsula has a complex terrain and highly variable climate producing a wide range of microclimates (Oliva et al. 2018). These microclimates exist throughout the peninsula as well as within individual mountain systems. Generally, precipitation decreases from North to South and from West to East across the peninsula. Areas that are Atlantic-influenced range from over 2000-2500mm to a minimum of 600-900mm in the Sierra Nevada (Oliva et al. 2019). Conversely, temperature increases from North to South and West to East across the peninsula (Oliva et al. 2019). Below I present the general characteristics of faunal assemblages from a range of Middle Paleolithic rock shelter sites throughout Spain (as well as one example from southeastern France) in order to examine variation in faunal exploitation throughout MIS 5 through 3. These sites include Teixoneres Cave, Abric Romani, Navalmaillo Rock shelter, Cueva Anton, and Bolomor Cave (Figure 2.1).

### **2.1.1. MIS 5**

MIS 5 is dated to between 130 and 80kya. Known as the last interglaciation, this was a period of warming intermixed with cold oscillations separated by ~1-3kya (Sprovieri et al. 2006). It is suggested that this period saw increased precipitation and more humid conditions within the Iberian Peninsula. Additionally, it is thought that the summers were drier, and the winters were wetter indicating increased seasonality. Studies of  $\delta^{18}\text{O}$  and  $\delta^{13}\text{C}$  values suggest that there was high water availability which supported a well-developed Mediterranean

vegetation cover (Pérez-Mejias et al. 2019). Sites with MIS 5 occupations include Bolomor Cave, and Cueva Anton.

Bolomor Cave is located on the Central Mediterranean coast of Spain near Valencia 100m above sea level (asl). It was occupied intermittently during MIS 9-MIS 5e. Specifically, providing MIS 5 evidence is level IV which dates to 121 +/- 18kya. This level was sporadically used by Neanderthals with primary access to ungulates. There is some evidence of carnivore use of the shelter, as indicated by the presence of pits, puncture, and scores on bone specimens. The site has a uniquely broad-spectrum diet including the remains of over 30 very large (e.g., megaceros *Megaloceros giganteus*, narrow-nosed rhinoceros *Stephanorhinus hemitoechus*, and hippopotamus *Hippopotamus amphibius*) to small animals (e.g., rabbit *Oryctolagus cuniculus* and Hermann's tortoise *Testudo hermanni*). The dominant species is red deer (*Cervus elaphus*) but there is also habitual consumption of small prey such as birds and leporids. The assemblage is dominated by cranial remains for ungulates and limb elements for small prey. Percussion pits, marks, and notches, as well as cut marks, are noted on large- and medium-sized mammals. Cut marks are present on 7.2% of all identified species, pointing to defleshing and disarticulation activity. Additionally, 61.5% of the faunal assemblage is burnt (Blasco and Fernandez Peris 2012a; Blasco and Fernandez Peris 2012b; Sañudo, Blasco, and Fernandez Peris 2016).

Cueva Anton is a limestone rock shelter in southeastern Spain found 359m above sea level (asl). The site has layers dating to the end of MIS 5 through late MIS 3. The assemblage is comprised of large, medium, and small taxa including horse, ibex, rabbit, large birds, and tortoise. However, raptor activity is likely to be the main source of the rabbit accumulation (Zilhão et al. 2016). Remains of red deer and steppe rhino are present but scarce. There is also a limited number of carnivore remains. Medium size mammals are well represented. Like Bolomor

Cave, Cueva Anton is dominated by cranial remains. Gnawing evidence is present but anecdotal. Anthropogenic evidence on the faunal remains includes percussion marks, cut marks, and burnt remains. Percussion scars are present in 20% of the assemblage (Sanz et al. 2019). Most of the burnt remains are only partially burnt with few carbonized remains. The anthropogenic evidence points to defleshing, skinning, evisceration, disarticulation, and marrow extraction. It is believed that the site was used for on-site processing of complete carcasses as well as introduction of portions from different parts of a carcass. The overall stratigraphic sequence at Cueva Anton shows no significant change suggesting that the subsistence strategy, mobility, and site function remains consistent from MIS 5 through MIS 3 (Angelucci et al. 2013; Sanz et al. 2019, Zilhão et al. 2016).

### **2.1.2 MIS 4**

MIS 4 (71 to 59kya) was a period that saw the expansion of high-latitude global ice sheets and a decrease in precipitation (Pérez-Mejias et al. 2019). Specifically, there is a lack of evidence that paleo-glaciers retreated in Northern Iberia (Burjachs and Allue 2003). Sea surface temperatures as well as the relative sea level decreased as well (Pérez-Mejias et al. 2019).

Although relatively cool and humid, this stage was interspersed with small warm and cold peaks throughout (Hodgkins et al. 2016; Pérez-Mejias et al. 2019; Suarez-Bilbao et al. 2021). This period saw a gradual development of semi-desert vegetation and the expansion of grasslands across Iberia as well (Burjachs and Allue 2003; Fletcher et al. 2010; Mallol et al. 2019).

Navalmaillo is an example of a site with late MIS 5 and MIS 4 evidence. The site is a rock shelter located 55km north of Madrid (Moclan et al. 2021). The shelter sequence shows the

presence of over 20 different species including very large (i.e., steppe rhino), large (i.e., red deer), medium (i.e., roe deer), and small size (i.e., rabbit and tortoise) taxa. Carnivores like panther, wolf, lynx, and fox are also present. The most common taxa are large and medium-sized mammals. Cranial remains are most common followed by appendicular bones. Axial remains are poorly represented. In the level F assemblage, 6.0% have cut marks and 1.2% show percussion marks. There is also clear evidence of intentional fracturing of long bones for marrow as documented on the specimens of very large-, large-, and medium-sized species. Neanderthals appear to have had primary access to large bovids and cervids which were transported back to Navalmaillo and intensively processed as every phase of butchering is represented in the assemblage (Moclan et al. 2021).

### **2.1.3 MIS 3**

MIS 3 occurred from about 60-30kya and is characterized by recurrent fast and extreme changes from cold to milder climatic conditions, followed by a slow return to colder conditions (Kjellstrom et al. 2010). Specifically, there was a colder phase from 50-47kya and until about 42kya, during which glaciers continued to advance in Central Spain. From 42kya to about 33kya, glaciers retreated in Central Spain (Ballesteros et al. 2020). The average estimated winter temperatures were between -4 to 0 degrees Celsius and 12-18 degrees Celsius in the summer (Hodgkins et al. 2016). Conifers dominated the landscape (Burjachs and Allue 2003). Sites that have evidence of MIS 3 occupation include Abric Romani, and Teixoneres Cave.

Abric Romani is a travertine rock shelter located in northeastern Iberia near Barcelona 280m asl. Level M and O are dated to MIS 3. The site has thin archaeological levels that are



separated by thick sterile layers. M and O contain very small, small, medium, large, and very large-sized mammals (i.e., *S. hemitoechus* (steppe rhino), *Cervus elaphus* (red deer), *Rupicapra rupicapra* (roe deer), *Felis sylvestris* (wild cat), and *O. cuniculus* (rabbit)). The surfaces of the faunal specimens have evidence of both plant and water modifications. While Level M is dominated by cranial and limb bones, Level O has more forelimbs. There is also evidence of anthropic activity including cut marks, intentional bone breakage, and burning. Cut marks and percussion cones are mostly found on large and medium-sized animals. Incision marks are associated with defleshing, skinning, and viscera removal. In level O, about 5% of the remains have cut marks. Burnt remains indicate exposure to low to moderate temperatures. Level M includes 61.3% burnt remains while level O has 43.0% burnt remains. The shelter was used as a recurrent camp site where carcasses were delivered and consumed (Gabucio et al. 2016; Gabucio, Fernandez-Laso, and Rosell 2017).

Teixoneres Cave is a limestone rock shelter located in northeastern Iberia near Barcelona around 900m asl (Lopez-Garcia et al. 2012). It was formed by recurrent roof collapses. Although the site has layers dating from MIS 5c to MIS 2, level III and II specifically date to MIS 3 (51,000 to 44,210 and 42,210 to 33,060 cal BP respectively). Environmental data suggests that level III had a warm climate with high humidity. The faunal assemblage comprises very large, large, medium, and small-sized taxa (i.e., *Mammuthus primigenius* [mammoth], *Cervus elaphus* [red deer], *Capra pyrenaica* [Iberian Ibex], *Vulpes vulpes* [fox], leporids [rabbits], and tortoises [*Testudo* sp.]). Carnivore remains were identified including cave bear (*Ursus spelaeus*), wolf (*Canis lupus*), lynx (*Lynx* sp.), and badger (*Meles meles*). There is also anthropic evidence in the form of burnt bones, cut marks, percussion notches, impact flakes, intentional bone breakage, lithic tools, and hearths (Álvarez-Lao et al. 2017). Remains of large, medium, and small sized

mammals show burning and cut marks indicative of skinning, defleshing, and disarticulation. Carnivore accumulations were documented in the inner areas of the shelter while the Neanderthal accumulations are closer to the main entrance. The shelter was used for short term occupation (Rosell et al. 2010; Rufà et al. 2014; Álvarez-Lao et al. 2017).

Overall, faunal assemblages from the Iberian Peninsula during MIS 3 are mainly constituted by species of temperate environmental preferences (i.e., red deer) as well as typically interglacial taxa (steppe rhino and fallow deer). There is some evidence of cold adapted large mammals (i.e., woolly mammoths, woolly rhinoceros, reindeer, arctic fox, etc.) in southern Iberia but these occurrences are infrequent (Álvarez-Lao et al. 2009; Álvarez-Lao and Garcia 2010; Álvarez-Lao and Garcia 2011; Álvarez-Lao et al. 2017).

Faunal assemblages from rock shelters dated to MIS 5-3 within Spain spanning these periods are relatively consistent in showing generalist broad spectrum hunting. This includes the procurement of large and medium sized ungulates like deer, horse, and wild goat, as well as the use of small sized fauna like tortoise and rabbits. Additionally, the rock shelters all seem to have been used as recurrent short term occupation sites where consumption of animals occurred.



Figure 2.2: Map of Spain showing Abric del Pastor with photos of the site. The top right photo is an aerial view of the cave shelter. The bottom right photo shows the opening of the rock shelter and the excavation area.

## 2.2 Abric del Pastor

Abric del Pastor is a rock shelter located 820m above sea level on a northern facing slope on the right side of the Barranc del Cinc ravine in the Mariola mountains of Alcoy, Alicante, in the southeastern Spain (Figure 2.2). This small rock shelter (60m<sup>2</sup>) is an eroded karstic tube made of limestone cobble conglomerate (Machado et al. 2013; Connolly et al. 2019). The current climatic conditions are sub-humid meso-Mediterranean with an average yearly temperature between 13 and 17 degrees Celsius and an average of 600-1000mm of precipitation annually (Vidal-Matutano et al. 2015).

The first excavations at Pastor were led by Mario Brotons in 1953 (Machado et al. 2013). Brotons concentrated his efforts in what is now the central area of the excavation surface where

he recovered a significant number of faunal and lithic artifacts. Due to poor record keeping, these artifacts are lacking any reliable contextual information. Brotons' work affected a small area of the modern excavation area (uppermost layers of SU I, II, and III). Therefore, most of the site was left intact (Vidal-Matutano et al. 2015; Connolly et al. 2019). Although Brotons claimed to have recovered Middle Paleolithic artifacts, we now know that he was digging a bioturbated deposit. The soil had been churned up by shepherds mixing the Middle Paleolithic and Holocene deposits.

Since 2005, excavations have been directed by the Universidad de la Laguna, Tenerife (Connolly et al. 2019). These meticulous excavations, still ongoing, have yielded features such as hearths, as well as lithics, fauna, and charcoal (Vidal-Matutano et al. 2015). Current excavations cover 42 m<sup>2</sup> (70%) of the available surface. These excavations have shown that the site was formed by a series of brief Middle Paleolithic occupation events centered around single hearths. The deposit has been separated into six stratigraphical-units ("SU," numbered I–VI; Figure 2.3) that date to early MIS 3 and cover most of MIS 4 (43-72 ka). The stratigraphic units were distinguished based on macroscopic and micromorphological sedimentological properties (Machado et al. 2013; Vidal-Matutano et al. 2015).

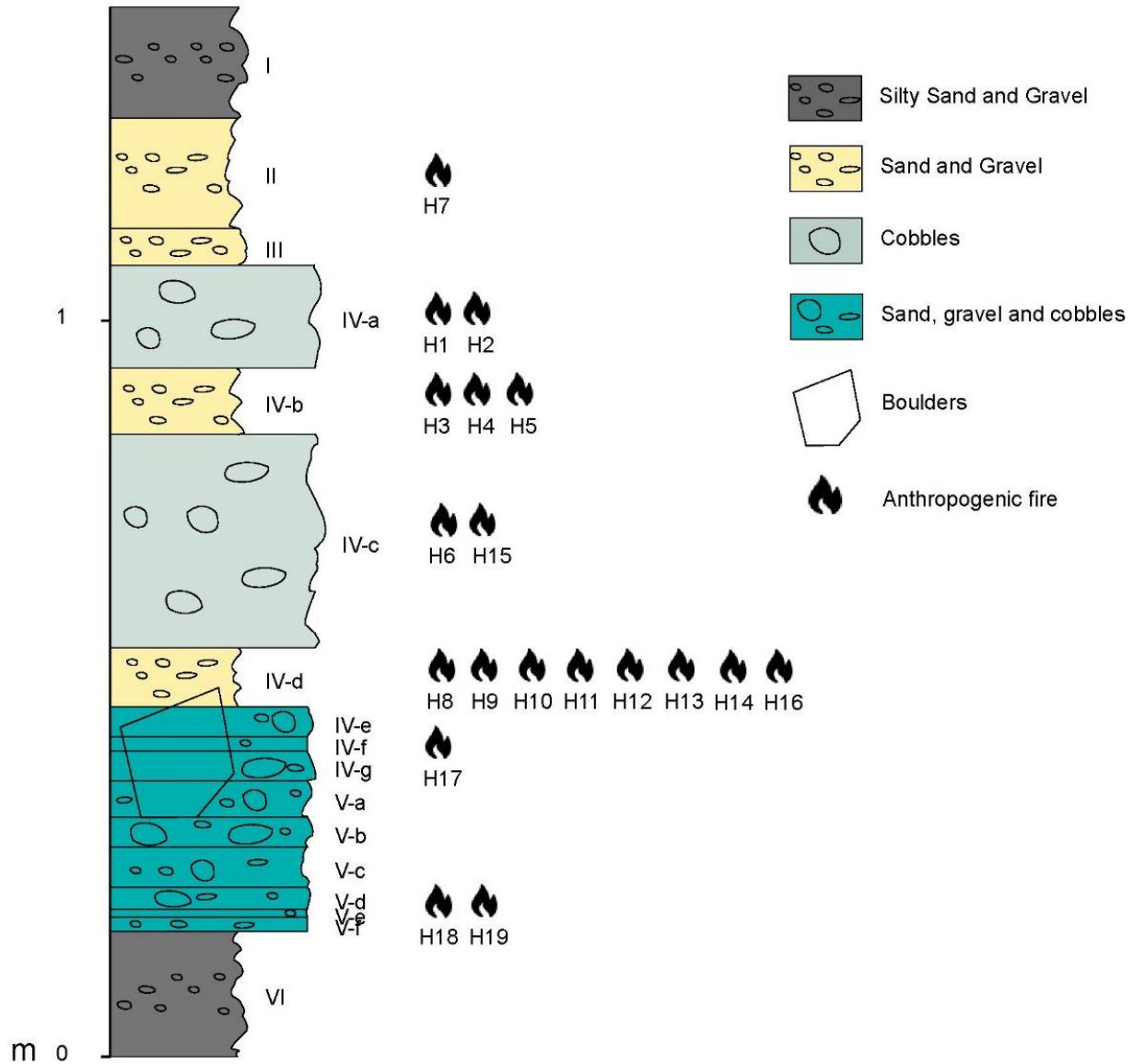


Figure 2.3: Stratigraphic diagram noting the type of sediment, the sublayers, as well as the presence of hearths.

Layer I is a Holocene deposit affected by the activities of shepherds. Layers II, IV, V, and VI have yielded Middle Paleolithic archaeological remains in a calcitic matrix (Mallol et al. 2019). Layer III is archaeologically sterile. Layer IV is about 70cm thick and ranges in texture

from fine sand to cobbles. A total of 17 possible combustion features were identified. Sublayers IVa and IVc are very loose, clast-supported layers that have few archaeological remains.

Sublayers IVb and IVd, on the other hand, are fine grained in texture and comprise the bulk of the archaeological remains. ESR/U-series provided a date of 48kya  $\pm$  5 for sublayer IVb while sublayer IVd was dated to 63kya  $\pm$  5 using OSL (Mallol et al. 2019).

Sublayer IVa contains a total of 114 faunal remains composed of Bovidae, Corvidae, Equidae, and Testudinidae. Among the few remains that could be identified, Testudinidae is the most common taxon. The faunal remains from this sublayer were spatially correlated to hearths H1 and H2 and may be result of one or two occupation events. The underlying unit, IVb, has 159 faunal remains composed of Bovidae, Canidae, Caprinae, Cervidae, Corvidae, Equidae, Leporidae, Rhinocerotidae, Suidae, and Testudinidae. Like IVa, indeterminate remains comprise the largest portion of the IVb assemblage, followed by Bovidae. Some of the faunal remains are burnt. The IVb remains were linked to hearths H3, H4, and H5. It is thought that IVb comprises between two and three occupation events. The faunal assemblage from IVc is also structured around a hearth. It contains 362 faunal remains including Bovidae, Cervidae, Equidae, Leporidae, and Testudinidae. Once again, indeterminate remains make up the majority of the assemblage. IVc also has a notably large number of tortoise remains (N=108, 29.8% of the assemblage). It has been interpreted as consisting of a single occupation event dedicated to animal processing and consumption (Machado et al. 2013; Machado et al. 2019). Throughout IVa, IVb, and IVc, a sector located along the length of the back wall—extending about 1m towards the front of the shelter—is devoid of faunal remains (Machado et al. 2013).

Layer IVd was composed of *Bos primigenius*, canids, *Capra pyrenaica*, *Cervus elaphus*, corvids, rabbits, and tortoises (Machado et al. 2019). Testudines is the most frequently identified

taxon (Connolly et al. 2019). The assemblage is dominated by cranial fragments, mainly bovine and goat teeth. Additionally, there are frequent long bone fragments of red deer as well as numerous tortoise carapace fragments (Mallol et al. 2019). The material is heavily fragmented. Post-depositional damage includes concretions, manganese, root-marks, corrosion, weathering, and gnaw marks. Anthropogenic marks were identified on 5.4% of the faunal remains with incisions being the most prevalent. Percussion notches and scrape marks were also identified. The marks suggest on-site butchering activities including disarticulation, defleshing, and periosteum removal. Burnt remains comprise 14.7% of the assemblage. Tortoise bones are the most commonly burnt remains. Most of the burnt remains indicate exposure to low fire temperatures but some are more severely burnt (Connolly et al. 2019). This occupation also contains evidence of in-situ burning (Mallol et al. 2019).

Further down the sequence, Layer IVf contained a well preserved, in situ, simple, open hearth. The ash layer of the earth was comprised of juniper wood and contained molecular traces of herbivore fat. Two species were identified in sublayer IVf, *Capra pyrenaica* and *Cervus elaphus* (Sossa-Ríos et al. 2022). Medium-sized mammals represent over 70% of the assemblage. Appendicular remains are prevalent. Anthropogenic modifications, including cut marks (6.3% of the assemblage) and burnt remains (24% of the assemblage), were noted in this layer. Burning on the specimens varies from mild to near calcination. The overall assemblage is highly fragmented and shows a high degree of post-depositional damage including manganese, corrosion, weathering, and root marks (Sossa-Ríos et al. 2022).

Overall, the stratigraphic units above layer V include remains of Bovidae, Canidae, Caprinae, Cervidae, Corvidae, Equidae, Pantherinae, Leporidae, Rhinocerotidae, Suidae, and Testudinidae, as well as anthropic activity. Anthropogenic marks include burnt remains and cut marks

that suggest that animal processing and consumption occurred within the rock shelter (Machado et al. 2013; Machado et al. 2019; Pérez et al. 2020; Sossa et al. 2022).

Layer V was first reached in 2005 in a test pit in the center back along the cave wall. The rest of the layer was excavated starting in 2017. The bottom of V<sub>f</sub> was reached across the entire excavation surface by the end of the 2022 season. Dates taken from stratigraphic layers above and below layer V (IV<sub>b</sub>: 48kya +/- 5kya; IV<sub>d</sub>: 63kya +/- 5kya; VI: 62+/- 12kya) place this sequence securely within MIS 4. The layer yielded lithic and faunal artifacts, as well as remnants of hearths. Layer V is the focus of this thesis and a more detailed description of the excavation and faunal remains from this layer are provided in the subsequent chapters.

### **2.3 Time Perspectivism**

The notion of time perspectivism was originally discussed in the 1980s by Binford (1981), Bailey (1981), and Foley (1981). The concept was born out of the shift in archaeology from focusing on chronological reconstruction to the analysis of behavioral practices (Schiffer 1976). Bailey, Binford, and Foley all emphasized how archaeological deposits represent remains of repeated events providing the opportunity to study processes beyond the time span of single events. These multiple events, resulting from many generations of individuals, represent the remnants of past behavioral systems. It is thus the task of the archaeologist to define this behavioral system (Bailey 1981; Binford 1981; Foley 1981; Holdaway and Wandsnider 2008).

Eventually, Bailey (1983, 1987, 2005, 2007, 2008) promoted the concept of time perspectivism. He defines this framework as one that considers: “that different timescales bring into focus different sorts of processes, requiring different concepts and different sorts of explanatory



variables” (Bailey 1987:7). Moreover, time perspectivism calls for the exploration of different time scales and the interactions between them as different phenomena are better studied at varying temporal resolutions. Bailey asserts that time perspectivism relies on a better understanding of the palimpsest. A palimpsest is a superimposition of material traces of overlapping layers of activity over varying time scales. Key to palimpsest is the variable degree of erasure and preservation of previous activities by the subsequent activities, the most extreme case being the obliteration of the previous activities. It is the very nature of the palimpsest that allows for the opportunity to examine behavior at different scales (Bailey 2007). Researchers have thus relied on new methods involving archaeostratigraphic, micromorphological, and geoarchaeological analyses to examine excavation units at a relatively high temporal resolution (Harding 2005; Machado and Pérez 2016; Pérez et al. 2020).

It is important not to overstate the ability of the archaeologist to identify single events of anthropogenic activity. Like all divisions of archaeological strata, there is still an arbitrary nature to the separation of single occupations. The successive nature of the palimpsest can cause prior occupations to be disturbed and altered by later occupations. Moreover, looking at too short of a time frame may affect the ability to make any generalizations or conclusions about the usage of the site. Therefore, it is important to examine both longer and shorter time scales in order to identify the nature of a site through time.

The palimpsest nature of many Middle Paleolithic sites (~300–40 ka) makes these sites adequate case studies to implement a time perspectivist framework. Specifically applying this framework to the study of faunal assemblages has allowed researchers to infer temporal indicators of seasonal human occupations and led to the identification of specific activities, such as changes in diet and animal management, among others. Because of this, a spatiotemporal perspective has more often

been employed to address the palimpsest problem, understand site formation, and illuminate the subsistence behavior of Neandertals during the Middle Paleolithic (Machado et al. 2013; Machado and Pérez 2016; Pérez et al. 2020; Real et al. 2018; Sanz et. al 2015; Sossa-Ríos et al. 2022). This project takes a spatiotemporal approach by drawing upon aspects of the time perspectivism framework using Abric del Pastor as a case study. Abric del Pastor provides a prime opportunity to explore subsistence behavior on varying timescales. First, the identification of hearths within the site provides crucial temporal markers in the palimpsest dissection. The direct association between faunal remains and the identification of hearths allows for identification of shorter time scales. Additionally, the detailed nature of the archaeological excavation (elaborated on in the methods section), with its focus on geoarchaeological analysis, allows for the precise division of layers. Finally, the fact that 70% of the surface area of the site has been excavated allows for a relatively comprehensive view of the rock shelter. The next chapter details the methods performed in excavating, examining, and analyzing the layer V faunal remains.

### Chapter 3: Materials and Methods

This thesis uses well-established, robust zooarchaeological and taphonomic methods in order to derive information on two time scales: i) a longer time frame focused on large scale human occupation and use and ii) another, shorter time span as an attempt to distinguish possible single anthropogenic events (Pérez et al. 2020). In application, the longer time span looks at two occupation events at Abric del Pastor: Occupation A and Occupation B (described below) while the shorter time span is based on sub-divisions (sublayers) of Occupation B. Below, I outline how the material was obtained, recorded, and analyzed. For the purposes of project consistency and continuity as well as ease of comparison to other faunal assemblages from the Iberian Peninsula, Spanish terms have been used throughout this thesis when referring to coding and features of the site.

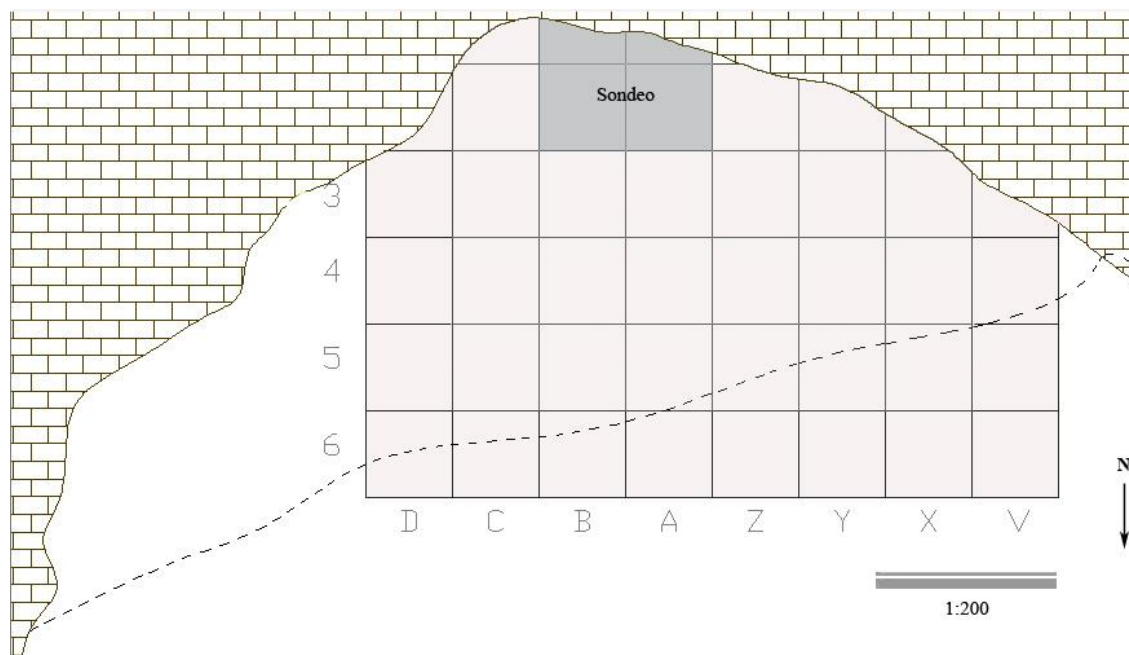


Figure 3.1: Excavation map of Abric del Pastor. Along the X axis the squares occur in alphabetical order from D-V while the Y axis follows a numerical order from 1-6. The dotted line represents the drip line.

## 3.1 Faunal Samples

### 3.1.1 Obtaining the Material

The faunal remains from layer V were obtained over a series of excavation seasons starting in 2006. In 2006, layer V was only reached within the “Sondeo” or trench (Figure 3.1). The majority of the remains come from the 2018, 2019, 2021, and 2022 excavations seasons. A few additional specimens derive from the 2017 season. The bottom of Vf (the deepest sublayer of layer V) was reached across the shelter excavation surface by the end of the 2022 season.

The site is excavated on an X-Y grid. The X axis is labeled from left to right: D, C, B, A, Z, Y, X, V. The Y axis is labeled numerically 1 through 6 from south to north (Figure 3.1). All artifacts, including faunal remains, that are spotted while excavating are left in situ. Before being removed from the surface, the X, Y, and Z coordinates are recorded using a total station. All sediment that is removed during the excavation process is sieved. The material caught in the sieve is examined for any lithics or faunal material while the rest of the material (i.e., limestone cobbles and gravels) is discarded. The sediment that was collected below the sieve in the bucket is placed into a plastic bag and saved for further analysis. All sediment is floated and sorted in heavy and light fraction.

I analyzed and recorded faunal remains located in situ and in the sieve. Generally, faunal fragments discovered in the heavy fraction are set aside for a micromammal specialist. However, because fragments from one bag were unusually large, they were set aside to be included in my analysis. This bag had 110 fragments from sublayer Va. This bag doubled the number of indeterminate fragments from sublayer Va, while representing 18% of the indeterminate

fragments from the whole assemblage. This unlikely created a slight bias as not all sediment bags have been floated and sorted in heavy fraction.

### 3.1.2 Division of Time scales

To apply a time perspectivist framework, the faunal remains from layer V are analyzed on varying time scales. Those time scales include the longer scale (occupation events A and B) as well as a shorter scale (by sublayer of Occupation B). Occupation events were identified using a three-dimensional scatterplot in Past 4.03. From the scatterplot, two occupation events were identified based on a clear horizontal separation between two distinct groups of faunal remains. Each accumulation was then analyzed for taxonomic composition, taphonomic characteristics, and traces of anthropogenic activity. Those patterns were then analyzed on the micro scale for Occupation B where multiple sublayers were identified using macro and micromorphological sedimentological characteristics. Because occupation A contains a single sublayer (Vd), trends could not be evaluated in this case.

The focus on piece-plotted remains has some drawbacks because the remains collected in the sieve could not be included in this thesis. Not including this material can create a bias toward larger specimens as it is easier to miss smaller fragments while excavating. Additionally, this reduced the sample size by almost 50% as there are only 640 remains with associated coordinate data while there are over 1,300 fragments—not including remains those recovered in the heavy fraction—within layer V as a whole.

## 3.2 Database

Each fragment was examined and recorded in a FileMaker database. The database has multiple layouts. The primary layout is the principal layout (Figure 3.2). From the principal

layout, one can navigate to the other databases. These databases include one for teeth, osteometry, and marks.

The screenshot displays the main data entry form for specimen 1025 in the Abric del Pastor database. The interface is organized into several functional areas:

- Navigation and Overview (Top):** Includes a search bar with '1025', a 'Records' indicator showing '1025 Total (Unsorted)', and buttons for 'Show All', 'New Record', 'Delete Record', 'Find', and 'Sort'. Below this is a 'Layout: ZARPITAS' dropdown and 'View As' options.
- Provenience Information (Left, White):** Contains fields for 'Nº REGISTRO' (1025) and 'Nº INVENTARIO', 'YACIMIENTO' (Abric del Pastor), 'UE', 'FECHA', 'CAPA/FACIES', 'LEVANTAMIENTO', 'CUADRO', 'SUBCUADRO', and coordinates 'X', 'Y', 'Z'. It also includes 'ORIENTACION' and 'PENDIENTE'.
- Taxonomía (Teal):** A section for taxonomic classification with fields for 'ORDEN', 'FAMILIA', 'SUBFAM.', 'GENERO', 'ESPECIE', and 'INDETER.'.
- Anatomía (Light Green):** A section for anatomical data with fields for 'HUESO', 'GRUPO', 'GRCA', 'DIENTES', 'FRAGMENTO', 'LONGITUD', 'ZONA', 'LATERALIDAD', 'CIRCUNFER.', 'CARA', and 'LAT. A/B'.
- Tafonomía (Red):** A section for tafonomía (fractures and alterations) with sub-sections:
  - FRACTURAS:** 'ORIGEN' and 'MORFOTIPO'.
  - ALTERACIONES:** 'CORROSION', 'RASPADO', 'INCISION', 'TAJO', 'HORADACION', 'HUNDIMIENTO', 'PUNCIÓN', and 'ARRASTRE'.
  - ALTERACIONES DIAGENÉTICAS:** 'METEORIZACION', 'EROSION', 'CONCRECION', 'CORROSION', and 'MANGANESO'.
  - ALTERACIONES TERMOALTERACIONES:** 'COLOR 1', 'COLOR 2', 'PARTE 1', 'PARTE 2', 'LOC. 1', and 'LOC. 2'.
- Medidas (Dark Grey):** A section for measurements with fields for 'LONGITUD', 'ESPESOR', 'ANCHURA', and 'INTERVALO'. It includes buttons for 'BD DIENTES' and 'BD OSTEOMETRICA'.
- Alteraciones Diagenéticas (Light Beige):** A section for diagenetic alterations with fields for 'SUP. OBSERVABLE', 'PISOTEO', 'PRESION', 'ROEDORES', and 'RAICES'.
- Notas (Light Beige):** A section for notes with fields for 'SEPARADO', 'RESTAURACION', 'REVISION', 'FOTO', and 'REMONTAJE'.
- Observaciones (Light Beige):** A section for observations with a 'MODIFICACIONES' field.

Figure 3.2: The principal layout for the Abric del Pastor database.

Each database (principal, teeth, marks, and osteometry) has the white section on the far left-hand side (Figure 3.3). This white section includes all the provenience information. Each fragment entry corresponds to a new register number. A separate inventory number is also assigned to each specimen. The inventory number is either a whole number (i.e., 1, 2, 3, 4, etc.) that corresponds to the number assigned to the data point taken with the total station, or “Criba-#” if the specimen was recovered in the sieve.

Nº REGISTRO	Nº INVENTARIO	
1124	47	
		
		X <input type="text" value="5"/>
YACIMIENTO		
<input type="text" value="Abric del Pastor"/>		
UE		
<input type="text" value="V7"/>		
FECHA		
<input type="text" value="2022"/>		
CAPA/FACIES	LEVANTAMIENTO	
<input type="text" value="Gr"/>	<input type="text"/>	
CUADRO	SUBCUADRO	
<input type="text" value="D3"/>	<input type="text" value="4"/>	
X <input type="text"/>		
Y <input type="text"/>		
Z <input type="text"/>		
ORIENTACIÓN	PENDIENTE	
<input type="text" value="0"/>	<input type="text" value="0"/>	

Figure 3.3: Example of how the information about provenience is recorded in the database.

### 3.3 Taxonomic Classification

Recording of all fragments occurred in the field at the dig house in Alcoy, Alicante. There was limited access to a comparative collection. Identification relied mostly on photographs and other identification guides (Barone 1976; Hillson 1996, 2005; Pritchard et al. 2009; Schmid 1972; Sobolik and Steele 1996). Assistance was also provided by Dr. Leopold Pérez.

The image shows a teal-colored form titled "TAXONOMÍA". It contains six rows of input fields for taxonomic classification. Each row has a label on the left and a white input box on the right. To the left of the input boxes for "SUBFAM.", "GÉNERO", and "INDETER." are small white buttons with the text "GO" in black. The labels are: "ORDEN", "FAMILIA", "SUBFAM.", "GÉNERO", "ESPECIE", and "INDETER.".

Figure 3.4: The section of the database where taxonomic information is recorded.

The taxonomic information is recorded in the blue box labeled “Taxonomia” (Figure 3.4). If the taxa of the specimen could not be determined to taxon, the specimen was either attributed to size class (large, large/medium, medium, medium/small, small, very small) or left indeterminate.

During the initial sorting, fragments were first separated between mammal, bird, and micromammal specimens. Except for one bird remain that was identified as *Pyrrhocorax* sp., the bird and micromammal fragments were only identified to this taxonomic level (Aves or micromammal) as these will be examined by other specialists. The bird and micromammal fragments were not recorded in the database. They were recorded in a separate excel sheet noting the unit provenience, whether it was from a bird or micromammal, the element (i.e., long bone, fragment, mandible, etc.), and whether it was found in situ or in the sieve. Additionally, any notable taphonomic attributes were noted in the comments section. If the bird or micromammal remain had any anthropic marks, it was included in the main database instead of the separate excel sheet.



All the mammal fragments were examined and classified as specifically as possible, preferably to the genus and species level. However, some could only be determined to body size categories: very small, small, medium and large (Table 3.1). Some fragments were recorded as medium/large or small/medium categories.

Size Class	Weight (Kilos)	Thickness of the cortical bone	Taxa Examples
Large	100-300kg	5-8mm	<i>Cervus elaphus</i> <i>Sus scrofa</i>
Medium	10-100kg	2-5mm	<i>Capra pyrenaica</i> <i>Rupicapra</i> sp. <i>Canis lupus</i> <i>Cuon</i> sp. <i>Panthera pardus</i> <i>Lynx</i> sp.
Small	5-10kg	1-2mm	<i>Oryctolagus cuniculus</i> <i>Testudo hermanni</i> Avifauna
Very Small	<5kg	<2mm	Avifauna Micromammals

Table 3.1: Body size class classification.

### 3.4 Anatomic Group Classification

In the section labeled “Anatomia”, the anatomical data was recorded for each specimen (Figure 3.5). In this section, the bone, the anatomic group, and the skeletal portion of the remain was recorded. If the fragment is a tooth, the specific tooth (i.e., dp4, lower 3<sup>rd</sup> molar, etc.) was identified in the bone (“Hueso”) box. The portion of the fragment was recorded in the “fragmento” box. Additionally in this section, the longitude (“longitud”), circumference (“circunfer.”), zone (“Zona”), “cara” (face) and side (“lateralidad and “Lat. A/B”) were recorded.

ANATOMÍA

HUESO  GRUPO  GRCA

DIENTES  FRAGMENTO

LONGITUD  ZONA  LATERALIDAD

CIRCUNFER.  CARA  LAT. A/B

Figure 3.4: The section in which the anatomical data for each specimen is recorded.

### 3.4.1 Anatomic Group

The element and anatomic group for each specimen was recorded using the codes listed in Appendix 1. Fragments were categorized as either flat bone, cancellous or spongy bone, long bone, or splinter. Long bone fragments were coded according to the size class of the specimen. For instance, “Lt1” corresponds to a long bone fragment of a medium-sized animal. When the size of the taxa could not be assessed, it was coded as Lt (Table 3.2).

Anatomic Group	Bone	Abbreviation
<b>Indeterminate Element Fragments</b>	Long Bone Indeterminate	Lt
	Long bone-Medium	Lt1
	Long bone-Large	Lt2
	Long bone-Small	Lt3
	Flat	Pl
	Spongy	E
	Splinter	Esq

Table 3.2: Indeterminate anatomic group bones and the abbreviations that are used in the database.

### 3.4.2 Tooth Database

When a tooth is identified, more detailed information and measurements were recorded for dental remains (Figure 3.6). The register number (seen in the top left corner of Figure 3.6) connects the principal database information with the tooth database. The database includes information about the specific tooth present, its localization (superior or inferior), side (left or right), and measurements. For all taxa besides equids, the measurements are recorded in boxes M1-M13. The measurements correspond to the standard measurements used for teeth (Rivals [2004] for cervids/caprines, Testu [2006] for carnivores, Lacomat [2006] for rhinoceros and Castaños [1988] for equids). For equids, the measurements are recorded in the far-right section labeled “Équidos”. Diagrams of the standard measurements can be referenced under the tabs labeled “cerv/capr,” “Equidae,” “rhino,” and “carnivora” tabs.

The screenshot displays a web-based form for recording tooth data. It is organized into several vertical panels:

- Registration Information:** Located at the top left, it includes fields for 'Nº REGISTRO' (997) and 'Nº REG. DIENTES' (22). Below these are icons for adding, editing, and deleting records, along with a search field.
- Location and Date:** A green sidebar on the left contains fields for 'YACIMIENTO' (Abric del Pastor), 'UE' (VI), and 'FECHA' (2022).
- Taxonomic Information:** A central panel titled 'TAXONOMÍA/ANATOMÍA' contains dropdown menus for 'ORDEN' (Artiodactyla) and 'GÉNERO' (Capra), and input fields for 'HUESO' (P/2) and 'FRAGMENTO'.
- Species Selection:** A panel titled 'DIVERSAS ESPECIES' features a 'BD PRINCIPAL' button and four tabs: 'CERV/CAPR', 'EQUIDAE', 'RHINO', and 'CARNIVORA'.
- Measurements:** A central panel lists measurements M1 through M13, each with a corresponding input field.
- Equid Measurements:** A panel titled 'ÉQUIDOS' is divided into 'MOLARIFORME SUPERIOR' and 'MOLARIFORME INFERIOR'. It lists specific measurements such as 'L DIENTE', 'M1 L DIENTE', 'A DIENTE', 'M2 A DIENTE SC', 'M3 L MESOSTILO', 'M4 L PARASTILO', 'M5 L PROTOCONO', 'M6 L MITAD ANT PROTOCONO', 'M7 L MITAD POST PROTOCONO', 'M8 A ISTME', 'M9 A POST PROTOCON', 'M10 DIST HIPOCONO POST PROTOCONO', 'M11 L PLEGIO CAVALLINO', 'M12 L FOSA LUNATA ANT', 'M13 L FOSA LUNATA POST', and 'M14 A EMBOCADURA ENTRANT ANT'. The inferior section includes 'L DIENTE PUNT P', 'A DIENTE PUNT P', 'L PROTOCON PUNT P', and 'H DIVERGENCIA-MESOSTILO'.
- Wear and Divergence:** At the bottom right, there are input fields for 'CABRA: FASES DESGASTE', 'CIERVO: FASES DESGASTE', and 'FASES DESGASTE'. Below these are 'INDICE PROT A', 'INDICE PROT A EN P', 'INDICE PROTOCON B', 'INDICE PROTOCON C', and 'INDICE PROTOCON D'. At the very bottom, there are 'DESGASTE M SUP' and 'DESGASTE M INF' fields, each with a 'GO' button.

Figure 3.6: Tooth database layout.

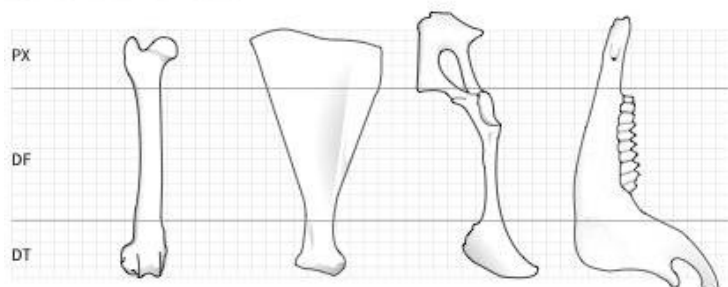
### 3.4.3 Portion

The portion is recorded using a series of three numbers (1, 5, or 0) with the position of the number correlating to the proximal, diaphysis, and distal end, respectively, of the specimen (Figure 3.7). A “1” is noted when that portion of the element is complete, a “5” when it is fragmented, and “0” when absent. For instance, if the specimen is a shaft fragment of a long bone, it would be recorded as “050.” In place of a numerical designation, “X” is used to denote an unfused epiphysis (i.e., “X11” or “11X”).

## FRAGMENTO DE HUESO

PX + DF + DT  
 (parte proximal) (parte diáfisis) (parte distal)

### DEFINICIÓN DE CADA PARTE



### CANTIDAD QUE QUEDA DE CADA PARTE

- 1 completa
- 5 fragmentada
- 0 ausente

### EJEMPLOS DESTACADOS

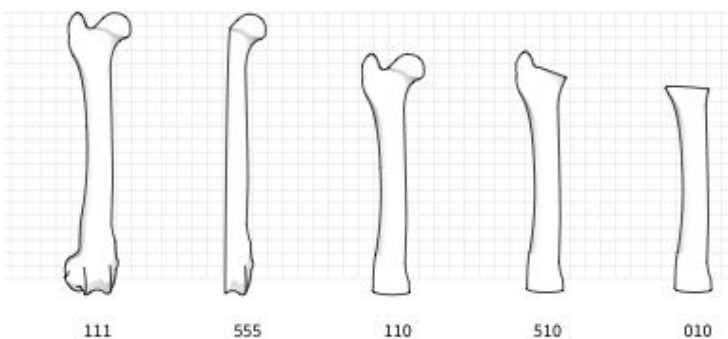


Figure 3.7: The diagrams showing how the portion of the fragment is identified and recorded.

### 3.4.4 Length and Circumference

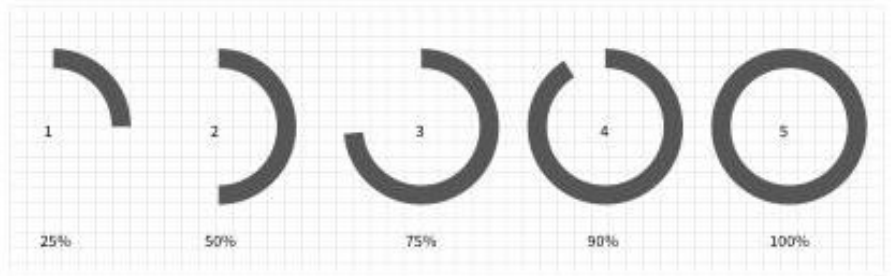
The length of the diaphysis that is preserved in each specimen is recorded in the “longitud” box (Figure 3.5) on a scale from 1-5. The circumference (recorded in the “circunfer.” box) of the diaphysis is also recorded on a scale from 1-5. The scale correlates to the percent of

the diaphysis circumference preserved: “1” is 0-25%, “2” is 25-50%, “3” is 50-75%, “4” is 90%, and “5” is 100% (Figure 3.8).

**CARACTERÍSTICAS DE LA DIÁFISIS**

circunferencia + longitud + zona cara

**CIRCUNFERENCIA DE LA DIÁFISIS**



**ZONA Y CARA DE LA DIÁFISIS**

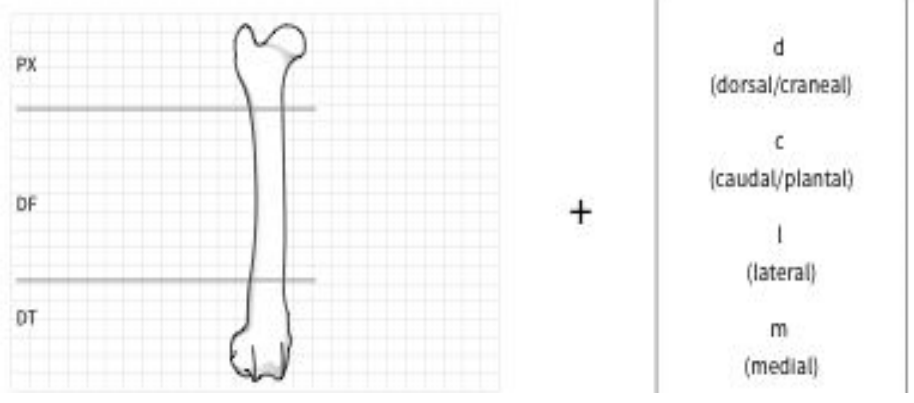


Figure 3.8: Diagrams describing how circumference and bone region are recorded.

### 3.4.5 Zone and Bone Region

The zone box indicates whether the fragment is the proximal, diaphysis, or distal portion of the specimen. This section also contains the box labeled “cara” or bone region. This box provides more detail as to what portion of the bone is present using a series of numbers and letters. The number is either “1”, “2”, or “3” which corresponds to the proximal, diaphysis, or distal end of the bone respectively. Then, any combination of the following letters, (d) dorsal, (c) caudal, (m) medial, (l) lateral, is added to describe the specimen more precisely (Figure 3.8).

### 3.4.6 Side

“Lateralidad” records the side for paired elements (i.e., right, or left). If the side cannot be determined the box was left blank. Lat. A/B is for phalanges of two-toed animals to identify whether it is from the right (A) or left (B) side of the foot.

### 3.4.7 Age and Sex

Age and sex data are recorded in the sections labeled “Edad” and “Sexo” (Figure 3.9). Age data are recorded in two boxes: “fusión” and “estimada”. The “fusión” section provides information on the fusion status of the epiphyses using “0” (unfused), “1” (fusing), “2” (fused), or “X” (not present). The other box, “estimada,” is the age estimate: neonatal, very young, young, subadult, adult, or old. Sex includes male, female, or indeterminate. However, because of a lack of data, age and sex could not be considered in this analysis.

EDAD	FUSIÓN	<input type="text"/>
	ESTIMADA	<input type="text"/>
SEXO		<input type="text"/>

Figure 3.9: The section where sex and age data are recorded.

#### 3.4.8 Osteometry and the Osteo-metric Database

The osteo-metric data is recorded in the section labeled “Medidas.” This includes the length, width, and thickness of the cortical bone (Figure 3.10). All fragments were measured to the nearest millimeter for length and width using metal calipers. The length of small indeterminate splinters was recorded as an interval in centimeters (e.g., 0-2, 2-3, 3-4, 4-5, >5). The thickness of the cortical bone was measured for all long bone specimens. Length was measured at the longest point, whereas width was measured at the widest point of the fragment. Identified elements were also measured using the standard system developed by Von den Driesch (1976) in the separate osteo-metric database (Figure 3.11).



Figure 3.10: The section where osteo-metric data are recorded. The link to the osteo-metric database is provided by the gray button in the lower right-hand corner.

Figure 3.11: The osteo-metric database layout.

### 3.5 Taphonomy

Taphonomy, derived from the Greek words *taphos* meaning burial and *nomos* meaning rules or systems, describes the component of studying animal remains that aims to understand the agents that were involved in, and affected, the deposition of the faunal remains. This

includes analysis of the post-depositional damage (i.e., anthropic modifications, carnivore modifications, weathering, manganese, etc.) that affects the preservation, recovery, and identification of faunal remains. Taphonomic analysis aids in distinguishing the effects of cultural versus natural agents on an assemblage (Lyman 2008; Gifford-Gonzalez 2018). Within the principal database, there are four boxes in which taphonomic information is recorded: fractures (Figure 3.12), post-depositional damage (Figure 3.14), marks (Figure 3.15), and thermo-alteration (Figure 3.16).

### 3.5.1 Fractures

Figure 3.12: Where the fracture data is recorded including the origin (i.e., fresh, ancient, or mixed) and the morphology.

In the section on fractures, the origin “A” for ancient, “R” for recent, or “In” for Indeterminate and morphotype of the fracture is recorded. The morphotype corresponds to the type and shape of fracture (fresh, dry, mixed, indeterminate; Figures in Appendix).

Whether the fracture was a green bone fracture or dry bone fracture was recorded in the database. The identification of green bone fractures versus dry bone fractures followed the protocol of Villa and Mahieu (1991). Villa and Mahieu suggest that dry bone fractures tend to occur at right angles, have jagged or rough edges, or tear along the longitudinal plane into splinters. On the other hand, green bone or fresh fractures are classically spiral or curved in

cross-section. Green bone fractures can also result in obtuse or acute angles, have smooth margins, and sharp fracture edges. Fracture morphotypes are recorded in the database using a numerical system that identifies where the dry and/or fresh fractures are located on the specimen. There are various diagrams illustrating the numerical system that corresponds to various skeletal elements. The diagrams are included in the appendix.

### 3.5.2 Refits

Refits are noted in the “remontaje” box in the “Notas” section. This section is also used to record whether the specimen has been photographed as well as all other interesting observations about the specimen (Figure 3.13). Refits were attempted within each bag, sub-square, square, between squares, as well as within and between sublayers.



The image shows a screenshot of a form titled "NOTAS" (Notes) on a light beige background. The form contains several input fields and labels:

- SEPARADO**: A label followed by a small white rectangular input field.
- RESTAURACIÓN**: A label followed by a small white rectangular input field.
- REVISIÓN**: A label followed by a small white rectangular input field.
- FOTO**: A label followed by a small white rectangular input field.
- REMONTAJE**: A label followed by a large white rectangular input field.

Figure 3.13: The section where refits, photographs, and possible future revisions are noted.

### 3.5.3 Post-Depositional Damage

Post-depositional damage caused by natural agents was examined on all specimens with a focus on weathering, erosion, concretions, corrosion, manganese, and root marks. Weathering was assessed according to the criteria outlined by Gifford-Gonzalez 2018 (Table 3.3).

0	Fresh bone, no weathering cracks, bone is greasy and soft tissue may still be attached
1	Cracking, usually parallel to the fiber orientation of the bone. Articular surfaces may display mosaic cracking. Soft tissues may still be present
2	Outermost layers of bone exhibit flaking, usually beginning from cracks that continue to develop in the bone. In long bones, long thin flakes are normal. Flaking continues, becoming extensive and gradually removing all outer bone. Tissue may still be present
3	Bone surface displays patches of rough, evenly weathered compact bone, showing the underlying fibrous texture of the bone. Weathering does not penetrate more than 1.0-1.5mm at this stage. Patches of the exposed bone gradually spread over most of the bone. Break surfaces may be rounded at this stage. Tissue seldom present.
4	Bone surface is coarsely fibrous, with rough texture. Large and small splinters of bone may fall from the bone. Weathering penetrates bone cavities. Cracks in bone are open, with rounded or splintered edges.
5	Bone is falling apart in place. Large splinters lie around the main bone, which splinters or breaks up when moved.

Table 3.3: Weathering stage criteria from Gifford-Gonzalez (2018).

The other forms of natural taphonomic characteristics (concretions, erosion, manganese, corrosion, trampling, and root marks) are assessed on a scale from one to five (Table 3.4). Each of the numbers in the coding system corresponds to the percentage of the fragment's surface that is affected. The corresponding numbers for both the weathering criterion and the damage scale were recorded into the database under the "Alteraciones Diageneticas" section (Figure 3.14). These characteristics aid in assessing how well preserved or how damaged the assemblage is.

Scale Number	Percentage of Surface area affected by post-depositional damage
1	25% of the fragment's surface affected
2	25-50% of the fragment's surface affected
3	50% of the fragment's surface affected
4	>50-75% of the fragment's surface affected
5	80-100% of the fragment's surface affected

Table 3.4: Scale from 1-5 that corresponds to the percentage of surface area affected by post-depositional damage.

ALTERACIONES DIAGENÉTICAS		SUP. OBSERVABLE	
METEORIZACIÓN	<input type="text"/>		<input type="text"/>
EROSIÓN	<input type="text"/>	PISOTEO	<input type="text"/>
CONCRECIÓN	<input type="text"/>	PRESIÓN	<input type="text"/>
CORROSIÓN	<input type="text"/>	ROEDORES	<input type="text"/>
MANGANESO	<input type="text"/>	RAICES	<input type="text"/>

Figure 3.14: The database layout where post-depositional damage is recorded.

#### 3.5.4 Marks

Anthropogenic marks include cut marks (incision), scrape marks (“raspado”), and percussion notches (“muesca”). Each fragment was examined for these marks using a 40x magnification hand lens. The bones were also examined for marks produced by other agents including carnivores and prey birds. Possible marks from those agents include corrosion from digestion, punctures (“puncion”), furrowing, crenulated edges, and peeling. When present, these

marks were recorded in the box labeled “Alteraciones” (Figure 3.15). Marks were recorded on a presence or absence basis. Further information about the marks is recorded in the separate marks database. The presence of these marks aid in identifying whether the assemblage was modified by hominins, carnivores, or prey birds.

The image shows a red rectangular form titled "ALTERACIONES". It contains two columns of input fields. The left column lists: CORROSIÓN, RASPADO, INCISIÓN, TAJO, HORADACIÓN, HUNDIMIENTO, PUNCIÓN, and ARRASTRE. The right column lists: FURROWING, BORDE CRENU., PEELING, PÉRDIDA OSEA, and MUESCA. Each label is followed by a white rectangular input field. At the bottom right of the form is a red button with the text "BD MARCAS".

Figure 3.15: The section of the database where anthropic marks are recorded.

### 3.5.5 Thermo-alteration

The image shows a beige rectangular form titled "TERMOALTERACIONES". It contains several input fields. On the left side, there are three rows: "COLOR 1" with a white input field, "PARTE 1" with a white input field, and "LOC. 1" with a white input field. On the right side, there are three rows: "COLOR 2" with a white input field, "PARTE 2" with a white input field, and "LOC. 2" with a white input field. At the bottom left, there is a label "MODIFICACIONES" followed by a long white input field.

Figure 3.16: The section where evidence of burning on fragments is noted.

Thermo-altered specimens were noted in the section labeled “termoalteraciones” (Figure 3.16). The color, the proportion of the surface area affected, as well as portion of the bone burnt are recorded. Color was used as a proxy to estimate the specimen’s exposure to fire (Shipman, Foster, and Schoeninger 1984; Stiner et al. 1995; Lambrecht and Mallol 2020). The amount of surface area of the fragment that has been thermo-altered is assessed using general terms like point (Figure 3.17), part (Figure 3.18), or total (Figure 3.19) within the “parte” box. The location of the color change on the specimen was recorded using the same series of numbers and letters that is used for bone region (see above).



Figure 3.17: Example of a burnt remain where only a “point” on the surface area was affected by thermo-alteration. The arrow indicates the burnt point.



Figure 3.18: Example of a burnt remain where part of the surface area was affected by thermo-alteration. The arrow indicates the part of the specimen where the surface area has been burnt.



Figure 3.19: Example of a burnt remain where the “total” amount of surface area was affected by thermo-alteration.

### 3.5.6 Marks Database

The last database focuses on marks (Figure 3.20). Like the osteo-metric and tooth database, the marks database is also linked to the principal database through the registration number. This database includes: the type of mark present, its probable origin, the agent who

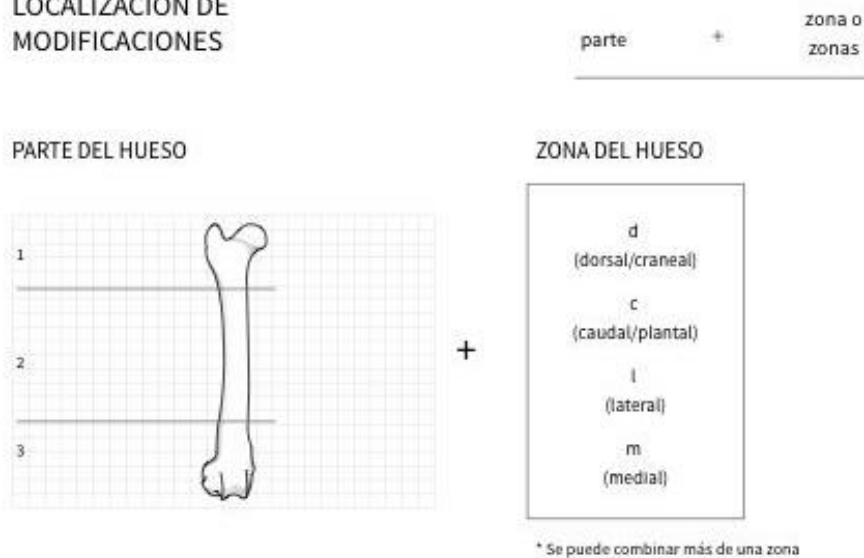


created the mark, along with information on localization, morphology, distribution, direction, intensity, and quantity. “Origin” refers to whether the marks were made by teeth, using a stone tool edge, percussion, digestion, etc. The various agents include hominins, carnivores, rodents and raptors. Localization was specified using the same numerical and alphabetical system described above (i.e., “2dm” =diaphysis, dorsal, medial; see Figure 3.21). Morphology describes the shape of the mark such as: linear, semi-circular, circular, triangular, and irregular. The distribution box contains data on whether the marks occur only on one (unilateral) or both sides (bilateral). The direction of the marks is described as either longitudinal or transverse. The intensity—whether light, moderate, or heavy—is recorded in the box below direction. The number of marks on the fragment were also recorded numerically (i.e., 1, 2, 3, etc.) or qualitatively (e.g., singular, multiple).

<p>N° REGISTRO <b>980</b></p> <p>N° REG. MARCAS 75</p> <p>YACIMIENTO Abric del Pastor</p> <p>UE Ve</p> <p>FECHA 2022</p> <p>CAPA/FACIES Gr-CI</p> <p>LEVANTAMIENTO</p> <p>CUADRO C5</p> <p>SUBCUADRO 3</p> <p>BD PRINCIPAL</p> <p>FOTOGRAFÍAS</p> <p>CÓDIGOS</p>	<p><b>TAXONOMÍA/ANATOMÍA</b></p> <p>ORDEN</p> <p>GENERO Indeterminado</p> <p>HUESO L11</p> <p>FRAGMENTO 050</p> <p>LATERALIDAD</p>	<p><b>CARACTERÍSTICAS</b></p> <p>TIPO DE MARCA Inclión</p> <p>ORIGEN Lítica</p> <p>AGENTE Antropico</p> <p>A. ESPECÍFICO</p> <p>LOCALIZACIÓN 2</p> <p>MORFOLOGÍA Corta</p> <p>DISTRIBUCIÓN Unilateral</p> <p>DIRECCIÓN Tr</p> <p>INTENSIDAD Leve</p> <p>CANTIDAD Multiple</p>	<p><b>MEDIDAS</b></p> <p>LONGITUD 1</p> <p>ANCHURA 1</p> <p>LONGITUD 2</p> <p>ANCHURA 2</p> <p>NOTAS</p> <p>FOTO <input checked="" type="checkbox"/></p> <p>OBSERVACIONES</p>
--	--	---	---

Figure 3.20: Marks database layout.

## LOCALIZACIÓN DE MODIFICACIONES



## EJEMPLOS

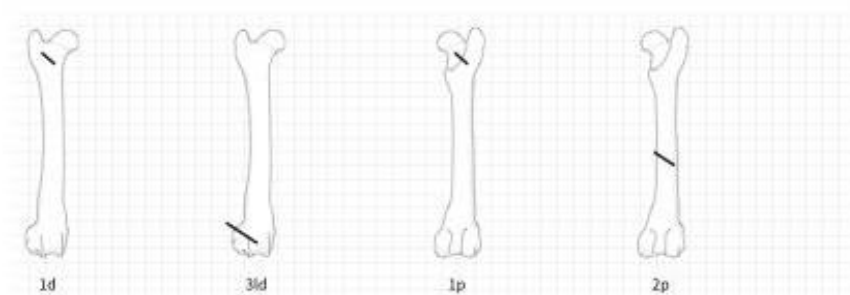


Figure 3.21: Diagrams explaining how the location of marks on a specimen are recorded.

## 3.6 Quantification

After all the specimens were recorded in the FileMaker database, the data were exported into an Excel file. The data were then analyzed on two-time scales: the main occupations (A or B) and the sublayers of Occupation B. The remains were quantified using NISP, MNE, and MNI. A spatial analysis was conducted in ArcGIS Pro as well.

### 3.6.1 Counts

Quantification provides the basis for interpretation of subsistence patterns and comparison between assemblages. Below I describe the methods used to quantify the faunal assemblage including the number of specimens (NSP), the number of identified specimens (NISP), the minimum number of elements (MNE), and the minimum number of individuals (MNI).

The number of specimens (NSP) is the total number of fragments in the faunal assemblage, including both the identified and indeterminate specimens. NSP is cumulative and corresponds to the sum of specimens entered into the FileMaker database. NISP is the portion of NSP that are identified to taxon. Identifying an element to taxon can refer to varying levels of specificity, from species to taxonomic order depending on numerous factors including preservation, fragmentation, identifiability of the element, and the analyst's skill level. The operationalization of NISP is straightforward: you identify as many specimens to taxon as possible, and then tally how many specimens are present for each taxon (Lyman 2008). NISP can be calculated per stratigraphic unit, sublayer, feature, or the entire site. NISP is advantageous as it is easily calculated and additive (Lyman 2008). However, NISP is also heavily affected by interdependence (counting the same element or individual animal multiple times), fragmentation, preservation, density, analyst experience, and differences in the number of bones between various species (Lyman 2008; Morin et al. 2017). To mitigate the problem of counting the same element more than once, I calculated NISP taking refits into consideration.

MNE is the minimum number of a particular skeletal element per taxon in a faunal sample. MNE is a derived unit that is strongly correlated with NISP (Lyman 2008). Although MNE is simply defined, determining MNE is complicated as practices vary between analysts and

can be affected by fragmentation, the size of the NISP sample, how excavation units are derived, as well as differences in identifiability between elements (Lyman 2008; Morin et al. 2017). I calculated MNE by first sorting the identified specimens by element according to side. However, if the side could not be determined, I divided the paired elements by 2 to represent both sides. Age (fusion state) was taken into consideration, as well as the portion (proximal, diaphysis, distal, medial, and/lateral) of the element. The side with the highest value for each element determined the MNE value of that element. Indeterminate tooth and maxilla fragments were not included in the calculation of MNE. These pieces were often found together in caches but were not always able to be refit. By including these fragments, the number of cranial elements would have been heavily inflated.

MNI is the minimum number of individual animals (Stock 1929; Howard 1930; Lyman 1994). MNI is a derived method calculated based on the most abundant skeletal element per taxon. Like MNE, MNI can over-represent rare species, be affected by fragmentation, the size of the NISP sample, how excavation units are derived, differences in identifiability between elements, as well as inter-analyst variation (Lyman 2008; Morin et al. 2017). Because MNI can be calculated in a multitude of ways (Grayson 1984; Banning 2000; Lyman 2008), it is important that analysts explicitly detail their method. I calculated MNI taking refits, age, side, and portion into consideration. Ultimately, the highest MNE for each species forms the basis for the MNI of each species.

### 3.6.2 Statistical Analysis

To determine whether taxonomic, taphonomic, and anthropogenic patterns are significantly different, a chi-square test of independence was conducted. All samples were tested to make sure they met the small frequency requirements outlined by Zar (1996). The adjusted standardized residuals and  $p$ -values for all chi-square tests of independences are presented in tables in the results section. In order to evaluate whether perceived increases and decreases in the data were indeed statistically significant, Cochran's linear test was performed.

### 3.6.3 Spatial Analysis

To understand and identify spatial patterns at various scales, all the fragments with spatial data were entered into an ArcGIS Pro project. Once in ArcGIS, specimens with spatial data were plotted and two different analyses were run: Kernel Density Models (KDM) and Average Nearest Neighbor (ANN). Kernel Density Models were run to identify whether the faunal material show clustering or are randomly distributed across the excavation surface. The KDM helps to identify where those clusters are located and the density of those clusters.

To understand the degree to which remains were clustered, ANN was performed. The ANN tool in ArcGIS Pro calculates the Observed Mean Distance (OMD), the Expected Mean Distance (EMD), the ANN Ratio,  $z$ -score, and  $p$ -value. OMD is the average distance from each point to its closest neighboring point. EMD is calculated by scattering an identical number of points randomly across the space and taking the average distance from each of the random points to its nearest neighbor. The ANN ratio corresponds to the OMD divided by the EMD. If the ANN ratio

approaches 1, the distribution is considered random. An ANN ratio of less than 1 suggests clustering because the points are nearer to one another than if they had been randomly scattered across the surface. If the ratio is greater than 1, it suggests that the points are dispersed because the points are farther from each other than if they were randomly scattered across the surface. The probability that the observed points were sampled from a completely random universe of points (converted from a z-score) is calculated for each ANN ratio. The lower the probability, the more likely that a clustered pattern is in fact clustered as well as that a dispersed pattern is indeed dispersed (Thompson et al. 2022).

ANN was run in ArcGIS Pro with the following input feature classes: Occupation A and Occupation B. All the analyses were run using Euclidean distance (as opposed to Manhattan distance). A report on each analysis was generated recording the observed mean distance, expected mean distance, nearest neighbor ratio, z-score, and *p*-value (ANN reports are listed in the appendix). From the generated report it was recorded whether the results were clustered or dispersed and to what significance.

Kernel density models (KDM) help to visually identify clusters. These models predict the density of the input points by calculating the density of input features around each output cell using the smoothing parameter (Thompson et al. 2022). KD models were projected in ArcGIS Pro. The input parameters were as follows: Population field: None; Output cell size: 0.02800000000227 for Occupation A and 3.54892000057152E-02 for Occupation B; Area: Square Kilometers; Output Value: Densities; Method: Planar, Input Barrier feature: Polygon. In KD plots, the results are projected onto the surface area with a darker color indicating a higher density and then fading in opacity as the density decreases.

### **3.7 Summary**

In this chapter, I have described the methods and recording of identification, quantification, taphonomic and spatial data used in the analysis of the faunal material for this thesis. I have also highlight how and when the material was recovered from layer V of Abric del Pastor as well as what material was included in the analysis.

## Chapter 4: Results

Layer V at Abric del Pastor contains the remains of two occupation events (Figure 4.1 and Figure 4.2). Occupation A is the older accumulation, while Occupation B is stratigraphically above and younger. These occupations are separated by an archaeologically sterile layer. The taphonomic, taxonomic, and anthropic characteristics of these occupations are described on two time scales: 1) between occupations A and B, and 2) within the same occupation.

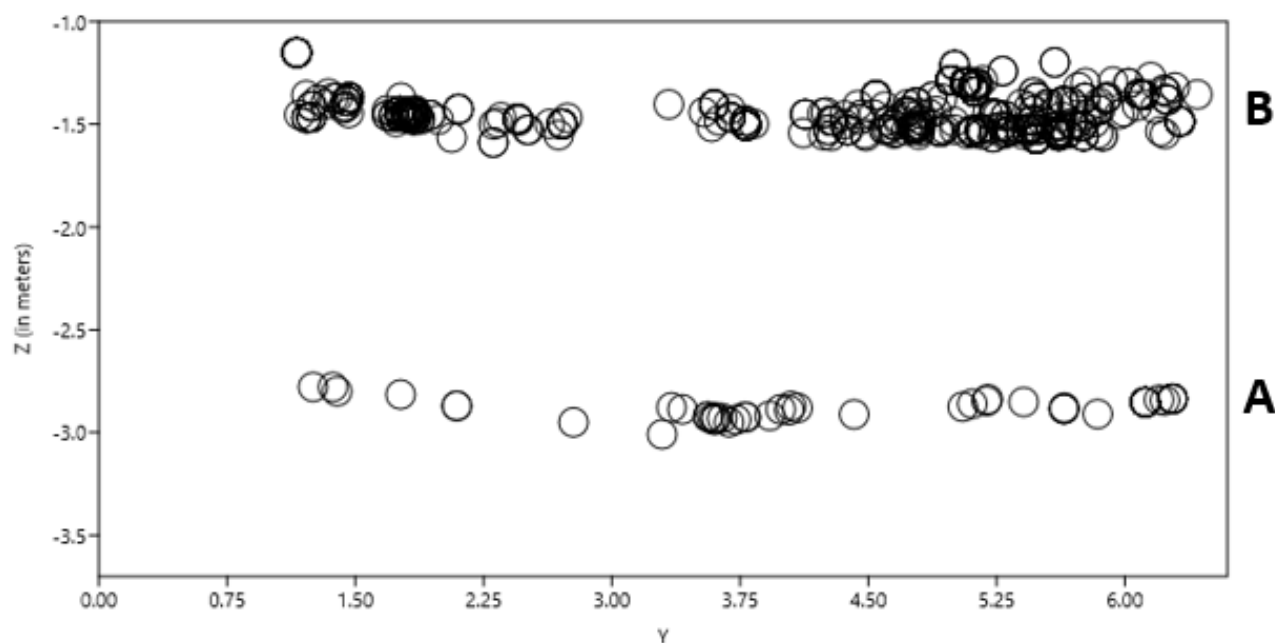


Figure 4.1: Cross-section of the y-axis showing the vertical distribution of all the faunal remains in Occupations A and B. The y-axis (in meters) correlates to rows 1-6 of the excavation surface.



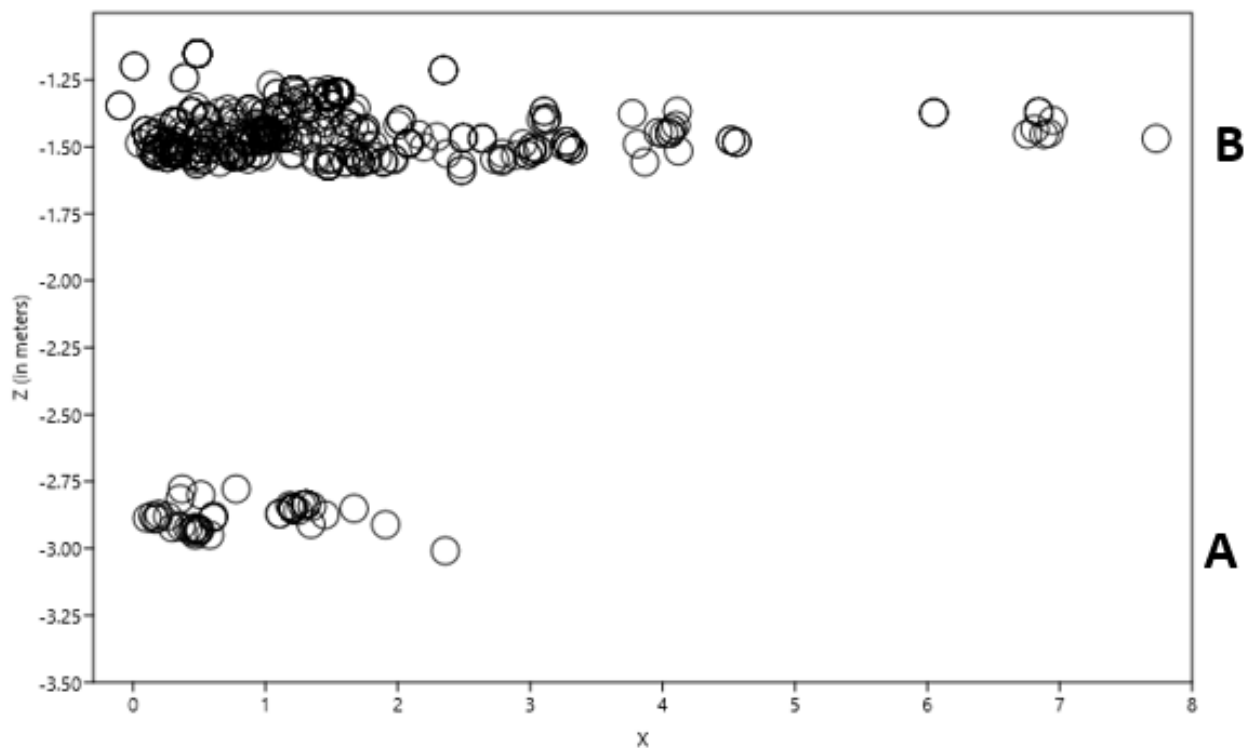


Figure 4.2: Cross-section of the x-axis showing the vertical distribution of all the faunal remains in Occupations A and B. The x-axis (in meters) correlates to columns D through W of the excavation surface.

#### 4.1 Occupation A

Occupation A is composed of 57 faunal remains all from sublayer Vd (Table 4.2). The remains are relatively well-preserved with approximately 80% of the specimens having less than 25% of their surface area affected by post-depositional damage, such as concretions, manganese, root marks, and traces of erosion (Table 4.1). Additionally, the fragments show, on average, only limited (level 1; NISP: 8; 88.9%) weathering according to Gifford-Gonzalez's (2018) classification.

Type of Damage	Percent of Surface Area Affected					Total
	>0-25	25-50	50	>50-75	75-100	
Concretions	27 (71.0)	8 (21.0)	0	1 (2.6)	2 (5.3)	38
Erosion	25 (80.6)	4 (12.9)	1 (3.2)	1 (3.2)	0	31
Root Marks	14 (70.0)	4 (20.0)	0	2 (10.0)	0	20
Manganese	47 (90.4)	5 (9.6)	0	0	0	52
<b>Total</b>	<b>113 (80.1)</b>	<b>21 (14.9)</b>	<b>1 (0.7)</b>	<b>4 (2.8)</b>	<b>2 (1.4)</b>	<b>141</b>

Table 4.1: Number and percentage of the faunal remains from Occupation A exhibiting various types of post-depositional damage. Percentage is listed in parentheses.

Taxa	Vd	
	N	%
Caprinae	3	42.8
<i>Oryctolagus cuniculus</i>	1	14.3
<i>Testudo hermanni</i>	2	28.6
<i>Pyrrhocorax</i> sp.	1	14.3
<b>Total</b>	<b>7</b>	<b>100</b>
Small-sized animals	17	37.0
Medium-sized animals	29	63.0
<b>Total</b>	<b>46</b>	<b>100</b>
Indeterminate	4	
<b>Total</b>	<b>57</b>	

Table 4.2: Taxonomic breakdown of Occupation A.

Size Class	Vd	
	N	%
Small size animals	21	39.6
Medium size animals	32	60.4
<b>Total</b>	<b>53</b>	<b>100</b>

Table 4.3: Percentage of specimens identified to small- and medium-sized animals from Occupation A after merging the species with those identified to body size class.

The majority of the faunal remains are identified to either taxon or body size class, while only four specimens remain indeterminate. The identified taxa include caprines, *Oryctolagus*

*cuniculus*, *Testudo hermanni*, and *Pyrrhocorax* sp. (Table 4.2). Medium-sized species dominate (60.4%) the assemblage. Small-sized taxa are also present whereas specimens from large-sized animals are absent (Table 4.3). Most of the remains are from forelimbs (40%) followed by cranial fragments (30%; Table 4.4). The occupation has a total MNE count of six and an MNI count of four for all species combined (Table 4.5 and 4.6).

Anatomical Group	Vd	
	N	%
Cranial	3	30.0
Axial	1	10.0
Forelimb	4	40.0
Hindlimb	1	10.0
Shell	1	10.0
<b>Total</b>	<b>10</b>	<b>100</b>

Table 4.4: Anatomic groups for all species combined that are present in Occupation A.

Element by Taxa	MNE	
	N	%
Caprine		
Inferior premolar <i>Oryctolagus cuniculus</i>	2	33.3
Pelvis <i>Pyrrhocorax</i> sp.	1	16.7
Ulna <i>Testudo hermanni</i>	1	16.7
Humerus	1	16.7
Carapace	1	16.7
<b>Total</b>	<b>6</b>	<b>100</b>

Table 4.5: MNE counts for Occupation A.

Taxa	MNI	
	N	%
Caprine	1	25.0
<i>Oryctolagus cuniculus</i>	1	25.0
<i>Pyrrhocorax</i> sp.	1	25.0
<i>Testudo hermanni</i>	1	25.0
<b>Total</b>	<b>4</b>	<b>100</b>

Table 4.6: MNI counts for Occupation A.

There are 8 specimens within Occupation A that show anthropic marks (percussion notches, cut marks, and scrape marks; Table 4.7). Of those, 62.5% are cut marks. Most marks are on fragments of small-sized taxa. Only one of the cut marks was on a specimen identified to taxon, *Testudo* (Table 4.8). All of the cut and scrape marks are located on the shaft of long bone fragments. Given their placement, these marks are likely the result of defleshing. There are only 2 (lightly) burnt fragments. Additionally, most of the fractures are fresh or intermediate between fresh and dry (43.4% and 52.8% respectively; Table 4.10). The average length of the fragments for medium-sized taxa is 27.1mm while those for small-sized animals average 19.7mm (Table 4.11). The majority (52.5%) of the long bone fragments have between 0-25% of the circumference preserved (Table 4.9).

Type of Mark	Vd	
	N	%
Cut Marks	5	8.8
Scrape Marks	2	3.5
Percussion Notches	1	1.8
<b>Total Marks</b>	<b>8</b>	<b>14.0</b>

Table 4.7: The number and percentage of each type of anthropic mark identified in Occupation A. The percentage of anthropic marks in Occupation A as a whole is listed in the total row.

Body Size Class	Cut Marks	Scrape Marks	Percussion Notches	Total
Small-sized taxa	5			5
Medium-sized taxa		2	1	3
<b>Total</b>	<b>5</b>	<b>2</b>	<b>1</b>	<b>8</b>

Table 4.8: The number and percentage of specimens for each type of anthropic mark by body size class in Occupation A.

Sublayer	Percent of Circumference preserved					Total
	>0-25	>25-50	>50-75	>75-90	>90-100	
Vd	21 (52.5)	6 (15.0)	6 (15.0)	6 (15.0)	1 (2.5)	40 (100)
<b>Total</b>	21	6	6	6	1	40

Table 4.9: The number and percentage of specimens of each category of percent of circumference preserved for long bone fragments from Occupation A. The percentage of the assemblage is listed in the parentheses.

Type of Fracture	Vd	
	N	%
Dry	2	3.8
Fresh	23	43.4
Mixed Fresh and Dry	28	52.8
<b>Total</b>	<b>53</b>	<b>100</b>

Table 4.10: Number and percentage of long bone fragments with dry, fresh, and mixed fractures from Occupation A.

Body Size Class	N	Average Length (mm)
Medium-sized taxa	32	27.1
Small-sized taxa	21	19.7
<b>Total</b>	<b>53</b>	<b>24.1</b>

Table 4.11: Average length of medium- and small-sized animal specimens from Occupation A.

No evidence of carnivore or raptor activity was found in Occupation A; nor were tooth marks, crenulated edges, corrosion from digestion, or beak marks observed. It is important to

note that the absence of evidence of carnivores or raptors involvement does not prove that Neanderthals were the only agents in the faunal accumulation. It only suggests that the impact of carnivores and raptors seems to have been limited.

A kernel density model, as well as an average nearest neighbor analysis (observed: 0.104003, expected: 0.218701,  $p < 0.001$ ), show that the faunal remains in Occupation A are clustered (Figure 4.3). The remains are clustered along the left (eastern) portion of the shelter, with the densest clusters being observed in squares D4 and C1.

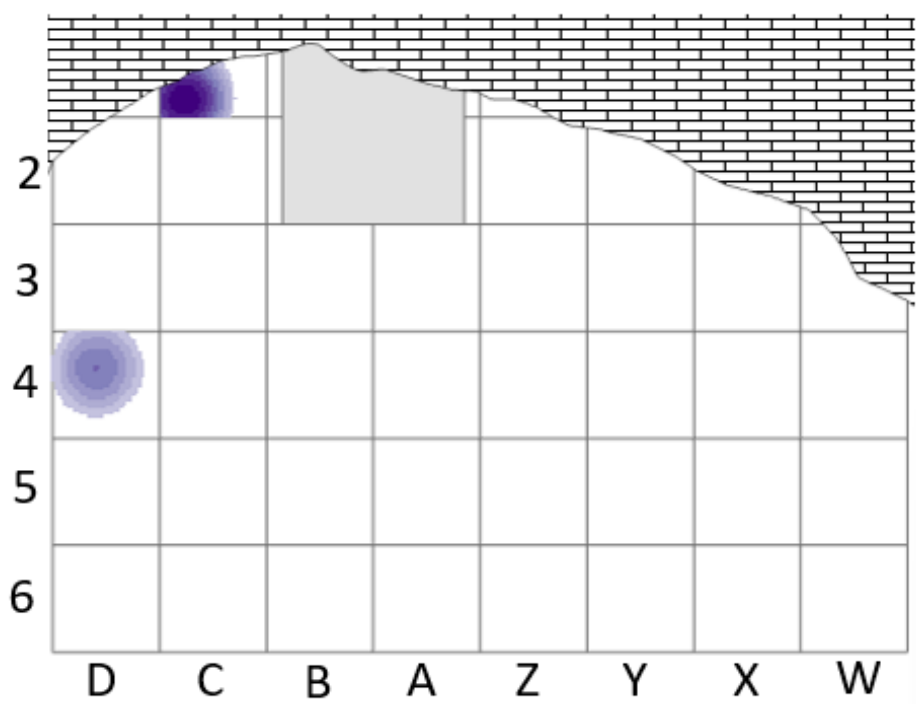


Figure 4.3: Kernel density model of Occupation A. The darker the color the denser the accumulation of faunal material. Squares are 1 x 1m.

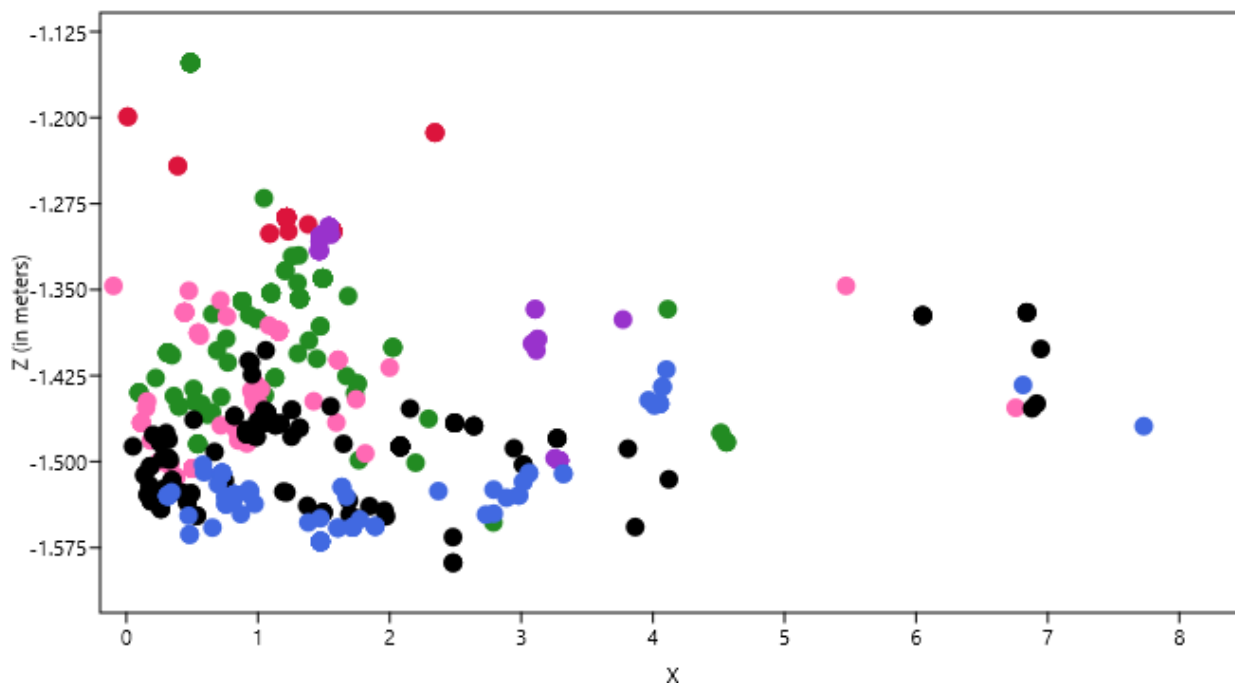


Figure 4.4: XZ plot of Occupation B with the sublayers color-coded as follows: Va is red, Vb is purple, Vc is green, Vd, is pink, Ve is black, and Vf is blue. The x-axis (in meters) correlates to columns D through W of the excavation surface.

## 4.2 Occupation B

Occupation B has more faunal remains than Occupation A with a NSP of 570 for all sublayers included (Va through Vf; Figure 4.4). The specimens are relatively well-preserved. On average, 25-50% of the surface area of each fragment has evidence of post-depositional damage including traces of erosion, concretions, manganese, and root marks (Table 4.12 and 4.13). Generally, the fragments are weathered corresponding to stage 3 according to Gifford-Gonzalez's (2018) classification of post-depositional damage (Table 4.14).

Sub-layer	Percent of Surface Area Affected						Percent of Surface Area Affected				
	Concretions						Manganese				
	0-25	35-50	50	>50-75	80-100	Total	0-25	35-50	50	>50-75	Total
Va	30 (61.2)	8 (16.3)	8 (16.3)		5 (10.2)	49 (100)	31 (62.0)	13 (26.0)	6 (12.0)		50 (100)
Vb	16 (51.6)	5 (16.1)	8 (25.8)	2 (6.4)		31 (100)	23 (88.5)	1 (3.8)	2 (7.7)		26 (100)
Vb/Vc			1 (100)			1 (100)	1 (100)				1 (100)
Vc	46 (50.0)	19 (20.6)	14 (15.2)	13 (14.1)		92 (100)	82 (76.6)	17 (15.9)	7 (6.5)	1 (0.9)	107 (100)
Vd	24 (68.6)	9 (25.7)	1 (2.9)		1 (2.9)	35 (100)	83 (93.2)	5 (5.6)	1 (1.1)		89 (100)
Ve	57 (70.4)	11 (13.6)	5 (6.2)	5 (6.2)	3 (3.7)	81 (100)	87 (74.3)	24 (20.5)	6 (5.1)		117 (100)
Vf	43 (75.4)	10 (17.5)	3 (5.3)		1 (1.8)	57 (100)	50 (56.8)	23 (26.1)	11 (12.5)	4 (4.5)	88 (100)
<b>Total</b>	<b>216 (62.4)</b>	<b>62 (17.9)</b>	<b>40 (11.6)</b>	<b>20 (5.8)</b>	<b>10 (2.9)</b>	<b>346 (100)</b>	<b>357 (74.7)</b>	<b>83 (17.4)</b>	<b>33 (6.9)</b>	<b>5 (1.0)</b>	<b>478 (100)</b>

Table 4.12: Number and percent of the surface area of fragments affected by concretions and manganese for each sublayer of Occupation B. The percentage is listed in the parentheses. Va is the most recent sublayer and Vf is the oldest sublayer.

Sub-layer	Percent of Surface Area Affected						Percent of Surface Area Affected					
	Erosion						Root Marks					
	0-25	35-50	50	>50-75	80-100	Total	0-25	35-50	50	>50-75	80-100	Total
Va	22 (91.7)	2 (8.3)				24 (100)	11 (61.1)	4 (22.2)	2 (11.1)		1 (5.5)	18 (100)
Vb	5 (25.0)	2 (10.0)	9 (45.0)	4 (20.0)		20 (100)	6 (37.5)	3 (18.7)	5 (31.2)	1 (6.2)	1 (6.2)	16 (100)
Vb/Vc										1 (100)		1 (100)
Vc	63 (78.7)	8 (10.0)		4 (5.0)	5 (6.2)	80 (100)	31 (53.4)	13 (22.4)	9 (15.5)	3 (5.2)	2 (3.4)	58 (100)
Vd	24 (64.9)	10 (27.0)	3 (8.1)			37 (100)	24 (54.5)	11 (25.0)	6 (13.6)	2 (4.5)	1 (2.3)	44 (100)
Ve	51 (54.8)	10 (10.7)	9 (9.7)	8 (8.6)	15 (16.1)	93 (100)	29 (42.0)	12 (17.4)	9 (13.0)	6 (8.7)	13 (18.8)	69 (100)
Vf	46 (63.0)	24 (32.9)	3 (4.1)			73 (100)	30 (52.6)	7 (12.3)	5 (8.8)	5 (8.8)	10 (17.5)	57 (100)
<b>Total</b>	<b>211 (64.5)</b>	<b>56 (17.1)</b>	<b>24 (7.3)</b>	<b>16 (4.9)</b>	<b>20 (6.1)</b>	<b>327 (100)</b>	<b>131 (49.8)</b>	<b>50 (19.0)</b>	<b>36 (13.7)</b>	<b>18 (6.8)</b>	<b>28 (10.6)</b>	<b>263 (100)</b>

Table 4.13: Percent of the surface area of the fragments affected by erosion and root mark damage for each sublayer in Occupation B. The percentage is listed in parentheses.



Sub-layer	Number corresponding to the weathering stage outlined by Gifford-Gonzalez (2018)					
	1	2	3	4	5	Total
Va		10 (25.0%)	22 (55.0%)	2 (5.0%)	6 (15.0%)	40 (100)
Vb			4 (40.0%)		6 (60.0%)	10 (100)
Vc	3 (8.6%)	13 (37.1%)	14 (40.0%)	3 (8.6%)	2 (5.7%)	35 (100)
Vd	6 (11.8%)	13 (25.5%)	17 (33.3%)	2 (3.9%)	13 (25.5%)	51 (100)
Ve	1 (1.8%)	7 (12.7%)	24 (43.6%)	5 (9.0%)	18 (32.7%)	55 (100)
Vf	2 (6.4%)	3 (9.7%)	7 (22.6%)	15 (48.4%)	4 (12.9%)	31 (100)
<b>Total</b>	<b>12 (5.4%)</b>	<b>46 (20.7%)</b>	<b>88 (39.6%)</b>	<b>27 (12.2%)</b>	<b>49 (22.1%)</b>	<b>222</b>

Table 4.14: Weathering stage for the fragments in each sublayer of Occupation B. Va is the topmost sublayer and Vf is the bottommost sublayer. The percentage is listed in the parentheses.

Taxa	Va		Vb		Vb/Vc		Vc		Vd		Ve		Vf		Total	
	N	%	N	%	N	%	N	%	N	%	N	%	N	%	N	%
Birds			4	23.5							1	16.7	2	20.0	7	8.1
Caprines	10	100	12	70.6			17	51.5	8	80.0	1	16.7	6	60.0	54	62.8
Cervids							2	6.1	1	10.0					3	3.5
<i>Oryctolagus c.</i>			1	5.9			1	3.0	1	10.0					3	3.5
<i>Testudo her.</i>							13	39.4			4	66.7	2	20.0	19	22.1
<b>Total</b>	<b>10</b>	<b>100</b>	<b>17</b>	<b>100</b>			<b>33</b>	<b>100</b>	<b>10</b>	<b>100</b>	<b>6</b>	<b>100</b>	<b>10</b>	<b>100</b>	<b>86</b>	<b>100</b>
Small-sized animals							3	5.9	5	10.2	3	4.6	6	13.3	17	6.9
Medium-sized animals	19	79.2	11	100	1	100	45	88.2	44	89.8	57	87.7	35	77.8	212	86.2
Large-sized animals	5	20.8					3	5.9			5	7.7	4	8.9	17	6.9
<b>Total</b>	<b>24</b>	<b>100</b>	<b>11</b>	<b>100</b>	<b>1</b>	<b>100</b>	<b>51</b>	<b>100</b>	<b>49</b>	<b>100</b>	<b>65</b>	<b>100</b>	<b>45</b>	<b>100</b>	<b>246</b>	<b>100</b>
Indeterminate	36		11				38		38		57		20		200	
M./Large-sized animals									6		9		23		38	
<b>Total</b>	<b>36</b>		<b>11</b>				<b>38</b>		<b>44</b>		<b>66</b>		<b>43</b>		<b>238</b>	

Table 4.15: Taxa identified in each sublayer of Occupation B. Va is the most recent sublayer and Vf is the oldest sublayer.

Size Class	Va		Vb		Vb/Vc		Vc		Vd		Ve		Vf		Total	
	N	%	N	%	N	%	N	%	N	%	N	%	N	%	N	%
Small size animals			5	17.9			17	20.2	6	10.2	8	11.3	10	18.2	46	13.8
Medium size animals	29	85.3	23	82.1	1	100	62	73.8	52	88.1	58	81.7	41	74.5	266	80.1
Large size animals	5	14.7					5	6.0	1	1.7	5	7.0	4	7.3	20	6.0
<b>Total</b>	<b>34</b>	<b>100</b>	<b>28</b>	<b>100</b>	<b>1</b>	<b>100</b>	<b>84</b>	<b>100</b>	<b>59</b>	<b>100</b>	<b>71</b>	<b>100</b>	<b>55</b>	<b>100</b>	<b>332</b>	<b>100</b>

Table 4.16: Percent distribution by body size class in the sublayers of Occupation B after merging taxonomically identified specimens with those attributed to body size class.

Most of the remains were determined to taxon or body size class (65%). The taxa present include birds, caprines, cervids, *Oryctolagus cuniculus*, and *Testudo hermanni* (Table 4.15). The most common taxon is caprines (62.8%). When classified by body size, medium-sized mammals comprise the largest proportion (n=266, 80.1%; Table 4.16). Specimens for small and large-sized taxa are also noted. Most of the specimens in Occupation B are cranial remains (Table 4.17). Occupation B has an MNE count of 36 and an MNI count of 9 (Table 4.18; Table 4.19).

Anatomic Groups	Va		Vb		Vc		Vd		Ve		Vf		Total	
	N	%	N	%	N	%	N	%	N	%	N	%	N	%
Cranial	30	93.7	18	56.2	17	47.2	5	26.3	4	20.0	23	53.5	97	53.3
Axial	1	3.1	5	15.6	2	5.5	3	15.8	7	35.0	11	25.6	29	15.9
Forelimb	1	3.1	2	6.2	3	8.3	1	5.3	1	5.0	1	2.3	9	4.9
Hindlimb					8	22.2	4	21.0	2	10.0	4	9.3	18	9.9
Shell					3	8.3			4	20.0	2	4.6	9	4.9
Flat			7	21.9	3	8.3	3	15.8	1	5.0			14	7.7
Cancellous							3	15.8	1	5.0	2	4.6	6	3.3
<b>Total</b>	<b>32</b>	<b>100</b>	<b>32</b>	<b>100</b>	<b>36</b>	<b>100</b>	<b>19</b>	<b>100</b>	<b>20</b>	<b>100</b>	<b>43</b>	<b>100</b>	<b>182</b>	<b>100</b>

Table 4.17: Anatomic groups present in the sublayers of Occupation B. All species combined.

Elements by Taxa	Va		Vb		Vc		Vd		Ve		Vf		Total	
	N	%	N	%	N	%	N	%	N	%	N	%	N	%
<b>Caprinae</b>														
Mandible							2	25.0					2	5.5
Incisor											1	16.7	1	2.8
Inferior Premolar							1	12.5					1	2.8
Superior Premolar	2	33.3	1	16.7	1	7.1							4	11.1
Inferior Molar			2	33.3							1	16.7	3	8.3
Superior Molar	2	33.3	2	33.3	2	14.3							6	16.7
Hyoid									1	50.0			1	2.8
Vertebra	1	16.7											1	2.8
Humerus	1	16.7											1	2.8
Femur							1	12.5			3	50.0	3	8.3
Tibia					1	7.1	1	12.5					1	2.8
Phalanx							1	12.5					1	2.8
<b>Cervinae</b>														
Ulna					1	7.1							1	2.8
2 <sup>nd</sup> Phalanx							1	12.5					1	2.8
<b><i>Oryctolagus cuniculus</i></b>														
3 <sup>rd</sup> Metacarpal			1	16.7									1	2.8
Femur							1	12.5					1	2.8
Calcaneus					1	7.1							1	2.8
<b><i>Testudo hermanni</i></b>														
Scapula					1	7.1							2	5.5
Pelvis					1	7.1							1	2.8
Femur					3	21.4							3	8.3
Tibia					2	14.3							2	5.5
Carapace					1	7.1			1	50.0	1	16.7	1	2.8
<b>Total</b>	<b>6</b>	<b>100</b>	<b>6</b>	<b>100</b>	<b>14</b>	<b>100</b>	<b>8</b>	<b>100</b>	<b>2</b>	<b>100</b>	<b>6</b>	<b>100</b>	<b>36</b>	<b>100</b>

Table 4.18: MNE counts for the sublayers of Occupation B.

Taxa	Va	Vb	Vc	Vd	Ve	Vf	Total
Caprinae	2	2	2	2	1	3	4
Cervinae			1	1			1
<i>Oryctolagus cuniculus</i>		1	1	1			1
<i>Testudo hermanni</i>			3		1	1	3
<b>Total MNI</b>	<b>2</b>	<b>3</b>	<b>7</b>	<b>4</b>	<b>2</b>	<b>4</b>	<b>9</b>

Table 4.19: MNI counts for the sublayers in Occupation B.

In the sublayers of layer V, there are more dry fractures than fresh fractures (Table 4.22). The majority of long bone fractures have less than 25% of the circumference preserved (Table 4.20). The average length of fragments in Occupation B is around 2.5cm. When body size is controlled for, small size animal fragments are on average slightly shorter (2.1cm), while large size animal fragments are slightly longer (3.2cm). Medium size animal fragments are on average 2.5cm long (Table 4.21).

Sublayer	Percent of Circumference Preserved					Total
	>0-25	>25-50	>50-75	>75-90	>90-100	
Va	20 (80.0)	3 (12.0)	1 (4.0)	1 (4.0)		25 (100)
Vb	1 (50.0)			1 (50.0)		2 (100)
Vb/Vc		1 (100)				1 (100)
Vc	24 (50.0)	10 (20.8)	3 (6.2)	11 (22.9)		48 (100)
Vd	22 (59.4)	4 (10.8)	7 (18.9)	3 (8.1)	1 (2.7)	37 (100)
Ve	39 (60.0)	21 (32.3)	2 (3.1)	3 (4.6)		65 (100)
Vf	19 (43.2)	21 (47.7)	3 (6.8)	1 (2.3)		44 (100)
Total	125 (56.3)	60 (27.0)	16 (7.2)	20 (9.0)	1 (0.4)	222 (100)

Table 4.20: The number and percentage of specimens attributed to each category of the percentage of the circumference preserved for long bone fragments in Occupation B. The percentage of specimens is listed in the parentheses.

Body Size Class	Sublayer							Total
	Va	Vb	Vb/Vc	Vc	Vd	Ve	Vf	
Small-sized		17.0 (5)		21.8 (17)	21.8 (6)	22.3 (8)	16.4 (10)	(46)
Medium-sized	18.0 (29)	19.4 (23)	31.0 (1)	24.2 (62)	29.2 (52)	28.4 (58)	23.1 (41)	25.0 (266)
Large-sized	30.2 (5)			30.4 (5)	29.0 (1)	39.0 (5)	29.5 (4)	32.2 (20)
Total	20.0 (34)	19.2 (28)	31.0 (1)	24.1 (84)	28.6 (59)	28.5 (71)	22.7 (55)	25.0 (332)

Table 4.21: The average length (in millimeters) of specimens per body size class in each sub-layer of Occupation B. The number of specimens is in the parentheses.

Sublayer	Type of Fracture			Total
	Dry	Fresh	Mixed: Fresh and Dry	
Va	50 (72.5)	1 (1.4)	12 (17.4)	69 (100)
Vb	32 (91.4)	2 (5.7)	1 (2.9)	35 (100)
Vb/Vc	-	1 (100)	-	1 (100)
Vc	62 (50.8)	28 (22.9)	28 (22.9)	122 (100)
Vd	26 (25.5)	30 (29.4)	45 (44.1)	102 (100)
Ve	32 (23.5)	47 (34.5)	38 (27.9)	136 (100)
Vf	52 (54.2)	21 (21.9)	18 (18.8)	96 (100)
Total	254 (45.3)	130 (23.2)	143 (25.5)	561 (100)

Table 4.22: The percentage of dry, fresh, and mixed fractures in each sublayer of Occupation B. Va is the most recent sublayer and Vf is the oldest sublayer. The percentage is listed in parentheses.

Anthropic marks were identified on 34 fragments in Occupation B with the majority of them being cut marks (79.4%, Table 4.23). Of those anthropic marks, the majority of them were located on specimens identified as *Testudo* (Table 4.24). Most of the cut and scrape marks (83.8%) are located on the diaphysis of long bone fragments. Cut and scrape marks in these locations were mostly assigned to defleshing activities. Burnt remains were also identified (n=41). Most of the burnt (63.4%) specimens were only lightly burnt. A small percentage of specimens are calcined (4.9%; Table 4.25). No evidence of carnivore or raptor activity was identified in Occupation B. For this reason, their impact on the faunal accumulation seems minimal.

Type of Mark	Va		Vc		Vd		Ve		Vf		Total		% of total assemblage
	N	%	N	%	N	%	N	%	N	%	N	%	
Cut marks	1	100	9	90.0	7	58.3	5	83.3	5	100	27	79.4	4.7
Scrape Marks			1	10.0	4	33.3	1	16.7			6	17.6	1.0
Percussion Notches					1	8.3					1	2.9	0.2
Total Marks	1	100	10	100	12	100	6	100	5	100	34	100	6.0

Table 4.23: Number and percentage of anthropogenic marks identified in the sublayers of Occupation B.

Species	Cut Marks		Scrape Marks		Percussion Notches		Total Number of Marks per Species	
	N	%	N	%	N	%	N	%
Caprine	2	22.2	1	50.0	1	100	4	33.3
Cervus	2	22.2					2	16.7
Testudo	5	55.6	1	50.0			6	50.0
Total	9	100	2	100	1	100	12	100

Table 4.24: Number and percentage of anthropogenic marks by species and type of mark in Occupation B.

Color	Va		Vb		Vc		Vd		Ve		Vf		Total		% of total assemblage
	N	%	N	%	N	%	N	%	N	%	N	%	N	%	
Brown					4	80.0	5	100	14	63.6	3	37.5	26	63.4	4.6
Brown/Gray			1	100					3	13.6	2	25.0	6	14.6	1.0
Brown/Black									3	13.6			3	7.3	0.5
Black									1	4.5			1	2.4	0.2
Black/Gray									1	4.5	1	12.5	2	4.9	0.3
Gray					1	20.0					1	12.5	2	4.9	0.3
Gray/White											2	25.0	2	4.9	0.3
Total	0	0	1	100	5	100	5	100	22	100	8	100	41	100	7.2

Table 4.25: Breakdown of burned specimens identified in the sublayers of Occupation B. Vb is the topmost sublayer with burnt remains and Vf is the bottommost sublayer.

A kernel density model and average nearest neighbor analysis (observed: 0.039063, expected: 0.154357,  $p < 0.001$ ) shows that the faunal remains are clustered along the left-hand (eastern) portion of the shelter (Figure 4.5). The densest clusters are observed in squares D2 and C2, while a second cluster occurs between columns D and C in row 6.

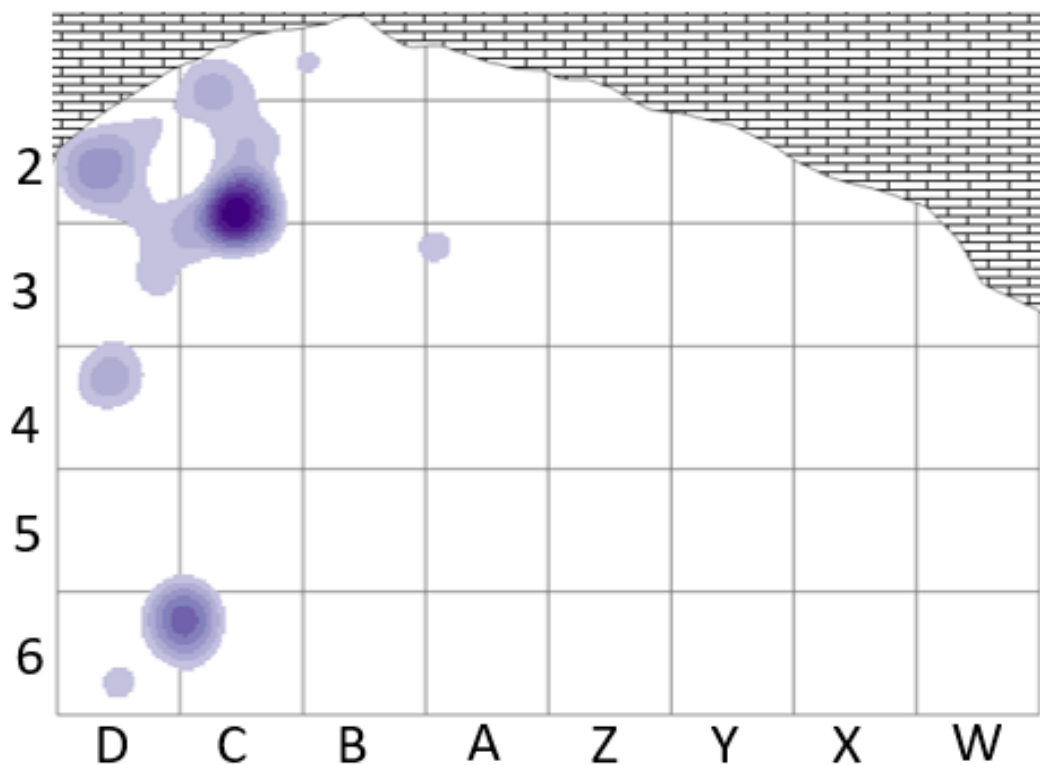


Figure 4.5: Kernel density model of Occupation B. The darker the color the denser the accumulation of faunal material. Each square is 1 x 1m.

#### 4.3 Finer Time Scale: Patterns Between Sublayers in Occupation B

In Occupation B, most of the specimens originate from sublayers Ve (24.0%) followed by sublayer Vc (21.4%). The sublayers show little variation in the proportion of specimens with manganese and concretions (Figure 4.7). However, there appears to be a small spike in weathering and erosion representation in sublayer Vb (Figure 4.6).

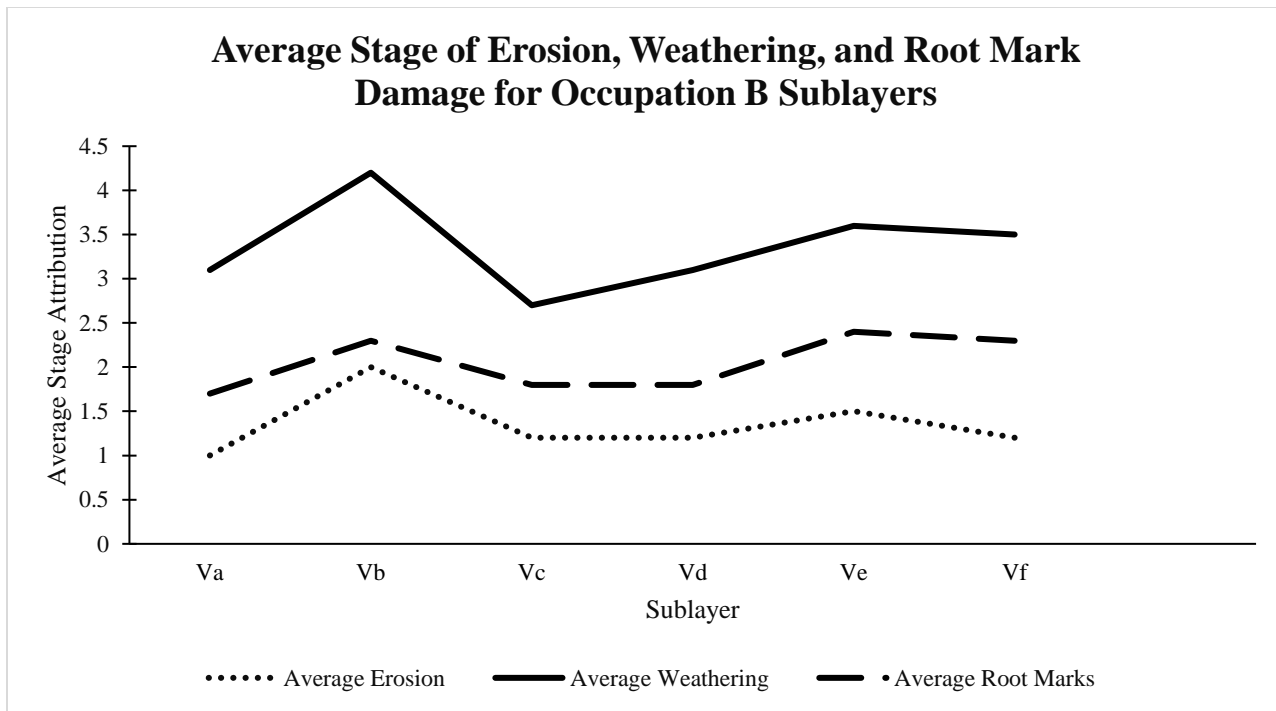


Figure 4.6: The average level of erosion, weathering, and root mark damage in the sublayers of Occupation B.

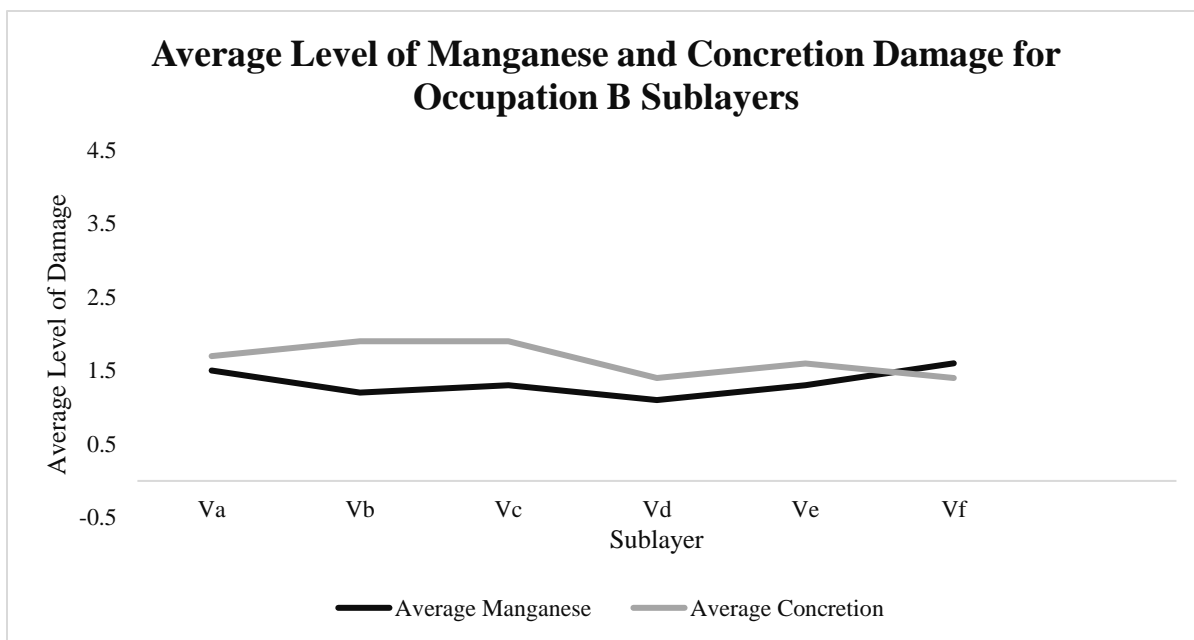


Figure 4.7: The average level of manganese and concretion damage in the sublayers of Occupation B. Va is the topmost sublayer and Vf is the bottommost sublayer.



The sublayers are mostly composed of identified specimens. However, sublayer Va has slightly more indeterminate than identified specimens (Figure 4.8). Although the difference in distribution of identified remains compared to indeterminate specimens is statistically significant ( $\chi^2 = 13.817$ ,  $p < 0.0168$ ), the effect size is small (Cohen's  $w$  index = 0.16; Table 4.24). Given that almost all of the sublayers, except for sublayers Vd and Vf, are significantly different, there is no clear pattern. This lack of patterning and the small effect size suggests that this difference may be the result of bias in methodology, rather than a result of human behavior.

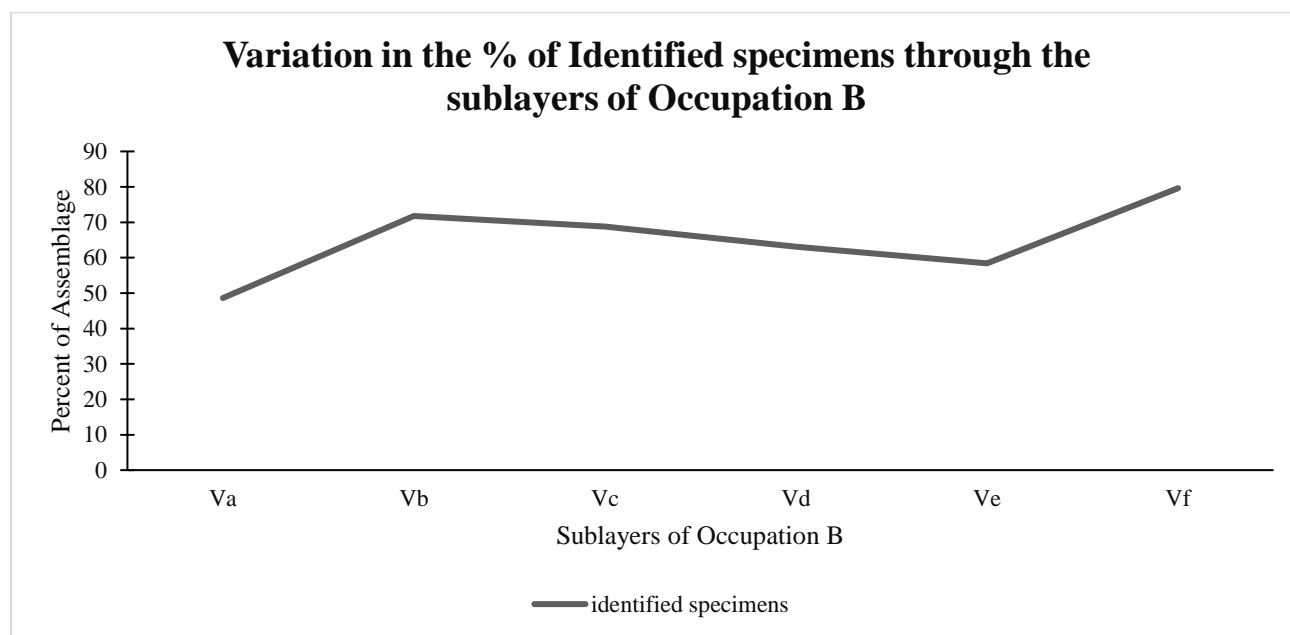


Figure 4.8: The percentages of determinate and indeterminate specimens through the sublayers of Occupation B. Va is the most recent sublayer and Vf is the oldest sublayer.

Sub-layer	Residual		<i>p</i> -value	
	Indeterminate	Identified	Indeterminate	Identified
Va	<b>1.74</b>	<b>-1.74</b>	<b>0.041</b>	<b>0.041</b>
Vb	<b>-1.79</b>	<b>1.79</b>	<b>0.037</b>	<b>0.037</b>
Vc	<b>-2.70</b>	<b>2.70</b>	<b>0.003</b>	<b>0.003</b>
Vd	0.20	-0.20	0.420	0.420
Ve	<b>1.73</b>	<b>-1.73</b>	<b>0.042</b>	<b>0.042</b>
Vf	0.45	-0.45	0.326	0.326

Table 4.26: Adjusted standardized residuals and *p*-values for the chi-square analysis of the distribution of identified and indeterminate specimens for the sublayers of Occupation B. Statistically significant outliers are in bold. Counts are drawn from Table 4.30.

Birds, caprines, cervids, rabbits, and tortoise are present in the sublayers of Occupation B (Figure 4.9). Caprines dominate in all sublayers except for sublayer Ve. Likewise, the body size data indicates that medium-size mammals dominate through all sublayers of Occupation B (Figure 4.10). The distribution of tortoise remains compared to the distribution of all other identified taxa is significantly different between the sublayers ( $\chi^2=22.705$ ,  $p<0.000$ ) with a large effect size (Cohen's *w* index= 0.52). The residuals indicate that the tortoise remains from sublayers Vb, Vc, and Ve contribute most to this difference (Table 4.25). In comparison to the other sublayers, the significantly higher proportion of tortoise remains—as indicated by an analysis of the residuals—likely contributes largely to the general increase in small-sized taxa in sublayer Vc. Overall, the distribution between body size classes through the sublayers varies significantly ( $\chi^2 = 18.413$ ,  $p<0.0484$ ), although it has a small effect size (Cohen's *w* index= 0.24, Table 4.27; Figure 4.11). For this reason, the observed pattern may have only limited implications in terms of cultural behavior.

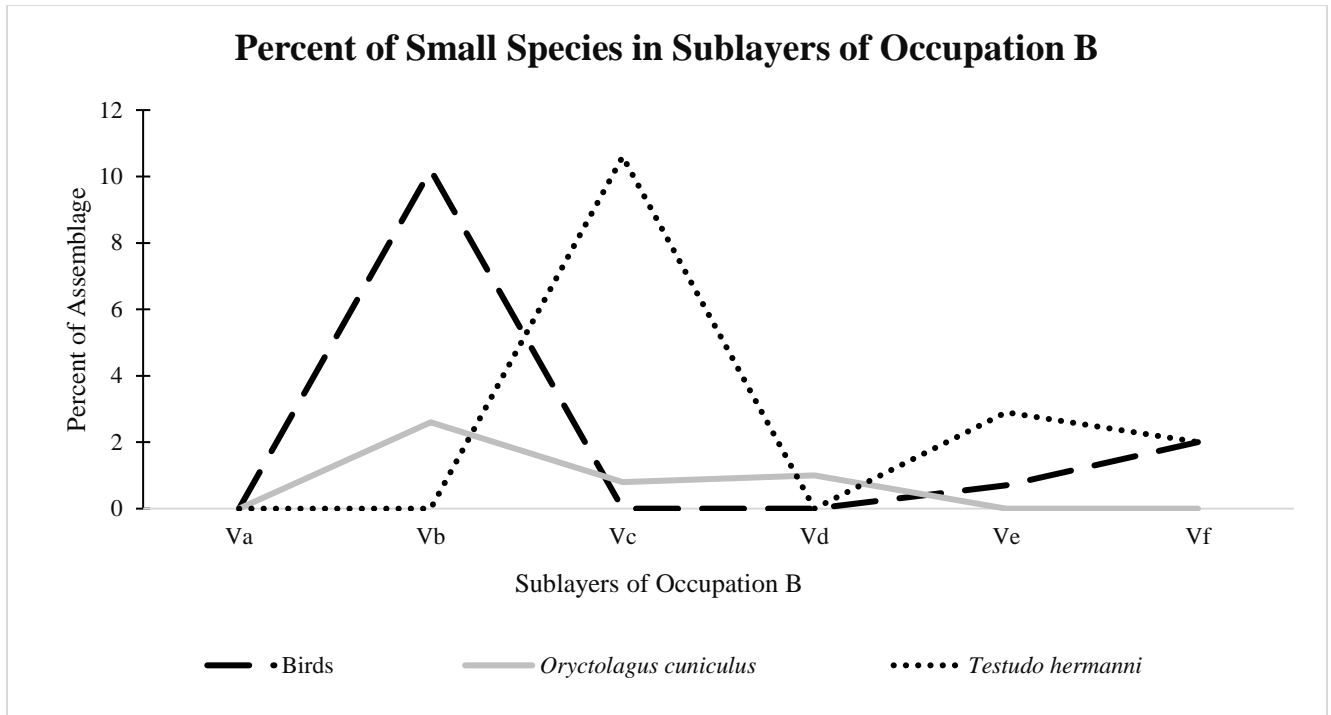


Figure 4.9: Percent of small-sized species through the sublayers of Occupation B.

Sublayers	Residuals		<i>p</i> -values	
	Tortoise	Other taxa	Tortoise	Other taxa
Va	<b>-1.81</b>	<b>1.81</b>	<b>0.035</b>	<b>0.035</b>
Vb	<b>-2.38</b>	<b>2.38</b>	<b>0.009</b>	<b>0.009</b>
Vc	<b>3.00</b>	<b>-3.00</b>	<b>0.001</b>	<b>0.001</b>
Vd	<b>-1.81</b>	<b>1.81</b>	<b>0.035</b>	<b>0.035</b>
Ve	<b>2.70</b>	<b>-2.70</b>	<b>0.003</b>	<b>0.003</b>
Vf	-0.19	0.19	0.425	0.425

Table 4.27: Adjusted standardized residuals and *p*-values for the chi-square analysis of the distribution of tortoises through the sublayers of Occupation B compared to other identified taxa. Statistically significant outliers are in bold. Counts are drawn from Table 4.15.

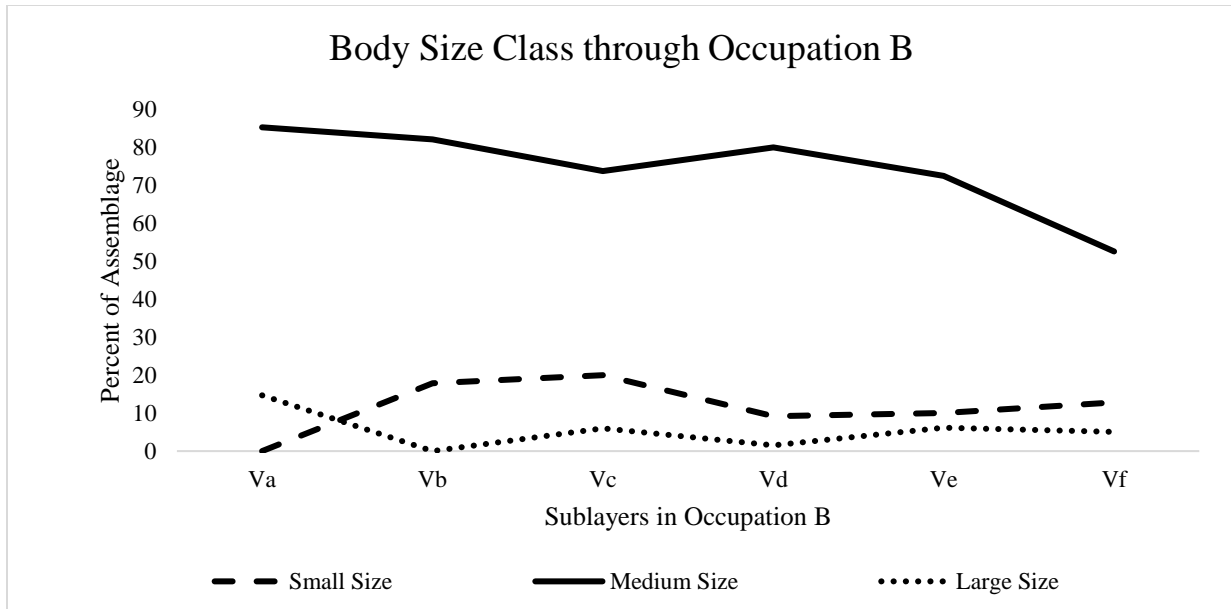


Figure 4.10: Percent of variation in body size classes (small, medium, and large) through the sublayers of Occupation B. Va is the most recent sublayer and Vf is the oldest sublayer.

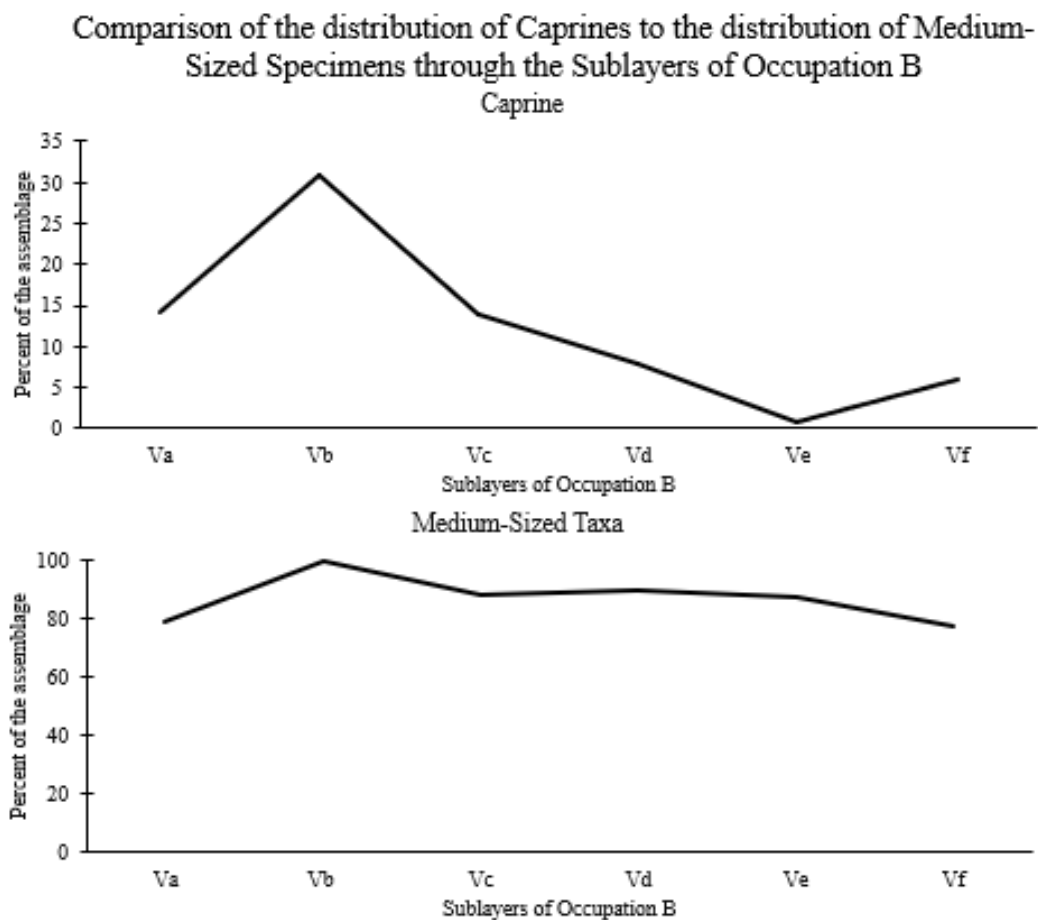


Figure 4.11: Comparing the percentage of caprines versus medium-sized mammals through the sublayers of Occupation B.

Sub-Layer	Residuals			<i>p</i> -values		
	Small	Medium	Large	Small	Medium	Large
Va	<b>-2.47</b>	0.81	<b>2.24</b>	<b>0.007</b>	0.210	<b>0.013</b>
Vb	0.63	0.29	-1.40	0.236	0.387	0.080
Vc	<b>1.94</b>	<b>-1.66</b>	-0.04	<b>0.026</b>	<b>0.048</b>	0.484
Vd	-0.91	<b>1.71</b>	-1.55	0.181	<b>0.043</b>	0.061
Ve	-0.72	0.39	0.40	0.235	0.349	0.345
Vf	1.01	-1.12	0.42	0.157	0.131	0.337

Table 4.28: Adjusted standardized residuals and *p*-values for chi-square analysis of the comparison of body size class distribution for each of the sublayers of Occupation B. Statistically significant outliers are in bold. Counts are drawn from Table 4.21.

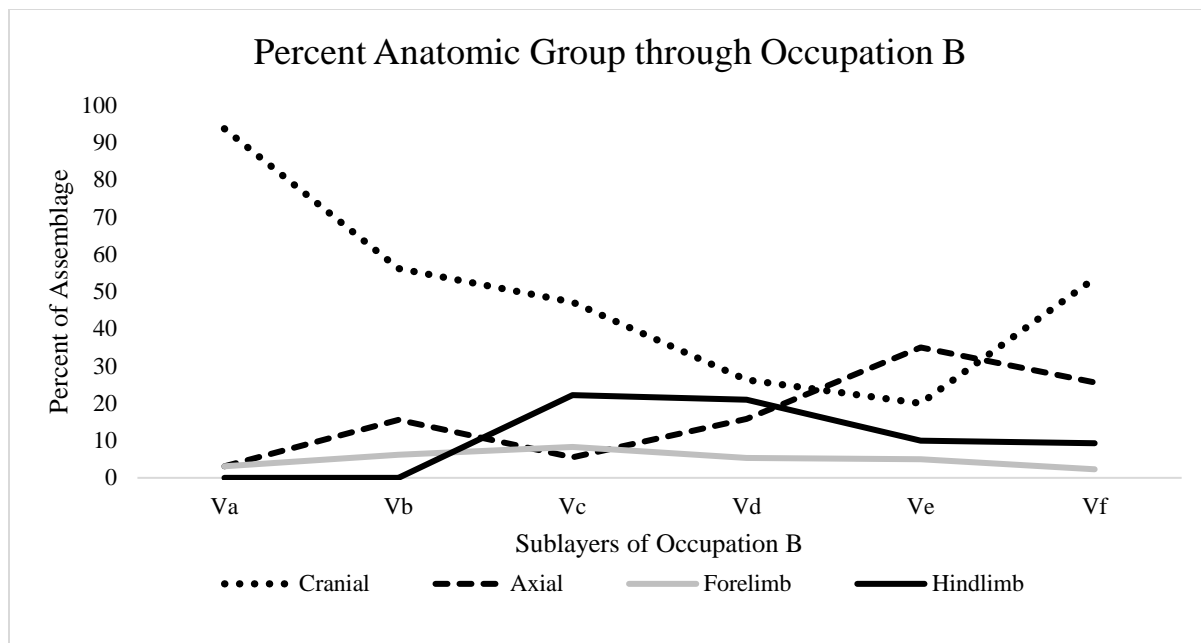


Figure 4.12: Variation in the percentage of the anatomic groups (cranial, axial, forelimb, and hindlimb) through the sublayers of Occupation B. Va is the most recent sublayer and Vf is the oldest sublayer.

As noted above, cranial remains are the most common element in Occupation B.

However, in sublayer Ve, axial remains are more common (Figure 4.12). The distribution of cranial remains is significantly different than that for the axial remains with a moderate effect size ( $\chi^2=21.410$ ,  $p<0.0007$ , Cohen's  $w$  index= 0.41; Table 4.27). The proportion of cranial remains significantly increase from sublayers Va and Ve ( $\chi^2_{\text{trend}}: 16.487$   $p\text{-value}<0.000$ ).

Throughout the sublayers of Occupation B, the proportion of forelimbs remains relatively constant whereas hindlimbs changes markedly. However, the overall difference between forelimbs and hindlimbs cannot be tested for statistical significance because the sample sizes are too small.

Sub-layer	Residual		<i>p</i> -value	
	Cranial	Axial	Cranial	Axial
Va	<b>3.01</b>	<b>-3.01</b>	<b>0.001</b>	<b>0.001</b>
Vb	0.16	-0.16	0.436	0.436
Vc	1.40	-1.40	0.080	0.080
Vd	-1.01	1.01	0.157	0.157
Ve	<b>-3.35</b>	<b>3.35</b>	<b>0.000</b>	<b>0.000</b>
Vf	-1.51	1.51	0.065	0.065

Table 4.29: Residuals and *p*-values for comparison of the distribution of cranial versus axial remains in the sublayers of Occupation B. Statistically significant outliers are in bold. Counts are drawn from Table 4.17.

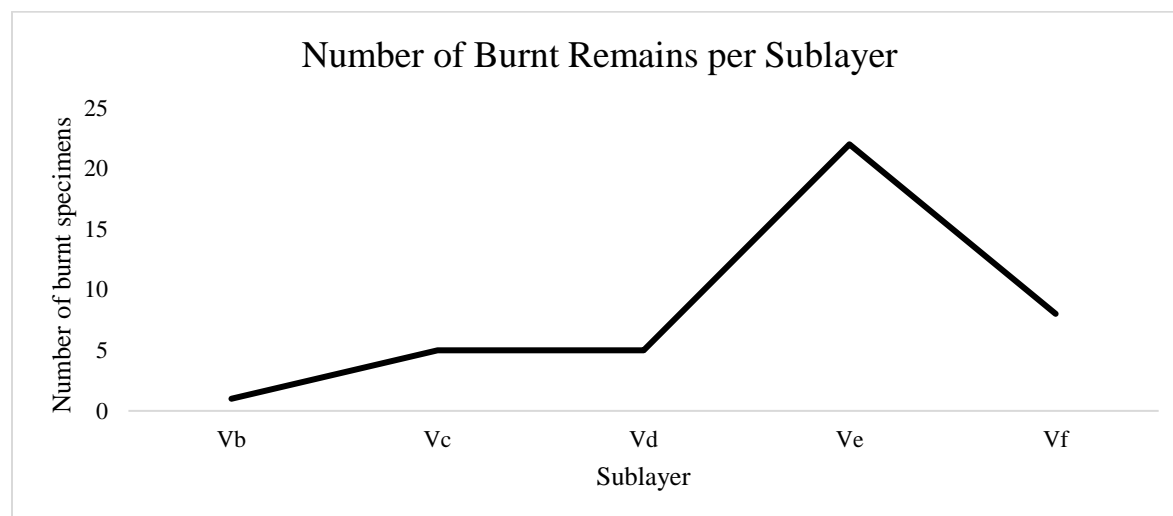


Figure 4.13: The number of burnt specimens per sublayer of Occupation B. Vb is the topmost sublayer with burnt remains and Vf is the bottommost sublayer.

Except for sublayer Va, all sublayers in Occupation B contain burnt specimens. Sublayer Ve has the highest proportion of burnt specimens (52.4%; Figure 4.13). Lightly burnt remains are present in all sublayers that have burnt specimens. Severely burnt specimens are concentrated in sublayers Vf and Ve. In the sequence, there is a statistically significant increase of burnt

remains relative to unburnt remains from sublayer Va to sublayer Ve ( $\chi^2_{\text{trend}}: 20.158; p\text{-value} < 0.000$ ).

Anthropogenic marks are present in most sublayers. They are most common in sublayer Vd (Figure 4.14). Since there are only 39 instances of anthropogenic marks in Occupation B, the sample size does not meet the small frequencies requirements suggested by Zar (1996) to perform a chi-square analysis. However, cut marks are the most frequent type of mark in all sublayers.

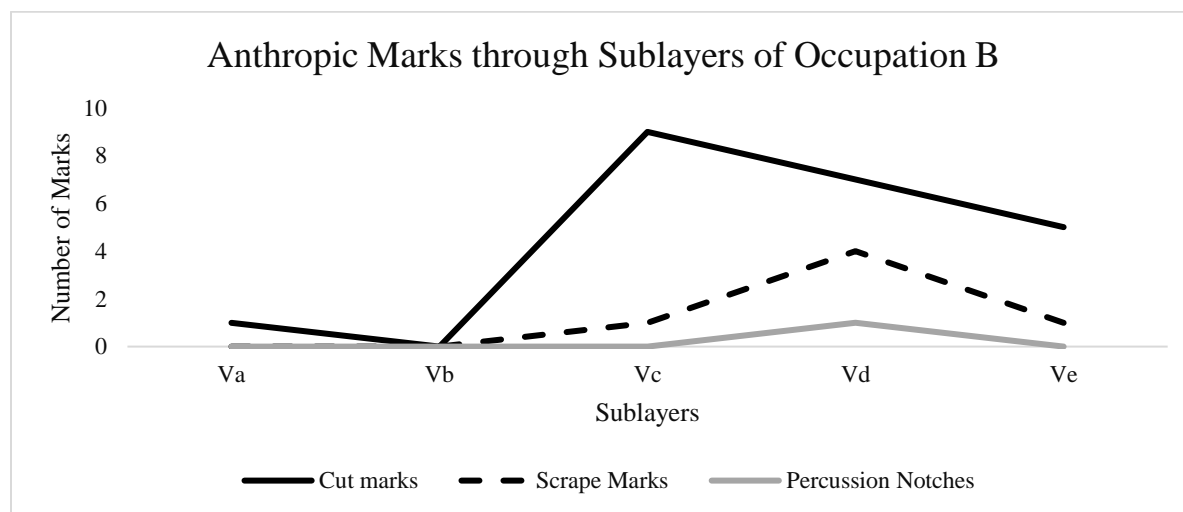


Figure 4.14 Anthropogenic marks through the sublayers of Occupation B.

#### 4.4 Comparison of the two Occupation Events

There are slight variations between the sublayers of Occupation B. Particularly significant differences were observed in the proportion of different body size classes, as well as in patterns of skeletal representation. Given these differences, it is likely that Occupation B is



comprised of multiple events. However, with some of the differences in distribution that tend to be small (i.e., differences in taxonomic composition and anthropic activity), Occupation B can be combined into a single palimpsest that can be compared with Occupation A. Occupation A is stratigraphically distinct, and composed of a single sublayer, making it likely that it is the result of one or few limited occupation events.

Sublayer	Occupation B														Occupation A			
	Va		Vb		Vb/Vc		Vc		Vd		Ve		Vf		Total		Vd	
	N	%	N	%	N	%	N	%	N	%	N	%	N	%	N	%	N	%
Identified	34	48.6	28	71.8	1	100	84	68.8	65	63.1	80	58.4	78	79.6	370	64.9	53	93.0
Indeterminate	36	51.4	11	28.2			38	31.1	38	36.9	57	41.6	20	20.4	200	35.1	4	7.0
<b>Total</b>	<b>70</b>	<b>100</b>	<b>39</b>	<b>100</b>	<b>1</b>	<b>100</b>	<b>122</b>	<b>100</b>	<b>103</b>	<b>100</b>	<b>137</b>	<b>100</b>	<b>98</b>	<b>100</b>	<b>570</b>	<b>100</b>	<b>57</b>	<b>100</b>

Table 4.30: Identified versus unidentified specimens per occupation and sublayer. Va is the most recent sublayer and Vf is the oldest sublayer.

	Occupation A				
	>0-25	35-50	50	>50-75	80-100
Erosion	25 (80.6)	4 (12.9)	1 (3.2)	1 (3.2)	-
Root Marks	14 (70.0)	4 (20.0)	-	2 (10.0)	-
Concretions	27 (71.0)	8 (21.0)	-	1 (2.6)	2 (5.3)
Manganese	47 (90.4)	5 (9.6)	-	-	-
<b>Total</b>	<b>113 (80.1)</b>	<b>21 (14.9)</b>	<b>1 (0.7)</b>	<b>4 (2.8)</b>	<b>2 (1.4)</b>
	Occupation B				
Erosion	211 (64.5)	56 (17.1)	24 (7.3)	16 (4.9)	20 (6.1)
Root Marks	131 (49.8)	50 (19.0)	36 (13.7)	18 (6.8)	28 (10.6)
Concretions	216 (62.4)	62 (17.9)	40 (11.6)	20 (5.8)	10 (2.9)
Manganese	357 (74.7)	83 (17.4)	33 (6.9)	5 (1.0)	-
<b>Total</b>	<b>915 (64.6)</b>	<b>251 (17.7)</b>	<b>133 (9.4)</b>	<b>59 (4.2)</b>	<b>58 (4.1)</b>

Table 4.31: Percentage of overall post-depositional damage including the effects of concretions, erosion, weathering, root marks, and manganese for Occupation A and Occupation B.

The Occupation A assemblage is obviously smaller in size than Occupation B. Both assemblages have a greater number of identified specimens than indeterminate specimens (Table 4.28). However, this is likely due to the bias created by only using piece-plotted faunal remains. Although both Occupations A and B are relatively well-preserved, Occupation B has slightly higher levels of post-depositional damage. Specifically, Occupation B, on average, has more weathering, root marks, and manganese (Table 4.29). Both assemblages are dominated by caprines and have similar proportions of *Testudo hermanni* remains (3.5% in Occupation A and 3.3% in Occupation B).

Both occupations have evidence of anthropogenic activity including percussion notches, scrape marks, cut marks (Figure 4.15), and burnt remains. Occupation A has limited evidence of anthropic activity, but a higher proportion of anthropic activity compared to Occupation B (17.5% and 13.9% respectively). The assemblages have similar distributions of cut marks, scrape marks, and percussion notches (Table 4.7 and Table 4.14). Additionally, both Occupation A and Occupation B's anthropic marks occur mostly on small-sized taxa (Table 4.8 and Table 4.24). Occupation B has a slightly higher proportion of burnt remains compared to Occupation A (7.7% and 3.6% respectively). Moreover, Occupation A shows the presence of lightly burnt remains while Occupation B includes lightly burnt to calcined remains.

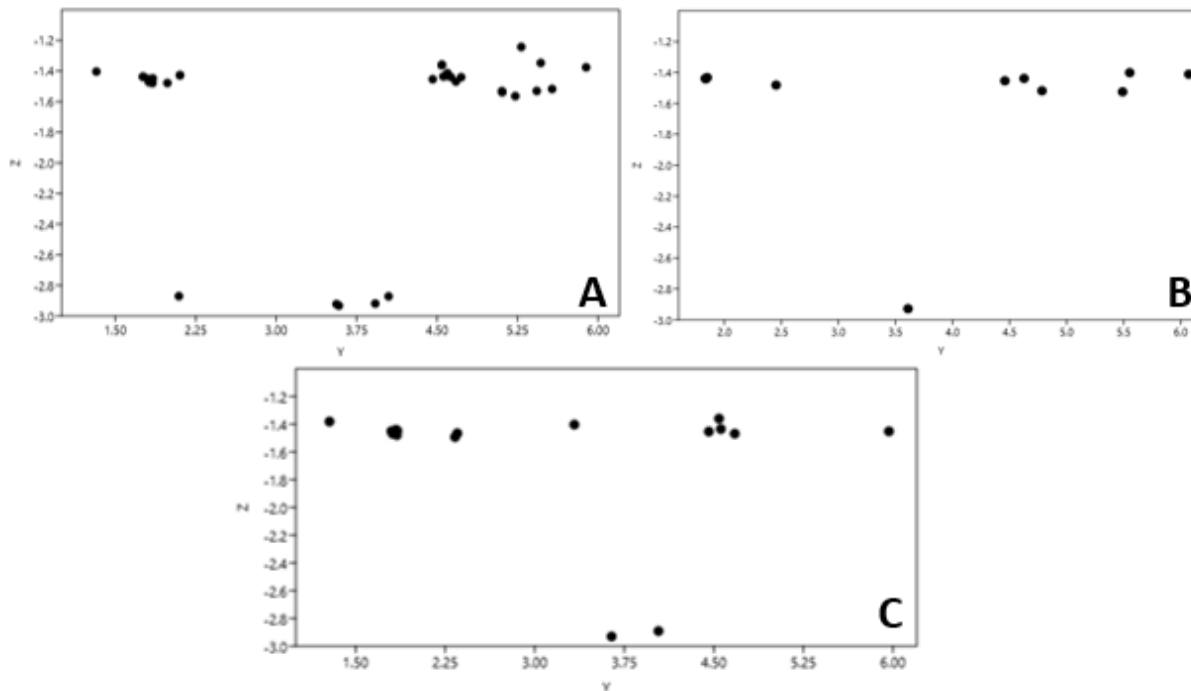


Figure 4.15: Vertical distribution of anthropic marks. A) cut marks B) percussion notches C) scrape marks.

#### 4.5 Summary

Layer V of Abric del Pastor is composed of two occupation events: Occupation A and Occupation B. The occupations show only minor differences in taphonomic and anthropic evidence. Overall, these two relatively well-preserved anthropogenic accumulations are dominated by medium-sized taxa but include small and large-sized taxa as well. The similar patterns between occupations suggests consistent behavioral patterns within layer V.

## Chapter 5: Discussion and Concluding Remarks

In the previous chapter, I outlined the results of the faunal analysis for layer V of Abric del Pastor. In this chapter, I will revisit my research questions: 1) what species were exploited by Neanderthals? 2) what agents were involved in the deposition of the faunal remains? 3) what activities took place during these accumulation events? 4) can we identify finer periods of accumulation in the stratigraphy? Lastly, I will touch on the limitations of this work, directions for future research, and provide concluding remarks.

### 5.1 What species were exploited?

The layer V faunal assemblage is comprised of small-, medium- and large-sized taxa encompassing a range of species. Medium-sized taxa are predominant. Although bird and micromammal fragments were identified, it is likely that these are naturally accumulated remains as they are few in number and have no observed anthropic marks. Additionally, no fish specimens have been noted at Abric del Pastor. The taxonomic breakdown is similar to other MIS 5–3 sites in the region including Teixoneres Cave (Lopez-Garcia et al. 2012; Álvarez-Lao et al. 2017; Rufà et al. 2014; Rosell et al. 2010), Navalmaillo rock shelter (Moclán et al. 2021), Abric Romani (Gabucio et al. 2016; Gabucio, Fernandez-Laso and Rosell 2017), Bolomor Cave (Blasco and Fernandez Peris 2012a; Blasco and Fernandez Peris 2012b; Sañudo, Blasco, and Fernandez Peris 2016), and Cueva Antón (Sanz et al. 2019; Zilhão et al. 2016)).

Despite the sequence dating to MIS 4—a relatively cool period—no cold-adapted mammals (i.e., woolly mammoth, woolly rhinoceros, reindeer, arctic fox, etc.) were identified.

This was not unexpected as these species were rare in the Iberian Peninsula until 44 ka BP. Moreover, the prevalence of cold-adapted species decreases moving south through the Iberian Peninsula (Alvarez-Lao and Garcia 2011). Similarly, other MIS 4 cave sites, like Navalmaillo rock shelter, also lack or have very few remains of cold-adapted species (Álvarez-Lao et al. 2017; Moclán et al. 2021).

While cold-adapted mammals are absent, Abric del Pastor has an abundance of *Testudo* remains. *Testudo* are typically found in warmer climates (Couturier et al. 2014; Sibeaux et al. 2016; Defleur and Desclaux 2019). The relative abundance of tortoise remains coupled with the absence of cold-adapted mammals points to the Abric del Pastor sequence being formed under temperate conditions during MIS 4. If we use the evidence from Abric del Pastor as a proxy, the present results suggest that the southern Iberian Peninsula may have been more temperate than anticipated. Alternately, the results may indicate the existence of a short warm interstadial within MIS 4.

## **5.2 What agents and activities were involved in the deposition of the faunal remains?**

No evidence of activity by carnivores or birds of prey was noted in the assemblage. Therefore, their impact on the assemblage appears to have been minimal. Evidence of anthropic activity was observed. Percussion notches, cut marks, and scrape marks point to carcass processing activities performed by hominins, including defleshing, and marrow cracking. This evidence indicates that the shelter was used to process and consume animals. Given that no complete carcasses were identified, it is likely that the animals were killed at another location and brought back to the rock shelter. Additionally, a hearth was identified as well as burnt faunal

remains. Although most of the anthropic evidence was observed on medium-sized taxa, *Testudo* remains have cut marks, scrape marks, and thermo-alterations which indicate that inhabitants of Abric del Pastor were exploiting small game as food resources during the Middle Paleolithic. The evidence from Abric del Pastor as well as other sites like Bolomor Cave (Blasco 2008; Blasco and Peris 2012a; Blasco and Peris 2012b) indicate that some small game procurement occurred during the Middle and Late Pleistocene (Blasco et al. 2022). Besides *Testudo* remains, rabbit specimens are few. No anthropic activity was observed on the rabbit fragments. Therefore, it is difficult to say whether these remains were the result of natural accumulations or anthropic activity. Ultimately, the anthropic activities identified in the layer V assemblage are typical of other cave shelters in the region.

The relative proportions of anatomical elements can be used to understand the possible procurement and transport strategies of early hominins (Binford 1978; Morin 2007). Occupation A has mostly forelimb fragments followed by cranial and axial specimens. The abundance of forelimb remains could point toward a focus on bone grease while the cranial and axial fragments imply a focus on meat procurement. Skeletal element distribution suggests that the transport decisions were based on a combination of both meat and grease resources. However, there is no independent indicators of bone grease rendering like crushing, tearing, or embedded lithic material in the cortical bone (Morin and Soulier 2017). The presence of cancellous bone was noted; however, this is insufficient evidence for arguing that bone grease rendering activities occurred at the site. Additionally, a few cut marks on long bone fragments were observed that suggest meat procurement, but the overall small number of remains with marks of anthropic activity in Occupation A makes it difficult to reach robust conclusions about overall procurement and transport strategies.

In Occupation B, the majority of remains are either cranial or axial, which likewise suggests that the inhabitants were focused on meat procurement. However, hindlimbs are more common than forelimbs which may indicate a secondary preference for marrow, as hindlimb elements tend to have greater quantities of marrow. Moreover, scrape marks, and percussion notches were observed on a caprine mandible, as well as cut marks on a caprine hyoid bone, and cut and scrape marks on long bones of small- and medium-sized taxa that further suggest a focus on meat consumption.

### **5.3 Can we identify finer periods of accumulation?**

Given the sterile layer between Occupation A and Occupation B, we can assume that at the very least layer V encompasses two occupation events with a period of “abandonment” in between. It is likely that there were more than two occupation events, however. This is because micromorphological changes in the sediment, and variation in patterns of skeletal element representation between sublayers that are consistent with more than one occupation event being represented. Variations in taxonomic distribution and anthropic activity were also observed although these are subtle. In essence, it is likely that there were at least two occupation events within layer V with the possibility of up to eight identifiable events if each sublayer is counted separately.

### **5.4 Limitations and Future Research Directions**

Although this zooarchaeological and taphonomic analysis was meant to be comprehensive, there are a few limitations to this research. First and foremost, only the plotted

faunal remains were considered in this analysis. Over 1,300 faunal fragments were recovered and analyzed from layer V. However, less than half (n=570) of the specimens were plotted. This could have led to biases in terms of body size class representation and taxonomic distribution, given that larger fragments are more likely to be piece-plotted during the excavation. Additionally, excavation and field practices tend to produce biases toward larger specimens over smaller fragments. This might have contributed to a lower representation of small game in the samples, including birds and leporids.

Another limitation is the lack of data on mortality profiles and sex ratios due to the small size of the samples. These data could have shed light on seasonal patterns of occupation. Likewise, the fact that a single layer was examined means that little can be said on long-term changes in subsistence practices. Future work should focus on an in-depth comparison between layers IV and V of Abric del Pastor to better understand shifts in subsistence behavior and adaptation to climate change.

Future research should compare the zooarchaeological remains to the lithic specimens as this may aid in illuminating subsistence behaviors as well as improving our understanding of how the cave was used over time. For instance, if there is a direct association between Mariola retouched flakes—which have been identified in layer IVf—and specimens with cut marks, we may be able to infer that carcass processing was occurring within a specific area of the rock shelter (Sossa-Ríos et al. 2022). Additionally, a comprehensive analysis considering all potential lines of evidence may provide a clearer picture of the type, duration, and intensity of anthropic activity and occupation of Abric del Pastor than possible with zooarchaeological data alone.



## **5.5 Concluding Remarks**

The layer V faunal remains from Abric del Pastor are the result of repetitive anthropic occupation events where carcasses were transported back to the site for processing and consumption. The assemblage is very typical of other MIS 5–3 rock shelter sites in the Iberian Peninsula. However, it is one of very few layers that securely dates within MIS 4 thus filling an essential gap in the literature on how hominins adapted to the changing environmental conditions in Middle Paleolithic Iberia.

REFERENCES CITED

Álvarez-Lao, D.J., Kahlke, R.D., García, N. and Mol, D.

- 2009 The Padul mammoth finds—On the southernmost record of *Mammuthus primigenius* in Europe and its southern spread during the Late Pleistocene. *Palaeogeography, Palaeoclimatology, Palaeoecology*, 278(1-4): 57-70.

Álvarez-Lao, D. J., and N. García

- 2010 Chronological distribution of Pleistocene cold-adapted large mammal faunas in the Iberian Peninsula. *Quaternary International* 212(2): 120-128.
- 2011 Geographical distribution of Pleistocene cold-adapted large mammal faunas in the Iberian Peninsula. *Quaternary International* 233(2): 159-170.

Álvarez-Lao D. J., F. Rivals, C. Sánchez-Hernández, R. Blasco, J. Rosell

- 2017 Ungulates from Teixonerres Cave (Moià, Barcelona, Spain): Presence of cold-adapted elements in NE Iberia during the MIS 3. *Palaeogeography, Palaeoclimatology, Palaeoecology* 466: 287-302.

Angelucci, D. E., D. Anesin, D. Susini, V. Villaverde, J. Zapata, J. Zilhão

- 2013 Formation processes at a high resolution Middle Paleolithic site: Cueva Antón (Murcia, Spain). *Quaternary International* 315: 24-41.

Bailey, G.

- 1981 Concepts, timescales and explanations in economic prehistory. In *Economic Archaeology*, Vol. 9, edited by A. Sheridan and G. Bailey, pp. 97-117. British Archaeological Reports International Series, Oxford.

- 1983 Concepts of time in Quaternary prehistory. *Annual Review of Anthropology* 12: 165-192.
- 1987 Breaking the time barrier. *Archaeological Review from Cambridge* 6: 5-20.
- 2005 Concepts of time. In *Archaeology: The key concepts*, edited by C. Renfrew and P. Bahn, pp.268-273, Routledge, London.
- 2007 Time perspectives, palimpsests and the archaeology of time. *Journal of Anthropological Archaeology* 26: 198-223.
- 2008 Time perspectivism: origins and consequences. In *Time in archaeology: time perspectivism revisited*, edited by Simon Holdaway and LuAnn Wandsnider, LuAnn, pp. 13-30, Utah University Press, Utah.
- Ballesteros D., A. Álvarez-Vena, M. Monod-Del Dago, L. Rodríguez-Rodríguez, J. Sanjurjo Sánchez, D. Álvarez-Lao, C. Pérez-Mejías et al.
- 2020 Paleoenvironmental evolution of Picos de Europa (Spain) during marine isotopic stages 5c to 3 combining glacial reconstruction, cave sedimentology and paleontological findings. *Quaternary Science Reviews* 248: 106581.
- Banning, E.B
- 2002 Quantification: Abundance and other measures in archaeology. In *The archaeologist's laboratory interdisciplinary contributions to archaeology* edited by M.A., Jochim, and R.S. Dickens. Springer, Boston, MA.
- Barone, R.
- 1976 *Anatomie comparée des mammifères domestiques. Tome premier: Ostéologie*. Vigot Frères, Paris.
- Binford, L.R.

- 1978 *Nunamiut ethnoarchaeology*. Academic Press, New York.
- 1981 Behavioral archaeology and the “Pompeii Premise.” *Journal of Anthropological Research* 37: 195–208.
- 1984 Butchering, sharing, and the archaeological Record. *Journal of Anthropological Archaeology* 3: 235-257.

Blasco, R.

- 2008 Human consumption of tortoises at Level IV of Bolomor Cave (Valencia, Spain). *Journal of Archaeological Science* 35(10): 2839-2848.

Blasco, R. and Fernandez Peris, J.

- 2012a A uniquely broad spectrum diet during the Middle Pleistocene at Bolomor Cave (Valencia, Spain). *Quaternary International* 252: 16-31.
- 2012b Small and large game: human use of diverse faunal resources at Level IV of Bolomor Cave (Valencia, Spain). *Comptes Rendus Palevol*, 11(4): 265-282.

Blasco, R., D. Cochard, A. C. Colonese, V. Laroulandie, J. Meier, E. Morin, A. Rufà, L. Tassoni, J. C. Thompson

- 2022 Chapter 8 - Small animal use by Neanderthals, In *Updating Neanderthals* edited by Francesca Romagnoli, Florent Rivals, and Stefano Benazzi, pp. 123-143. Academic Press, New York.

Burjachs, F. and Allue, E.

- 2003 Paleoclimatic evolution during the Last Glacial cycle at the NE of the Iberian Peninsula. *Quaternary climatic changes and environmental crises in the Mediterranean region*: 191-200.

Capaldo, S. D., and R. J. Blumenschine

1994 A quantitative diagnosis of notches made by hammerstone percussion and carnivore gnawing on bovid long bones. *American Antiquity* 59: 724-748.

Carvalho, M. and N. Bicho.

2022 Complexity in the Middle to Upper Paleolithic transition in peninsular Southern Europe and application of refugium concepts. *Journal of Quaternary Science*, 37(2): 380-393.

Castaños, P.M.

1988 Mamíferos prehistóricos de Vizcaya. *Caja de Ahorros Vizcaína*, Bilbao.

Connolly, R., M. Jambrina-Enríquez, A.V. Herrera-Herrera, P. Vidal-Matutano, A. Fagoaga, R. Marquina-Blasco, M. D. Marin-Monfort, et al.

2019 A multiproxy record of palaeoenvironmental conditions at the Middle Palaeolithic site of Abric del Pastor (Eastern Iberia). *Quaternary Science Reviews* 225: 106023.

Couturier, T., A. Besnard, A. Bertolero, V. Bosc, G. Astruc, M. Cheylan

2014 Factors determining the abundance and occurrence of Hermann's tortoise *Testudo hermanni* in France and Spain: Fire regime and landscape changes as the main drivers. *Biological Conservation* 170: 177-187.

Daura, J., M. Sanz, M. Demuro, L.J. Arnold, A.M. Costa, J. Moreno, M. da Conceição Freitas, et al.

2021 A new chronological framework and site formation history for Cova del Gegant (Barcelona): Implications for neanderthal and anatomically modern human occupation of NE Iberian Peninsula. *Quaternary Science Reviews* 270:107141.

Defleur, A. and E. Desclaux

2019 Impact of the Last Interglacial climate change on ecosystems and Neanderthals behavior at Baume Moula-Guercy, Ardèche, France. *Journal of Archaeological Science* 104.

Finlayson, C., F.G. Pacheco, J. Rodriguez-Vidal, D.A. Fa, J.M. Gutierrez López, A.S. Pérez, G. Finlayson, et al.

2006 Late survival of Neanderthals at the southernmost extreme of Europe. *Nature* 443: 850–853.

Finlayson, C. and Carrión, J. S.

2007 Rapid ecological turnover and its impact on neanderthal and other human populations. *Trends Ecol. Evol* 22: 213–222.

Fletcher W. J., M. Fernanda Sánchez Goñi, J. R.M. Allen, R. Cheddadi, N. Combourieu-Nebout, B. Huntley, I. Lawson, et al.

2010 Millennial-scale variability during the Last Glacial in vegetation records from Europe. *Quaternary Science Reviews* 29(21-22).

Foley, R.A.

1981 A model of regional archaeological structure. *Proceedings of the Prehistoric Society* 47, 1–17.

Gabucio, M. J., I. Cáceres, F. Rivals, A. Bargalló, J. Rosell, P. Saladié, J. Valverdú, M. Vaquero, E. Carbonell

2016 Unraveling a Neanderthal palimpsest from a zooarchaeological and taphonomic perspective. *Archaeological and Anthropological Sciences* 10: 197-222

Gabucio, M.J., M. Cristina Fernández-Laso and J. Rosell

2017 Turning a rock shelter into a home. Neanderthal use of space in Abric Romaní levels M and O. *Historical Biology* 30(6): 743-766.

Galván B., C. M. Hernández, C. Mallol, N. Mercier, A. Sistiaga, V. Soler

2014 New evidence of early neanderthal disappearance in the Iberian Peninsula. *Journal of Human Evolution* 75: 1-12.

Garralda, M.D., B. Galván, C.M. Hernández, C. Mallol, J.A. Gómez, and B. Maureille

2014 Neanderthals from El Salt (Alcoy, Spain) in the context of the latest Middle Palaeolithic populations from the southeast of the Iberian Peninsula. *Journal of Human Evolution*, 75: 1-15.

Gifford-Gonzalez, D.

2018 *An introduction to zooarchaeology*. Cham: Springer.

Grayson, D.K.

1984 *Quantitative zooarchaeology: topics in the analysis of archaeological faunas*. Academic Press, New York.

Harding, J.

2005 Rethinking the great divide: long-term structural history and the temporality of event. *Norwegian Archaeological Review* 38(2): 88-101.

Hardy, B.L., M.H. Moncel, C. Daujeard, P. Fernandes, P. Béarez, E. Desclaux, M.G.C. Navarro, S. Puaud, and R. Gallotti

2013 Impossible Neanderthals? Making string, throwing projectiles, and catching small game during Marine Isotope Stage 4 (Abri du Maras, France). *Quaternary Science Reviews* 82: 23-40.

Hillson, S.

- 1996 Mammal bones and teeth: An introductory guide to methods of identification  
The Institute of Archaeology. University of London.

Hillson, S.

- 2005 *Teeth*. Cambridge University Press.

Hockett, B., and J.A. Haws

- 2002 Taphonomic and methodological perspectives of leporid hunting during the Upper  
Paleolithic of the Western Mediterranean basin. *Journal of Archaeological  
Method and Theory* 9: 269–302.

Hodgkins, J., C. W. Marean, A. Turq, D. Sandgathe, S.J.P. McPherron, H. Dibble

- 2016 Climate-mediated shifts in Neandertal subsistence behaviors at Pech de l'Azé IV  
and Roc de Marsal (Dordogne Valley, France). *Journal of Human Evolution*, 96:  
1-18

Holdaway, Simon J. and LuAnn Wandsnider

- 2008 Time in archaeology: An introduction." In *time in archaeology: time  
perspectivism revisited* edited by Simon Holdaway and LuAnn Wandsnider,  
LuAnn, pp. 1-12, Utah University Press, Utah

Howard, H.

- 1930 A census of the Pleistocene birds of Rancho La Brea from the collections of  
the Los Angeles Museum. *Condor* 32: 81– 88.

Kjellström, E., J. Brandefelt, J.O. Näslund, B. Smith, G. Strandberg, A.H.L. Voelker, and

B. Wohlfarth



2010 Simulated climate conditions in Europe during the Marine Isotope Stage 3 stadial. *Boreas* 39: 436-456.

Lacombat, F.

2006 Morphological and biometrical differentiation of the teeth from Pleistocene species of *Stephanorhinus* (Mammalia, Perissodactyla, Rhinocerotidae) in Mediterranean Europe and the Massif Central, France. *Palaeontographica, Abteilung A*, 274: 71-111.

Lambrecht, G., and C. Mallol

2020 Autofluorescence of experimentally heated bone: Potential archaeological applications and relevance for estimating degree of burning, *Journal of Archaeological Science: Reports* 31: 102333.

Lopez-Garcia, J., H. A. Blain, F. Burjachs, A. Ballesteros, E. Allué, G. E. Cuevas-Ruiz et al.

2012 A multidisciplinary approach to reconstructing the chronology and environment of Southwestern European Neanderthals: The contribution of Teixoneres Cave (Moià, Barcelona, Spain). *Quaternary Science Reviews* 43: 33-44.

Lyman, R.L.

1994 *Vertebrate taphonomy*. Cambridge Manuals in Archaeology. Cambridge University Press, Cambridge.

2008 *Quantitative paleozoology*. Cambridge University Press, Cambridge.

Machado, J., C. M. Hernández, C. Mallol, B. Galván.

2013 Lithic production, site formation and Middle Palaeolithic palimpsest analysis: In search of human occupation episodes at Abric del Pastor stratigraphic unit IV (Alicante, Spain). *Journal of Archaeological Science* 40: 2254-2273.

Machado, J. and L. Pérez

- 2016 Temporal frameworks to approach human behavior concealed in Middle Paleolithic palimpsests: A high resolution example from El Salt stratigraphic unit X (Alicante Spain). *Quaternary International* 417: 66-81.

Machado, J. A. Mayor, C. M. Hernández, B. Galván

- 2019 Lithic refitting and the analysis of Middle Palaeolithic settlement dynamics: A high-temporal resolution example from El Pastor rock shelter (Eastern Iberia). *Archaeological and Anthropological Sciences* 11: 4539-4554.

Mallol, C., C. M. Hernández, N. Mercier, C. Falguères, Á. Carrancho, D. Cabanes, P. Vidal-Matutano, et al.

- 2019 Fire and brief human occupations in Iberia during MIS 4: evidence from Abri del Pastor (Alcoy, Spain). *Science Reports* 9: 18281.

Marín J., C. Daujeard, P. Saladié, A. Rodríguez-Hidalgo, D. Vettese, F. Rivals, N. Boulbes, et al.

- 2020 Neanderthal faunal exploitation and settlement dynamics at the Abri du Maras, level 5 (south-eastern France). *Quaternary Science Reviews* 243: 106472.

Moclán A., R. Huguet, B. Márquez, C. Laplana, M.Á. Galindo-Pellicena, N. García, H.A. Blain, et al.

- 2021 A Neanderthal hunting camp in the central system of the Iberian Peninsula: A zooarchaeological and taphonomic analysis of the Navalmaíllo Rock Shelter (Pinilla del Valle, Spain). *Quaternary Science Reviews* 269: 107142.

Morin, E.

- 2007 Fat composition and Nunamiut decision-making: a new look at the marrow and bone grease indices. *Journal of Archaeological Science* 34(1): 69-82.

Morin, E., and M.C. Soulier

2017 New criteria for the archaeological identification of bone grease processing.

*American Antiquity* 82(1): 96-122

Morin, E., E. Ready, A. Boileau, C. Beauval, and M. P. Coumont

2017 Problems of identification and quantification in archaeozoological analysis, part I: insights from a blind test. *Journal of Archaeological Method and Theory* 24: 886-

937.

Oliva M., J. Ruiz-Fernández, M. Barriendos, G. Benito, J.M. Cuadrat, J.M. García-

Ruiz, S. Giralt, et al.

2018 The Little Ice Age in Iberian mountains. *Earth Science Reviews* 177: 175-

208.

Oliva M., D. Palacios, J.M. Fernández-Fernández, L. Rodríguez-Rodríguez, J.M. García-Ruiz,

N. Andrés, R.M. Carrasco, et al.

2019 Late Quaternary glacial phases in the Iberian Peninsula. *Earth-Science*

*Reviews* 192: 564-600.

Pérez, L., J. Machado, A. Sanchis, C. M. Hernández, C. Mallol, and B. Galván.

2020 A high temporal resolution zooarchaeological approach to Neanderthal subsistence strategies on the Southeastern Iberian Peninsula: El Salt stratigraphic unit Xa (Alicante, Spain). In *Short-term occupations in Paleolithic archaeology* edited by J. Cascalheira and A. Picin, pp: 237-289. Springer, Cham.

Pérez-Mejías C., A. Moreno, C. Sancho, R. Martín-García, C. Spötl, I. Cacho, H. Cheng, R. L.

Edwards.

2019 Orbital-to-millennial scale climate variability during Marine Isotope Stages 5 to 3 in northeast Iberia. *Quaternary Science Reviews* 224: 105946.

Pritchard, P.C.H., R.J. Rabett, and P.J. Piper

2009 Distinguishing species of geomyid and trionychid turtles from shell fragments: evidence from the Pleistocene at Niah Caves, Sarawak. *International Journal of Osteoarchaeology*, 19(4): 531-550.

Rabassa J., and J. F. Ponce

2013 The Heinrich and Dansgaard-Oeschger climatic events during Marine Isotopic Stage 3: Searching for appropriate times for human colonization of the Americas. *Quaternary International* 299: 94-105.

Real, C., A. Eixea, A. Sanchis, J. Vicente Morales, N. Klasen, J. Zilhao, V. Villaverde

2018 Abrigo de la Quebrada Level IV (Valencia, Spain): Interpreting a Middle Paleolithic palimpsest from a zooarchaeological and lithic perspective. *Journal of Paleolithic Archaeology* 3: 187-224.

Rivals, F.

2004 *Les petits bovidés (Caprini et Rupicaprini) pléistocènes dans le bassin méditerranéen et le Caucase*. Archaeopress, Oxford, England.

Rosell, J., R. Blasco, F. Rivals, M. Gema Chacón, L. Menéndez, J. I. Morales, A. Rodríguez-Hidalgo et al.

2010 A stop along the way: The role of Neanderthal groups at level III of Teixoneres Cave (Moià, Barcelona, Spain). *Quaternary* 21(2): 139-154.

Rufà, A., R. Blasco, F. Rivals, J. Rosell

- 2014 Leporids as a potential resource for predators (hominins, mammalian carnivores, raptors): An example of mixed contribution from level III of Teixoneres Cave (MIS 3, Barcelona, Spain). *Comptes Rendus Palevol* 13: 665-680.

Sañudo, P., R. Blasco, and J. Fernandez Peris

- 2016 Site formation dynamics and human occupations at Bolomor Cave (Valencia, Spain): An archaeostratigraphic analysis of levels I to XII (100–200 ka). *Quaternary International*, 417: 94-104.

Sanz, M., J. Daura, N. Eguéz, D. Cabanes

- 2015 On the track of anthropogenic activity in carnivore dens: Altered combustion structures in Cova del Gegant (NE Iberian Peninsula). *Quaternary International* 2015: 1-13.

Sanz, M., F. Rivals, D. García, J. Zilhão.

- 2019 Hunting strategy and seasonality in the Last Interglacial occupation of Cueva Antón (Murcia, Spain). *Archaeological and Anthropological Sciences* 11: 3577-3594.

Schiffner M. B.

- 1976 *Behavioral archaeology*. Academic Press, New York.
- 1999 Behavioral archaeology: some clarifications. *Cambridge University Press* 64: 166-168.

Schmid, E.

- 1972 *Atlas of animal bones*. Elsevier Publishing Company, Amsterdam, London, New York.

Shipman, P., G. Foster, and M. Schoeninger

- 1984 Burnt bones and teeth: an experimental study of color, morphology, crystal structure and shrinkage. *Journal of Archaeological Science*, 11(4): 307-325.
- Sibeaux, A. C. L. Michel, X. Bonnet, S. Caron, K. Fourniere, S. Gagno, J.M. Ballouard.
- 2016 Sex-specific ecophysiological responses to environmental fluctuations of free-ranging Hermann's tortoises: implication for conservation. *Conservation Physiology* 4(1): 1-16.
- Sobolik, K.D. and D.G. Steele
- 1996 *A turtle atlas to facilitate archaeological identifications*. Hot Springs: Mammoth Site of Hot Springs in conjunction with the Office of Research and Public Services, University of Maine.
- Sossa-Ríos, S., A. Mayor, C.M. Hernández, M. Bencomo, L. Pérez, B. Galván, C. Mallol, M. Vaquero
- 2022 Multidisciplinary evidence of an isolated neanderthal occupation in Abric del Pastor (Alcoy, Iberian Peninsula). *Scientific Reports* 12(1): 1-12.
- Sprovieri, R., E. Di Stefano, A. Incarbona, D. W. Oppo
- 2006 Suborbital climate variability during Marine Isotopic Stage 5 in the central Mediterranean basin: Evidence from calcareous plankton record. *Quaternary Science Reviews* 25(17-18): 2332-2342.
- Stiner, M. C., S. L. Kuhn, S. Weiner, O. Bar-Yosef.
- 1995 Differential burning, recrystallization, and fragmentation of archaeological bone. *Journal of Archaeological Science* 22(2): 223-237.
- Stock, C.
- 1929 A census of the Pleistocene mammals of Rando La Brea, based on the collections

of the Los Angeles Museum. *Journal of Mammalogy* 10: 281– 289.

Suárez-Bilbao, A., N. Garcia-Ibaibarriaga, J.E. Ortiz, T. Torres, A. Arrizabalaga, M.J. Iriarte-

Chiapusso, X. Murelaga

2021 Late Pleistocene palaeoenvironmental variations from Marine Isotope Stages 5 and 4: small mammals at Artazu VIII Site (Arrasate, Northern Iberian Peninsula). *Ameghiniana*, 58(3): 223-241.

Testu, A.

2006 Etude paléontologique et biostratigraphique des Felidae et Hyaenidae pléistocènes de l'Europe méditerranéenne. Ph.D. dissertation, Université de Perpignan.

Thompson, A. E., J.P. Walden, A.S. Chase, S.R. Hutson, D.B. Marken, B. Cap, et al.

2022 Ancient lowland Maya neighborhoods: average nearest neighbor analysis and kernel density models, environments, and urban scale. *PLoS ONE* 17(11): e0275916.

Vidal-Matutano, P., C. M. Hernández, B. Galván, C. Mallol.

2015 Neanderthal firewood management: evidence from stratigraphic unit IV of Abric del Pastor (Eastern Iberia). *Quaternary Science Reviews* 111: 81-93.

Villa, P. and E. Mahieu

1991 Breakage patterns of human long bones. *Journal of Human Evolution* 21(1): 27-48.

Von den Driesch, A.

1976 *A guide to the measurement of animal bones from archaeological Sites*. Peabody Museum Press.

Zar, J. H.

1996 *Biostatistical analysis*. Upper Saddle River, New Jersey: Prentice Hall.

Zilhão, J., A. Ajas, E. Badal, C. Burow, M. Kehl, J.A. López-Sáez, C. Pimenta, R. C., Preece, A.

Sanchis, M. Sanz, G.C. Weniger

2016 Cueva Antón: A multi-proxy MIS 3 to MIS 5a paleoenvironmental record for SE Iberia. *Quaternary Science Reviews* 146: 251-273.



## APPENDIX 1

## Database Codes

<b>Anatomic Group</b>	<b>Bone</b>	<b>Abbreviation</b>
<b>C (cranial)</b>	Crania	Cr
	Maxilla	Mx
	Mandible	Hem
	Isolated Tooth (Superior)	Das
	Isolated Tooth (inferior)	Dai
	Isolated Tooth	Da
	Incisor (Superior)	Is
	Incisor (Inferior)	Ii
	Molar (Superior)	Ms
	Molar (Inferior)	Mi
	Premolar (Superior)	Ps
	Premolar (Inferior)	Pi

<b>Anatomic Group</b>	<b>Bone</b>	<b>Abbreviation</b>
<b>MA (Forelimb)</b>	Scapula	Es
	Humerus	H
	Radius	R
	Ulna	U
	Metacarpal	Mc
	Metacarpal 1	Mc1
	Metacarpal 2	Mc2
	Metacarpal 3	Mc3
	Metacarpal 4	Mc4
	Metacarpal 5	Mc5
	Carpal	Cp

<b>Anatomic Group</b>	<b>Bone</b>	<b>Abbreviation</b>
<b>A (Axial)</b>	Vertebra Indeterminate	V
	Vertebra Cervical	Vc
	Vertebra Thoracic	Vt
	Vertebra Lumbar	Vl
	Vertebra Caudal	Vcd
	Sacrum	Vs
	Ribs	Ct
	Sternum	Et

<b>Anatomic Group</b>	<b>Bone</b>	<b>Abbreviation</b>
<b>MP (Hindlimb)</b>	Pelvis	Cx
	Femur	F
	Tibia	T
	Fibula	Fi
	Metatarsal	Mt
	Metatarsal 1	Mt1
	Metatarsal 2	Mt2
	Metatarsal 3	Mt3
	Metatarsal 4	Mt4
	Metatarsal 5	Mt5
	Patella	Pa
	Talus	As
	Calcaneus	Ca
	Tarsal	Ta

<b>Anatomic Group</b>	<b>Bone</b>	<b>Abbreviation</b>
<b>E (Extremities)</b>	Phalanx	Fa
	1 <sup>st</sup> Phalanx	Fa1
	2 <sup>nd</sup> Phalanx	Fa2
	3 <sup>rd</sup> Phalanx	Fa3
	Sesamoid	Se
	Metapodial indeterminate	Mtp

<b>Anatomic Group</b>	<b>Bone</b>	<b>Abbreviation</b>
<b>Ave Specific Bones</b>	Furcula	Fa
	Coracoid	Fa1
	Carpometacarpus	Fa2
	Tarsometatarsus	Fa3
	Tibiotarsus	Se
	Synsacrum	Ss
	4 <sup>th</sup> Phalanx	Fa4
	5 <sup>th</sup> Phalanx	Fa5

<b>Anatomic Group-Tortoise Specific</b>	<b>Bone</b>	<b>Abbreviation</b>
<b>ES (Carapace)</b>	Indeterminate Platelet	PT
	Indeterminate Carapace	PTES
	Nuchal	PTNu
	Neural	PTN
	Costal/Pleural	PTPle
	Marginal/Peripheral	PTPer
	Suprapygal	PTSpy

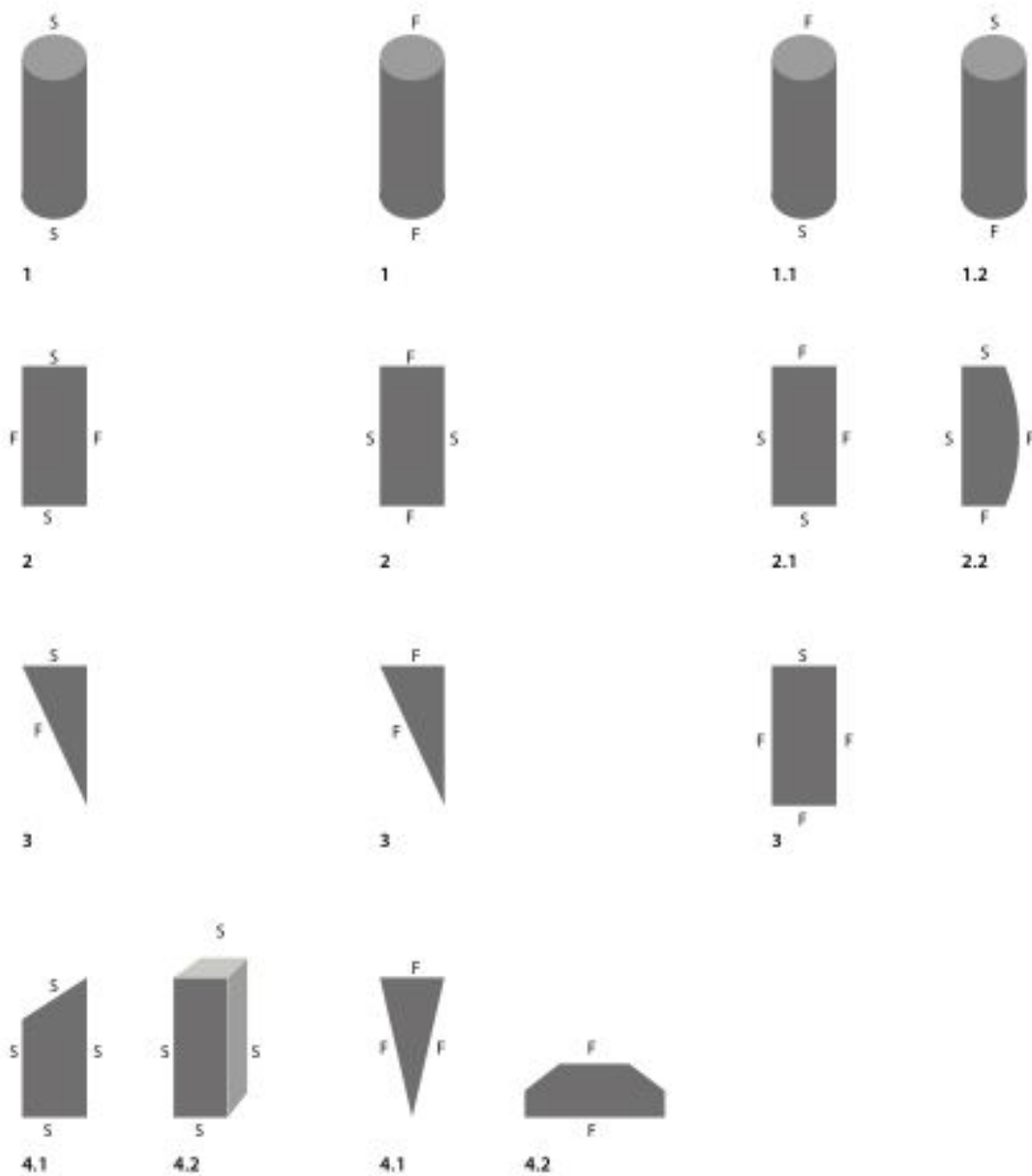
	Pygal	PTPy
<b>PL (Plastron)</b>	Indeterminate Plastron	PTPL
	Epiplastron	PTEpi
	Entoplastron	PTEnto
	Hioplastron	PTHio
	Hipoplastron	PTHipo
	Xiphiplastron	PTX

## APPENDIX 2

MORFOTIPOS  
DE DIÁFISIS

I. (seco)  
 II. (fresco)  
 III. (mixto)  
 IV. (indeterminado)

+ morfotipo específico



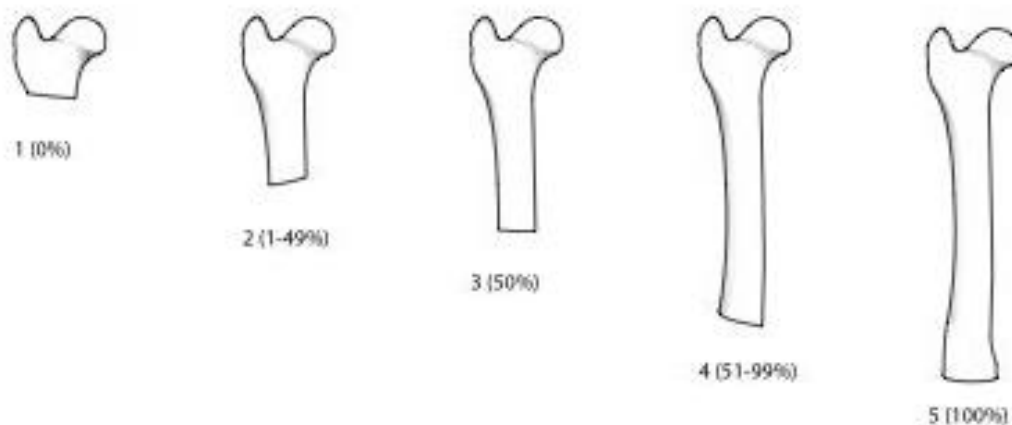
A 2.1. Figure that depicts the various morphotypes of long bone fractures and their corresponding database code.

## MORFOTIPOS DE ARTICULACIÓN

I. (seco)  
 II. (fresco)  
 III. (mixto)  
 IV. (indeterminado)

+ morfotipo específico

### CANTIDAD DE DIÁFISI CONSERVADA



### CANTIDAD DE EPÍFISIS CONSERVADA



\* caso específico del fémur proximal

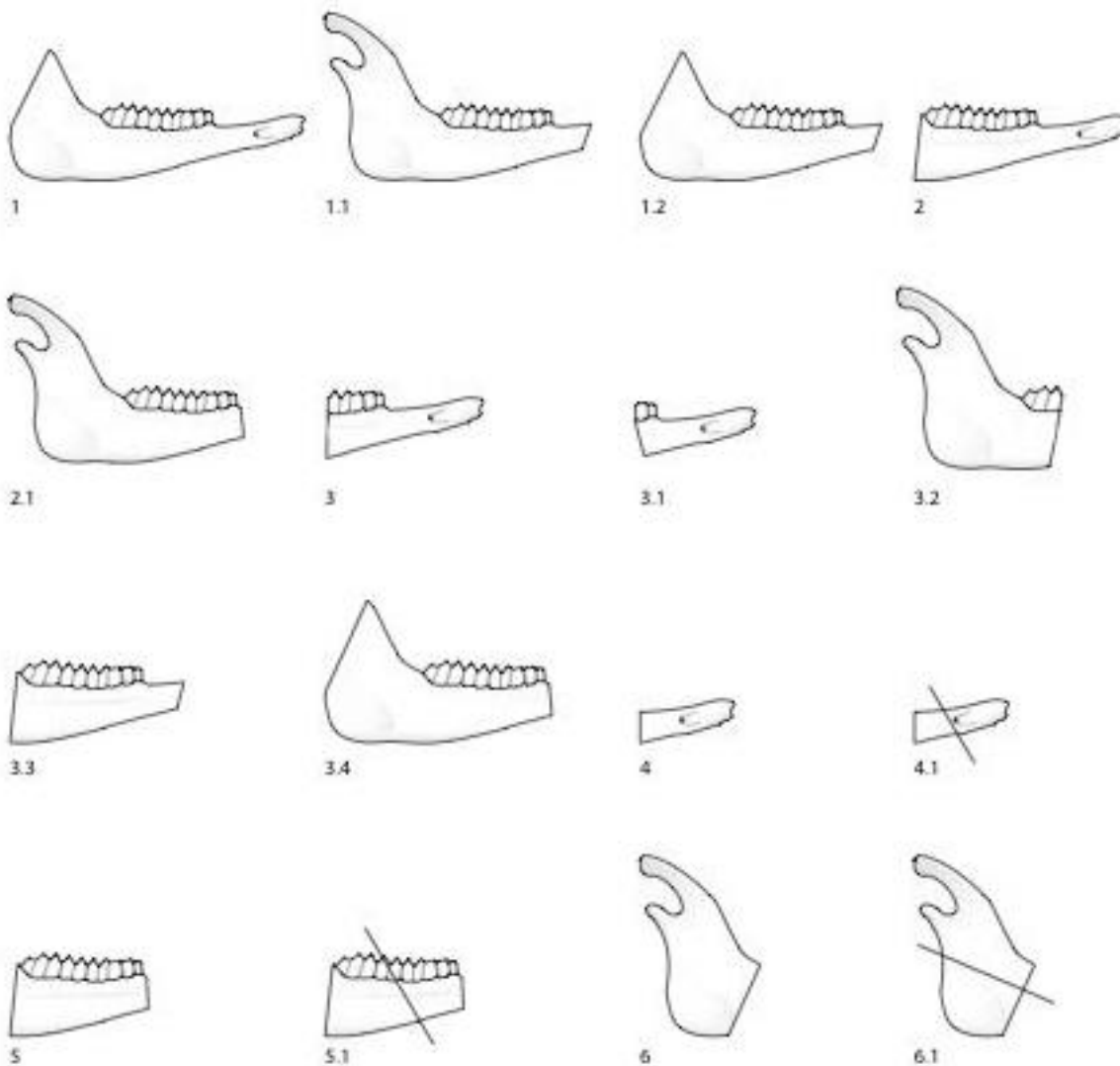
- 1.1 caput
- 1.2 gran trocante
- 2.1 cresta gran trocante
- 2.2 pequeño trocante

A 2.2. Figure that depicts the various morphotypes of epiphyses fractures and their corresponding database codes.

## MORFOTIPOS DE MANDÍBULA

I. (seco)  
 II. (fresco)  
 III. (mixto)  
 IV. (indeterminado)

+ morfotipo específico



1 D + CA + R fragmentado  
 1.1 D fragmentado + CA + R  
 1.2 CV + R y D fragmentados  
 2 D + CA  
 2.1 CA + R  
 3 D + 1/2 de CA  
 3.1 D + 1\* CA  
 3.2 1/2 de CA + R

3.3 D fragmentado + CA  
 3.4 CA + R fragmentado  
 4 D  
 4.1 D fragmentado  
 5 CV  
 5.1 CV fragmentado  
 6 R  
 6.1 R fragmentado

A 2.3. Figure depicting the various morphotypes of mandible fractures and their corresponding database codes.

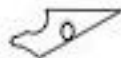
## MORFOTIPOS DE VÉRTEBRA

I. (seco)  
 II. (fresco)  
 III. (mixto)  
 IV. (indeterminado)

+ morfotipo específico



1.1



1.2



2.1



2.2



3.1



3.2



4.1



4.2

1.1 completa sin apófisis  
 1.2 fragmento indeterminado  
 2.1 arco completo  
 2.2 fragmento de arco

3.1 cuerpo completo  
 3.2 fragmento de cuerpo  
 4.1 apófisis completa  
 4.2 fragmento de apófisis

\* se añade ".1" si el resto conserva alguna apófisis

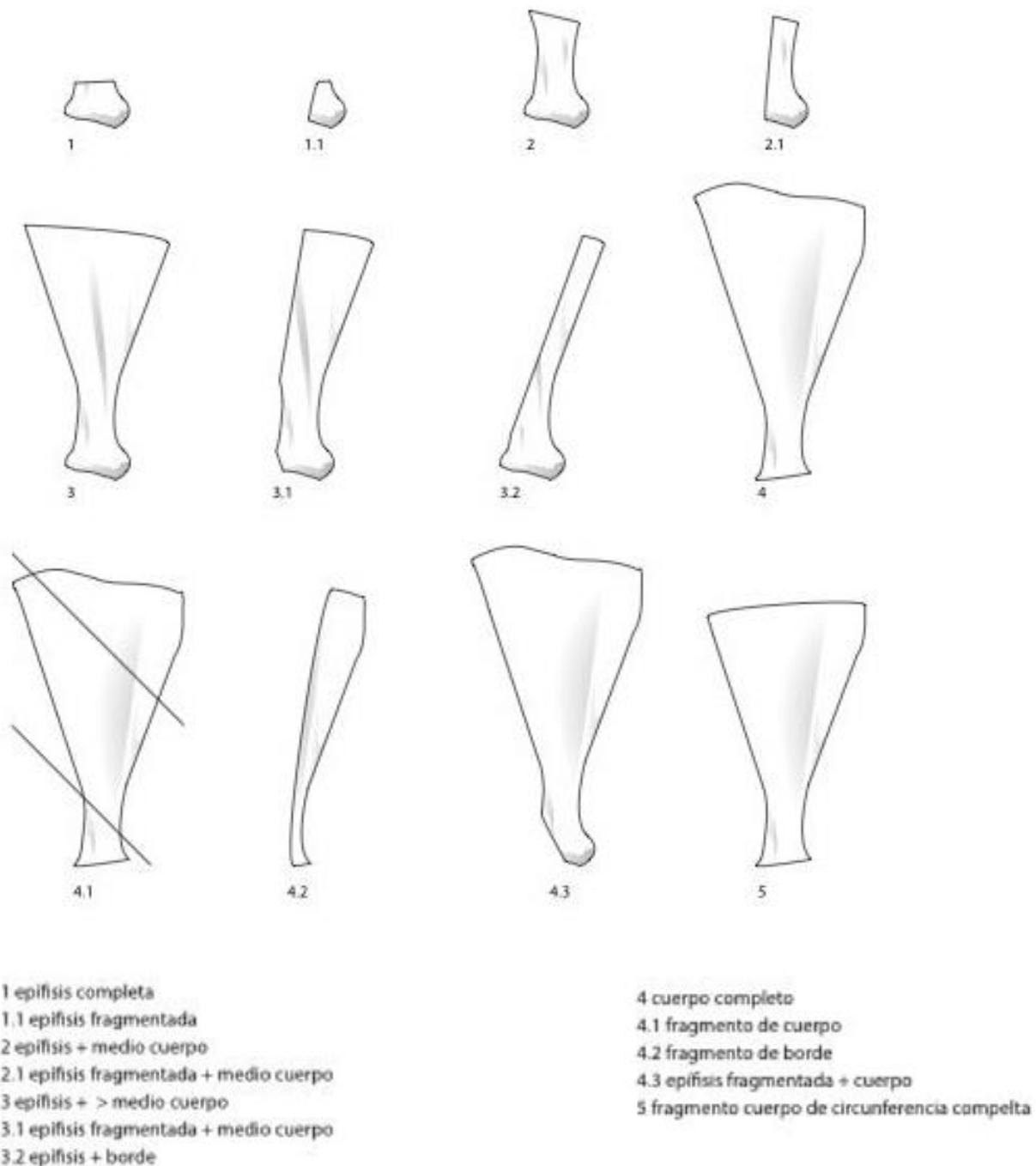
\* se añade ".2" si el resto conserva todas la epófisis

A 2.4. Figure depicting the various morphotypes of vertebra fractures and their corresponding database codes.

## MORFOTIPOS DE ESCÁPULA

I. (seco)  
II. (fresco)  
III. (mixto)  
IV. (indeterminado)

+ morfotipo específico



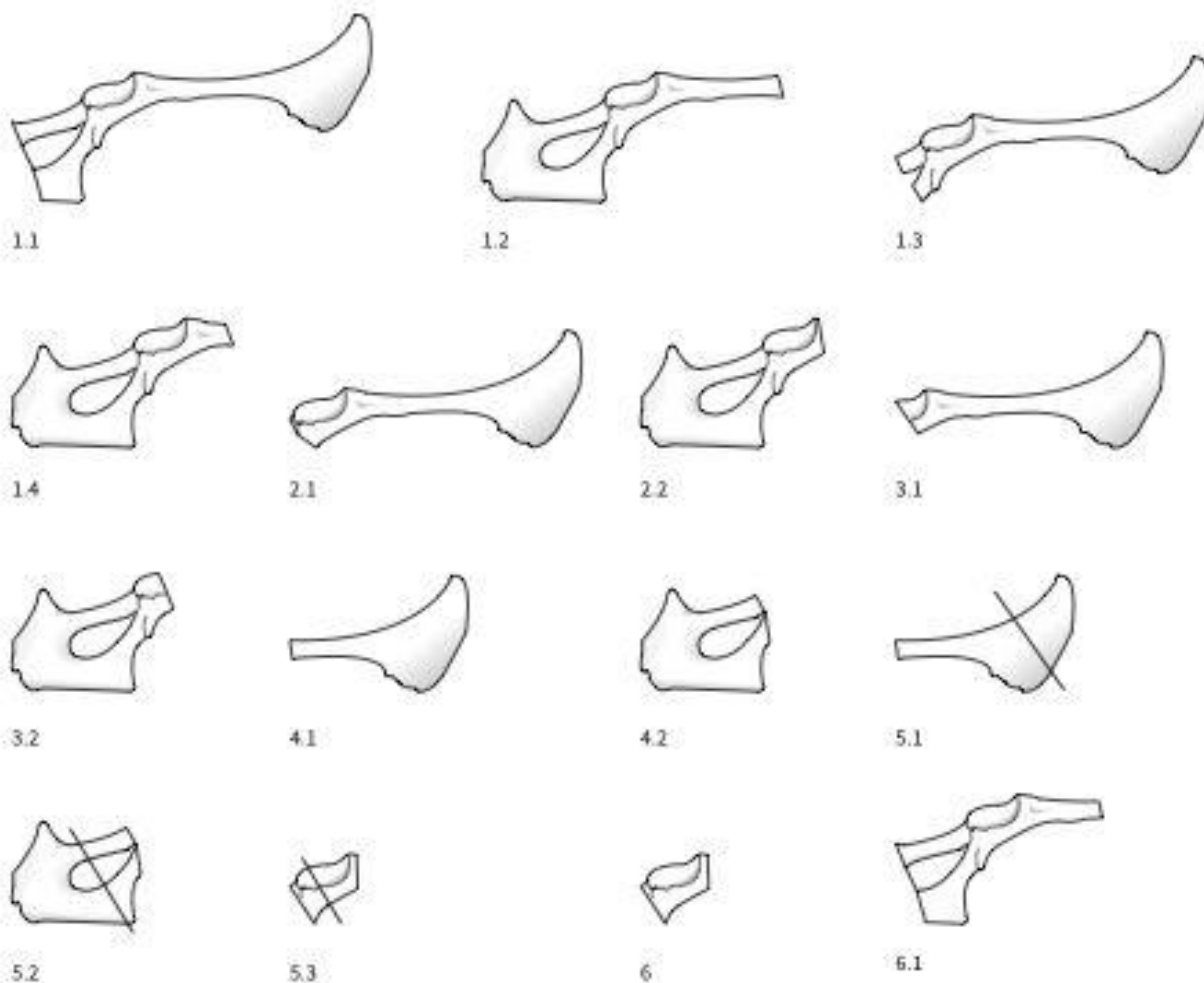
A 2.5. Figure depicting the various morphotypes of scapula fractures and their corresponding database codes.



## MORFOTIPOS DE COXAL

I. (seco)  
II. (fresco)  
III. (mixto)  
IV. (indeterminado)

+ morfotipo específico



1.1 ilion + 1/2 isquion  
1.2 isquion + 1/2 ilion  
1.3 ilion + acetabulo + <1/2 isquion  
1.4 isquion + acetabulo + <1/2 ilion  
2.1 ilion + acetabulo  
2.2 isquion + acetabulo  
3.1 ilion + 1/2 acetabulo  
3.2 isquion + 1/2 acetabulo

4.1 ilion completo  
4.2 isquion completo  
5.1 ilion fragmentado  
5.2 isquion fragmentado  
5.3 acetabulo fragmentado  
6 acetabulo completo  
6.1 acetabulo + ilion e isquion fragmentados

A 2.6. Figure depicting the various morphotypes of pelvis fractures and their corresponding database codes.

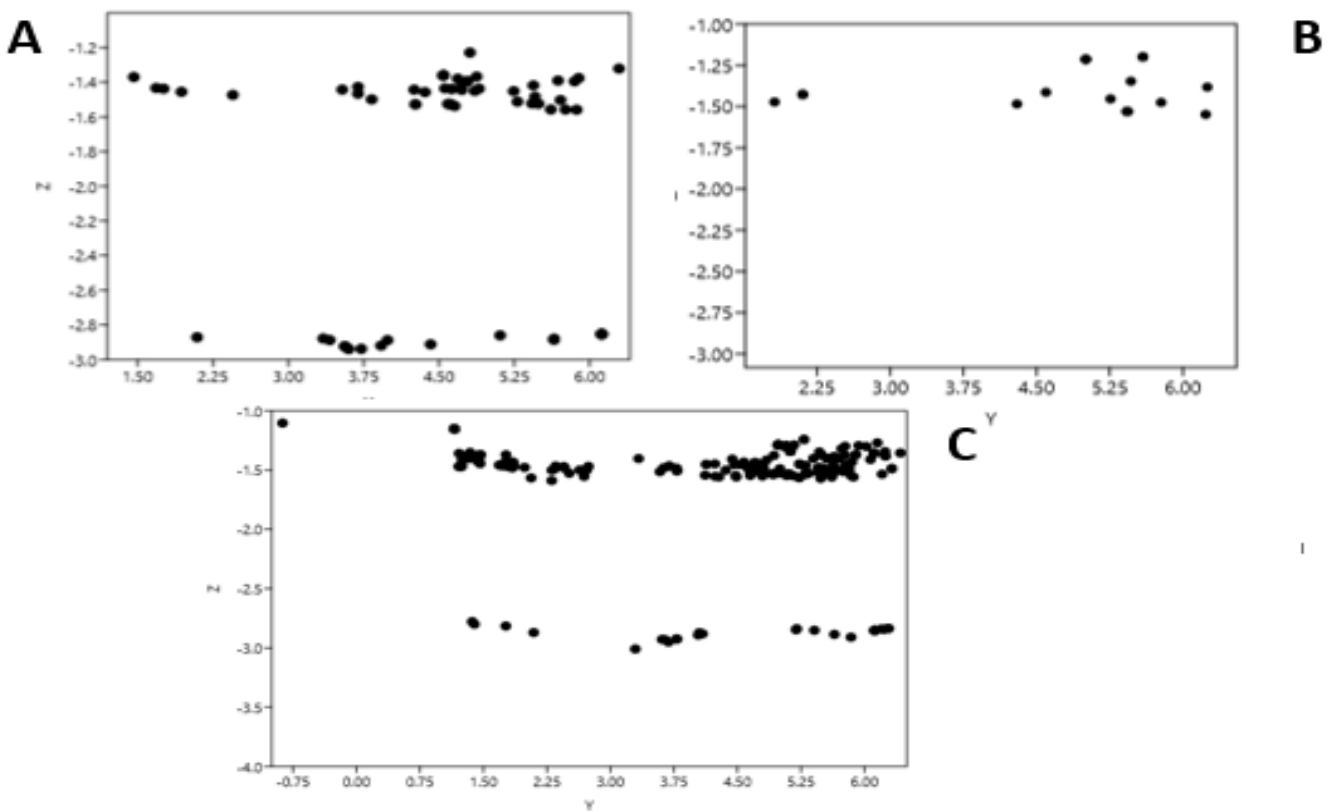
## APPENDIX 3

Occupation B	V		Va		Vb		Vb/Vc		Vc		Vd		Ve		Vf		Total N	Total %
<b>Determinate</b>	9	69.2	34	48.6	28	71.8	1	100	84	68.8	65	63.1	80	58.4	78	79.6	379	65.0
<b>Indeterminate</b>	4	30.8	36	51.4	11	28.2			38	31.1	38	36.9	57	41.6	20	20.4	204	35.0
<b>Total</b>	<b>13</b>	<b>100</b>	<b>70</b>	<b>100</b>	<b>39</b>	<b>100</b>	<b>1</b>	<b>100</b>	<b>122</b>	<b>100</b>	<b>103</b>	<b>100</b>	<b>137</b>	<b>100</b>	<b>98</b>	<b>100</b>	<b>583</b>	<b>100</b>

A 3.1. The number and percent of the determinate and indeterminate specimens through the sublayers of Occupation B.

Input Feature	Observed Mean Distance	Expected Mean Distance	Nearest Neighbor Ratio	z-score	p-value	Clustered or dispersed
Occupation A	0.104003	0.218701	0.475548	-7.574852	0.000000	Clustered
Occupation B	0.039063	0.154357	0.253067	-34.502199	0.000000	Clustered

A 3.2. Average Nearest Neighbor analysis output for both Occupation A and Occupation B.



A 3.3. Vertical distribution of specimens attributed to A) small-sized taxa, B) large-sized taxa, and C) medium-sized taxa.